

พอลิเมอร์ไรเซชันร่วมของเอทิลีนกับหนึ่งโอเลฟินด้วยตัวเร่งปฏิกิริยาเมทัลโลซีน
บนตัวรองรับซิลิกาทรงกลม



นางสาวเพชร รอดกิจ

ศูนย์วิทยทรัพยากร

วิทยานิพนธ์นี้เป็นส่วนหนึ่งของการศึกษาตามหลักสูตรปริญญาวิศวกรรมศาสตรมหาบัณฑิต

สาขาวิชาวิศวกรรมเคมี ภาควิชาวิศวกรรมเคมี

คณะวิศวกรรมศาสตร์ จุฬาลงกรณ์มหาวิทยาลัย

ปีการศึกษา 2552

ลิขสิทธิ์ของจุฬาลงกรณ์มหาวิทยาลัย

COPOLYMERIZATION OF ETHYLENE/1-OLEFIN WITH SPHERICAL
SILICA-SUPPORTED METALLOCENE CATALYSTS



Miss Prae Rothakit

A Thesis Submitted in Partial Fulfillment of the Requirements
for the Degree of Master of Engineering Program in Chemical Engineering

Department of Chemical Engineering

Faculty of Engineering
Chulalongkorn University

Academic Year 2009

Copyright of Chulalongkorn University

แพรว รลกิจ : พอลิเมอร์ไรเซชันร่วมของเอทิลีนกับหนึ่งโอเลฟินด้วยตัวเร่งปฏิกิริยา
เมทัลโลซีนบนตัวรองรับซิลิกาทรงกลม (COPOLYMERIZATION OF ETHYLENE/
1-OLEFIN WITH SPHERICAL SILICA-SUPPORTED METALLOCENE
CATALYSTS) อ. ที่ปริกษาวิทยานิพนธ์หลัก : รศ. ดร. บรรเจิด จงสมจิตร, 113 หน้า

ในปัจจุบันพอลิเมอร์ที่ได้รับความนิยมและมีปริมาณการใช้งานมากสุดในอุตสาหกรรมการผลิตพลาสติกคือพอลิเอทิลีนและพอลิโพรพิลีน ซึ่งพอลิโพรพิลีนในกลุ่มนี้ได้ถูกนำมาประยุกต์ใช้งานมากมาย เนื่องจากมีความคุ้มค่าในด้านของประสิทธิภาพและราคา พอลิเอทิลีนความหนาแน่นต่ำจึงได้ถูกจัดเป็นพอลิเอทิลีนที่มีความสำคัญในทางการค้า ซึ่งสามารถสังเคราะห์ได้จากปฏิกิริยาพอลิเมอร์ไรเซชันร่วมของเอทิลีนกับอัลฟาโอเลฟิน โดยระบบตัวเร่งปฏิกิริยาเมทัลโลซีนร่วมกับตัวเร่งปฏิกิริยาร่วมเมทิลอะลูมิเนียมออกเซนมีส่วนร่วมในการผลิตพอลิเอทิลีนความหนาแน่นต่ำเชิงเส้นที่มีจุดเด่นหลายประการ แต่ในระบบตัวเร่งปฏิกิริยาเมทัลโลซีนแบบไม่ใช้ตัวรองรับนี้ก็มีข้อเสียอยู่บ้าง เช่น ไม่สามารถควบคุมโครงสร้างสัณฐานของพอลิเมอร์ได้, ไม่สามารถใช้ระบบที่ไม่มีตัวรองรับนี้ในระบบสเลอร์และวัฏภาคแก๊สได้ และต้องใช้ตัวเร่งปฏิกิริยาร่วมจำนวนมากเพื่อให้ได้ความว่องไวในการเกิดปฏิกิริยาที่สูง ซึ่งปัญหาเหล่านี้สามารถแก้ไขได้โดยการซัดคัตตัวเร่งปฏิกิริยาเมทัลโลซีนลงบนตัวรองรับ โดยประสิทธิภาพของระบบตัวเร่งปฏิกิริยาเมทัลโลซีนแบบมีตัวรองรับและกลไกในการกระตุ้นให้เกิดการเร่งปฏิกิริยายังคงอยู่ในงานวิจัยนี้มุ่งเน้นการพัฒนาปรับปรุงตัวเร่งปฏิกิริยาเมทัลโลซีนโดยใช้ซิลิกาทรงกลมที่มีขนาดต่างๆ กันคือ ขนาดเล็กกว่าไมครอน, 3, 5 และ 10 ไมโครเมตรเป็นตัวรองรับ การศึกษาจะแบ่งเป็น 2 ส่วนซึ่งมีความแตกต่างกันในด้านการเคลือบฝังตัวเร่งปฏิกิริยาร่วมลงบนตัวรองรับ ในส่วนแรกเป็นการเกิดปฏิกิริยาพอลิเมอร์ไรเซชัน โดยใช้ระบบตัวเร่งปฏิกิริยาเมทัลโลซีน/เมทิลอะลูมิเนียมออกเซนแบบมีตัวรองรับที่เตรียมจากการเคลือบฝังตัวเร่งปฏิกิริยาร่วมแบบอินซิitu พื้นที่ผิวด้านนอกของตัวรองรับที่มีค่ามากส่งผลให้ค่าความว่องไวในการเกิดปฏิกิริยาพอลิเมอร์ไรเซชันของซิลิกาขนาด 3 ไมโครเมตรมีค่ามากขึ้นอย่างเห็นได้ชัด การเติมโคมอนอเมอร์เข้าไปในระบบส่งค่าความว่องไวในการเกิดปฏิกิริยาพอลิเมอร์ไรเซชันเพิ่มขึ้นอย่างเห็นได้ชัด ในส่วนที่สองจะเป็นการศึกษาในระบบตัวเร่งปฏิกิริยาที่คล้ายกับระบบแรก แต่เป็นการเคลือบฝังตัวเร่งปฏิกิริยาร่วมลงบนตัวรองรับแบบเอกซิtu พบว่าขนาดของอนุภาคซิลิกาทรงกลมที่เหมาะสมจะให้ค่าความว่องไวที่สูง แต่อันตรกิริยาระหว่างตัวเร่งปฏิกิริยากับตัวรองรับที่มีค่าสูงเกินไปจะส่งผลในแง่ลบต่อการเร่งปฏิกิริยา โคพอลิเมอร์ที่ได้ทั้งหมดจะถูกนำมาวิเคราะห์ด้วยเครื่อง ^{13}C NMR และเครื่อง DSC

ภาควิชา.....วิศวกรรมเคมี..... ถายมือชื่อนิสิต..... ๒๒๖. ๖๖๖.....

สาขาวิชา.....วิศวกรรมเคมี..... ถายมือชื่อ อ.ที่ปริกษาวิทยานิพนธ์หลัก..... *Jirada*.....

ปีการศึกษา.....2552.....

5170600521: MAJOR CHEMICAL ENGINEERING

KEYWORDS : SUPPORTED METALLOCENE CATALYST / SILICA / SPHERE / LLDPE / COPOLYMERIZATION OF ETHYLENE

PRAE ROTHAKIT : COPOLYMERIZATION OF ETHYLENE/1-OLEFIN WITH SPHERICAL SILICA-SUPPORTED METALLOCENE CATALYSTS.

THESIS ADVISOR : ASSOC. PROF. BUNJERD JONGSOMJIT, Ph.D., 113 pp.

At present, the first consideration and largest volume of polymers in the plastics industry (Polyolefins) are mostly consisting of polyethylenes and polypropylenes, which are often used in any application because of their excellent cost/performance value. LLDPEs (Linear low-density polyethylenes), synthesized by the copolymerization of ethylene with α -olefin, is the great commercial significance in polyethylene series. Which the metallocene / methylaluminoxane catalyst system participate in production of LLDPEs provide the great among of advantage. But there are only a few major problems, such as difficulty in controlling polymer morphology, inability to be used homogeneous metallocene in slurry or gas-phase, and need very large amount of methylaluminoxane to achieve maximum of catalytic activity. So, the way to wipe out the few constraints is attaching the metallocene to the support without losing the performances of the homogeneous complex and activation step of metallocene. This research proposed the development of metallocene catalyst by spherical silica supports with different particle diameter such as submicron, 3, 5, and 10 μm . This study was divided into two parts, which difference in the impregnation method. In the first part, the polymerization reaction was performed using a supported zirconocene/MAO catalyst, which was prepared by in situ impregnation method. The higher outer surface area of supports apparently resulted in increased polymerization activity for SiO_2 3 μm . The polymerization activity was also dramatically increased when comonomer was added. The second part was similar to the first, but catalyst precursors were prepared by ex situ impregnation method. The optimum particle size gave the better activity, but too strong interaction between MAO and support affected the negative result to the catalytic system. All copolymer were characterized by means of ^{13}C NMR and DSC.

Department :Chemical Engineering... Student's Signature... Prae Rothakit.....

Field of Study : Chemical Engineering... Advisor's Signature... Bunjerd Jongsomjit.....

Academic Year :2009.....

ACKNOWLEDGEMENTS

The author would like to express the great gratitude and appreciation to Associate Professor Dr. Bunjerd Jongsomjit, my advisor, for his invaluable suggestions, encouragement during my study and useful discussions throughout this research. His advice is always worthwhile and without him this work could not be possible.

In addition, I wish to thank Assistant Professor Dr. Montree Wongsri, as the chairman, and the entire member of thesis committee including Associate Professor Dr. ML. Supakanok Thongyai and Assistant Professor Dr. Sirirat Wacharawichanant for their valuable guidance and revision throughout my thesis.

Sincere thanks are given to the graduate school and department of chemical engineering at Chulalongkorn University for the financial support of this work. And many thanks are given to PTT Chemical Public Company Limited for ethylene gas supply and MEKTEC Manufacturing Corporation (Thailand) Limited for DSC and NMR measurements.

Many thanks for kind suggestions and useful help to Mr. Ekrachan Chaichana, Miss Mingkwan Wannaborworn, Miss Somsakun Pathomsap and many friends in the Center of Excellence on Catalysis and Catalytic Reaction Engineering, Department of Chemical Engineering, Faculty of Engineering, Chulalongkorn University for friendship and their assistance. To the many others, not specifically named, who have provided me with support and encouragement, please be assured that I think of you.

Finally, I would like to express my highest gratitude to my family who are always beside me and support throughout this study.

CONTENTS

	Page
ABSTRACT (IN THAI)	iv
ABSTRACT (IN ENGLISH)	v
ACKNOWLEDGEMENTS	vi
CONTENTS	vii
LIST OF TABLES	x
LIST OF FIGURES	xi
CHAPTER I INTRODUCTION	1
CHAPTER II LITERATURE REVIEW	5
2.1 Background of polyolefin catalyst	5
2.1.1 Metallocene catalysts	7
2.1.2 Structure of Metallocene Catalyst	9
2.1.3 Cocatalyst	11
2.1.4 Polymerization mechanism	14
2.1.5 Copolymerization	19
2.2 Supported metallocene catalysts	21
2.2.1 Catalyst Chemistry	23
2.2.2 Supporting Catalyst on Materials Treated with Alkylaluminum.....	24
2.2.3 Silica-supported catalytic system	25
CHAPTER III EXPERIMENTAL	32
3.1 Objectives of the Thesis	32
3.2 Scopes of the Thesis	32
3.3 Research Methodology	33
3.4 Experimental	34
3.4.1 Chemicals	34
3.4.2 Equipments	35
3.4.2.1 Cooling system.....	35
3.4.2.2 Magnetic stirrer and heater	36
3.4.2.3 Vacuum pump.....	36
3.4.2.4 Inert gas supply	36
3.4.2.5 Reactor	37
3.4.2.6 Schlenk line.....	37

	Page
3.4.2.7 Schlenk tube.....	37
3.4.2.8 Polymerization line	38
3.4.3 Supporting Procedure	38
3.4.3.1 Preparation of mesoporous silica sphere support.....	38
3.4.3.2 Preparation of supported MAO (catalyst precursor).....	39
3.4.4 Ethylene and ethylene/1-octene polymerization procedure	40
3.4.5 Characterization of supports and catalyst precursor.....	40
3.4.5.1 X-ray diffraction (XRD)	40
3.4.5.2 Scanning electron microscopy (SEM) and energy dispersive X-ray spectroscopy (EDX)....	41
3.4.5.3 N ₂ physisorption.....	41
3.4.5.4 Thermal gravimetric analysis (TGA).....	41
3.4.5.5 X-ray photoelectron spectroscopy (XPS)	41
3.4.6 Characterization of Polymer.....	42
3.4.6.1 Differential scanning calorimetry (DSC).....	42
3.4.6.2 ¹³ C NMR spectroscopy (¹³ C NMR)	42
CHAPTER IV RESULTS AND DISCUSSIONS	43
4.1 Characterization of supports and catalyst precursors	43
4.1.1 Characterization of supports with N ₂ physisorption.....	43
4.1.2 Characterization of supports and catalyst precursors with X-ray diffraction (XRD).....	45
4.1.3 Characterization of catalyst precursors with X-ray photoelectron spectroscopy (XPS).....	46
4.1.4 Characterization of supports and catalyst precursors with scanning electron microscope (SEM) and energy dispersive X-ray spectroscopy (EDX)	47
4.1.5 Characterization of supports and catalyst precursors with thermogravimetric analysis (TGA)	51
4.2 Characteristics and catalytic properties of ethylene and ethylene/1-octene polymerization which catalyst precursors prepared by in situ impregnation.	52
4.2.1 The effect of particle size of spherical silica supports and comonomer on the catalytic activity.....	52
4.2.2 The effect of particle size of spherical silica supports on the polymer microstructure	54

	Page
4.2.3 The effect of particle size of spherical silica supports on the polyethylene crystallinity	55
4.3 Characteristics and catalytic properties of ethylene and ethylene/1-octene polymerization which catalyst precursors prepared by ex situ impregnation.....	56
4.3.1 The effect of particle size of spherical silica supports and comonomer on the catalytic activity.....	56
4.3.2 The effect of particle size of spherical silica supports and comonomer on morphologies of polymers.....	58
4.3.3 The effect of particle size of spherical silica supports and comonomer on polymers microstructure	61
4.3.4 The effect of particle size of spherical silica supports on the polyethylene crystallinity	62
4.3.5 The effect of particle size of spherical silica supports on melting temperature of polymers	62
4.4 Comparison of catalytic activity between in situ and ex situ impregnation method	64
CHAPTER V CONCLUSIONS & RECOMMENDATIONS.....	66
5.1 Conclusions	66
5.2 Recommendations	67
REFERENCES.....	68
APPENDICES	75
APPENDIX A	76
APPENDIX B.....	81
APPENDIX C	94
APPENDIX D	101
APPENDIX E.....	107
APPENDIX F.....	111
VITA	113

LIST OF TABLES

Table	Page
2.1 Density range, molecular structure, synthesis, and applications of various type polyethylenes	6
4.1 BET surface area and pore characteristics of supports	44
4.2 Binding energy and surface concentration for Al 2p obtained from XPS	47
4.3 The average [Al] _{MAO} content on various spherical silica supports	51
4.4 Catalytic activity of various silica-supported MAO during ethylene (E) and ethylene/1-octene (EO) polymerization (In situ impregnation)	53
4.5 ¹³ C NMR analysis of and ethylene/1-octene copolymer (In situ impregnation)	54
4.6 Catalytic activity of various silica-supported MAO during ethylene (E) and ethylene/1-octene (EO) polymerization (Ex situ impregnation).....	57
4.7 ¹³ C NMR analysis of and ethylene/1-octene copolymer (Ex situ impregnation)	61
4.8 Melting temperatures of polymers obtained various silica supports (Ex situ impregnation)	63
4.9 Ethylene polymerization activities from various silica-supported MAO prepared by in situ and ex situ impregnation method.....	64
A-1 Binding energy (BE) and % mass concentration of SiO ₂ (0.56μm)	77
A-2 Binding energy (BE) and % mass concentration of SiO ₂ (3 μm)	78
A-3 Binding energy (BE) and % mass concentration of SiO ₂ (5 μm)	79
A-4 Binding energy (BE) and % mass concentration of SiO ₂ (10 μm)	80
E-1 Reactivity ratios of ethylene and 1-octene.....	109

ศูนย์วิทยทรัพยากร

จุฬาลงกรณ์มหาวิทยาลัย

LIST OF FIGURES

Figure	Page
2.1	History of metallocene catalyst development8
2.2	Typical chemical structure of a metallocene catalyst9
2.3	Schematic representations of metallocene symmetry (Type 1: C_{2v} -symmetric, Type 2: C_2 -Symmetric, Type 3 and Type 4: C_s -symmetric, Type 5: C_1 -symmetric) (<i>C</i> , italic. It is better to draw all the structures in a similar way)..... 10
2.4	Several kinds of cocatalysts 11
2.5	Structure of MAO proposed by Sinn et al. 12
2.6	The activation step of MAO cocatalyst 13
2.7	Cossee mechanism for Ziegler-Natta olefin polymerization 15
2.8	The propagation step according to the trigger mechanism 16
2.9	Propagation mechanism in polymerization..... 16
2.10	Chain transfer via β -H elimination 17
2.11	Chain transfer via β -CH ₃ elimination 17
2.12	Chain transfer to aluminum 18
2.13	Chain transfer to monomer 18
2.14	Chain transfer to hydrogen..... 18
2.15	Propylene polymerization profile shows the comparison of activity profile between 1-octene prepolymerized catalyst and untreated system21
2.16	Effect of surface hydroxyl groups on ionic metallocene catalysts24
2.17	Propene polymerization profiles of a silica supported metallocene/MAO catalyst prepared by suspension impregnation27
2.18	Structure of Et(Ind) ₂ ZrCl ₂ supported on silica.....28
2.19	Structure of Et(Ind) ₂ ZrCl ₂ supported on alumina28
2.20	Schematic representation of a model for the growth of a single polymer particle30
2.21	Schematic particle growth model for the propene polymerization of a silica-supported metallocene/MAO catalyst.....31
3.1	Flow diagram of research methodology33
3.2	Inert gas supply system.....36
3.3	Schlenk line.....37
3.4	Schlenk tube.....38
3.5	Diagram of system in slurry phase polymerization.38

Figure	Page
4.1 Pore size distribution of spherical silica supports.....	44
4.2 XRD patterns of different spherical silica supports.....	45
4.3 Typical XPS spectrum for Al 2p on various supports	46
4.4 SEM micrographs of various spherical silica supports before MAO impregnation.....	48
4.5 SEM micrographs of various spherical silica supports after MAO ex situ impregnation.....	49
4.6 Si and Al mapping of silica/MAO particles with ex situ impregnation.....	50
4.7 TGA profiles of supported MAO on spherical silica supports	51
4.8 XRD patterns of polyethylene (in situ impregnation).....	55
4.9 SEM micrographs of polyethylene obtained with various spherical silica supports	59
4.10 SEM micrographs of copolymers obtained with various spherical silica supports	60
4.11 XRD patterns of polyethylene (ex situ impregnation).....	62
A-1 The XPS profile of Al _{2p} on SiO ₂ (0.56 μm) support.....	77
A-2 The XPS profile of Al _{2p} on SiO ₂ (3 μm) support.....	78
A-3 The XPS profile of Al _{2p} on SiO ₂ (5 μm) support.....	79
A-4 The XPS profile of Al _{2p} on SiO ₂ (10 μm) support.....	80
B-1 SEM micrographs of various spherical silica supports before MAO impregnation.....	82
B-2 SEM micrographs of various spherical silica supports after MAO ex situ impregnation	83
B-3 SEM micrographs of polyethylene obtained with various spherical silica supports	84
B-4 SEM micrographs of copolymers obtained with various spherical silica supports	85
B-5 EDX mapping of SiO ₂ (0.56 μm) supports after MAO impregnation.....	86
B-6 EDX mapping of SiO ₂ (3 μm) supports after MAO impregnation.....	87
B-7 EDX mapping of SiO ₂ (5 μm) supports after MAO impregnation.....	88
B-8 EDX mapping of SiO ₂ (10 μm) supports after MAO impregnation.....	89
B-9 EDX profile of [Al] _{MAO} on SiO ₂ (0.56 μm).....	90
B-10 EDX profile of [Al] _{MAO} on SiO ₂ (3 μm)	91
B-11 EDX profile of [Al] _{MAO} on SiO ₂ (5 μm)	92
B-12 EDX profile of [Al] _{MAO} on SiO ₂ (10 μm)	93

Figure	Page
C-1 ¹³ C NMR spectrum of ethylene/1-octene copolymer (Homogenous by in situ impregnation)	95
C-2 ¹³ C NMR spectrum of ethylene/1-octene copolymer (SiO ₂ -0.56μm by in situ impregnation)	95
C-3 ¹³ C NMR spectrum of ethylene/1-octene copolymer (SiO ₂ -3μm by in situ impregnation)	96
C-4 ¹³ C NMR spectrum of ethylene/1-octene copolymer (SiO ₂ -5μm by in situ impregnation)	96
C-5 ¹³ C NMR spectrum of ethylene/1-octene copolymer (SiO ₂ -10μm by in situ impregnation)	97
C-6 ¹³ C NMR spectrum of ethylene/1-octene copolymer (Homogenous by ex situ impregnation).....	97
C-7 ¹³ C NMR spectrum of ethylene/1-octene copolymer (SiO ₂ -0.56μm by ex situ impregnation).....	98
C-8 ¹³ C NMR spectrum of ethylene/1-octene copolymer (SiO ₂ -3μm by ex situ impregnation).....	98
C-9 ¹³ C NMR spectrum of ethylene/1-octene copolymer (SiO ₂ -5μm by ex situ impregnation).....	99
C-10 ¹³ C NMR spectrum of ethylene/1-octene copolymer (SiO ₂ -10μm by ex situ impregnation).....	99
C-11 ¹³ C NMR spectrum of polyethylene for all support types	100
D-1 DSC curve of polyethylene produce with homogenous	102
D-2 DSC curve of polyethylene produce with SiO ₂ (0.56 μm).....	102
D-3 DSC curve of polyethylene produce with SiO ₂ (3 μm).....	103
D-4 DSC curve of polyethylene produce with SiO ₂ (5 μm).....	103
D-5 DSC curve of polyethylene produce with SiO ₂ (10 μm).....	104
D-6 DSC curve of ethylene/1-octene produce with homogenous.....	104
D-7 DSC curve of ethylene/1-octene produce with SiO ₂ (0.56 μm).....	105
D-8 DSC curve of ethylene/1-octene produce with SiO ₂ (3 μm).....	105
D-9 DSC curve of ethylene/1-octene produce with SiO ₂ (5 μm).....	106
D-10 DSC curve of ethylene/1-octene produce with SiO ₂ (10 μm).....	106

CHAPTER I

INTRODUCTION

Polyolefins are the largest volume polymers in the plastics industry today consisting mostly of polyethylenes (PE) and polypropylenes (PP), which are often considered first for use in any application because of their excellent cost/performance value. The utility and cost effectiveness of polyolefins have been proven in global market over many years cause the market for polyolefins in 2005 was 65 million tons with a 6% growth rate for PE and 40 million tons with an 8% growth rate for PP [Chum and Swogger, 2008]. LLDPEs (linear low-density polyethylenes), synthesized by the copolymerization of ethylene with higher α -olefins, such as 1-hexene, 1-octene, and 1-decene, are another type of polyolefins and have great commercial significance [Sarzotti et al., 2002]. Global LLDPE consumption is increasing at impressive rate and the driving force in this growth can be attributed to metallocene-catalyzed LLDPE resins [Britto et al., 2001]. The production of LLDPE with metallocene catalyst increased by 9% from 2001 to 2002 and is predicted to increase annually by 27% from 2001 to 2006 [Schumacher and Borruso, 2002]. Properties of olefins copolymers are greatly influenced by various factors, e.g. molecular weight, molecular weight distribution, comonomer content and monomer sequence distribution. In turn, some of these properties are dependent on nature of catalyst and cocatalyst and on the polymerization condition. There are a large number of metallocene and other single-site catalysts have been discovered and evaluated in the past decade [Kaminsky and Laban, 2001 ; Alt and Koppl, 2000 ; Hlatky, 2000 ; Ribeiro et al., 1997].

Since Sinn and Kaminsky's discovery of new catalytic systems in 1980s, group IV metallocenes activated by MAO has been the subject of intensive research and in vanguard. Metallocene-based catalysts are dramatically different from previous catalyst generation. In comparison with Ziegler-Natta systems, metallocene catalysts offer higher versatility and flexibility both for the synthesis and the control of the structures of polyolefins. The symmetry of the metallocene is the main factor in

determining polymer stereochemistry and minor effect may derive from the nature of cocatalyst and the polymerization temperature [Ciardelli et al., 1998]. For examples, metallocene catalysts can be tailored to produce polyolefins with special stereoregularities and high degree of tacticity. Moreover, these homogeneous systems are able to polymerize several olefins with high activities into high molecular weight polymers and copolymers, narrow molecular weight distribution (≈ 2) and homogeneous chemical composition [Ribeiro et al., 1997]. However, despite their numerous advantages, it was found that homogeneous metallocene catalyst have three main problems observed are (1) the difficulty in controlling polymer morphology (moreover, significant reactor fouling takes place) (2) inability to be used in slurry and gas-phase process, which is most of industrial olefin polymerization process technologies and (3) the very large amount of methylaluminoxane needed to achieve maximum metallocene catalytic activity. The immobilization of metallocenes on support is a technical and economical solution to these limitations. In this case, the aim is to find a way to attach the metallocene to the support without losing the performances of the homogeneous complex while improving the morphological characteristics of the polymers in order to meet the requirements for industrial applications.

To achieve heterogeneous metallocene catalyst, inorganic materials such as silica, alumina, silica-alumina, magnesium chloride, clays, zeolites and mesoporous materials have been employed as support [Grieken et al., 2007]. Silica is one of most frequently used supports, since they have relatively high surface area, pore volumes per unit mass leading to good morphological features for polymer particle [Pullukat and Hu, 2004]. Many types of supports have been studied and modified, then was found that support with different characteristic will achieve in various catalytic behaviors during polymerization reaction as well. [Silva et al., 2000 ; Jongsomjit et al. 2004a ; Jongsomjit et al., 2004b ; Smit et al., 2006 ; Jiamwjitkul et al., 2007 ; Bunchonturakarn et al., 2008 ; Pothirat et al., 2008 ; Marques et al., 2008 ; Wongwaiwattanukul and Jongsomjit, 2008]. Furthermore, mesoporous silica has attracted much attention because of their emerging applications in the areas of catalysis, adsorption, chromatography, and cosmetics [Zhang et al., 2008]. In order to

control polymer morphology, mesoporous silica spheres are promising support because of the shape and morphology of a polymer particle are determined by initial morphology of the original supported catalyst. Therefore, Many attempts have been made in the past to control morphology of polyolefins by using both spherical organic and inorganic supports [Roscoe et al., 1998; Galli and Vecellio, 2001; Zheng and Loos, 2006; Klapper et al., 2007].

In this present research, the ethylene/1-octene copolymerization using spherical silica supports with different particle diameters such as submicron, 3, 5 and 10 μm SiO_2 -supported MAO with zirconocene catalyst was investigate. This ethylene/1-octene copolymerization was compared with ethylene homopolymerization to study the commoner effect. The supports and catalyst precursors were prepared, characterized and investigated for the effect of particle size of supports on the catalytic activity and polymer properties. Moreover, the role of ex situ and in situ impregnation method was also studied.

The objective of this thesis was to study the effect of various size spherical supports and impregnation method on catalytic activity and polymer properties during ethylene and ethylene/1-octene polymerization with zirconocene/MAO catalyst. The spherical silica supports were impregnated with MAO cocatlyst before polymerization reaction. The supports and catalyst precursors were also characterized to make better understanding about these results.

This thesis was divided into five chapters. Chapter I involved an overview of the use of metallocene catalyst for the polyolefin industry. In Chapter II, knowledge and open literature dealing with metallocene catalysis for olefin polymerization were presented. The literature review was emphasized metallocene catalyst system used for copolymerization of ethylene with α -olefins. The experimental procedure as well as the instrument and techniques used for characterizing the supports, catalyst precursors and resulting polymers were also described in Chapter III.

In the Chapter IV, the results on ethylene and ethylene/1-octene polymerization with various spherical silica supports and impregnation methods were presented. The influences of different particle size of support on the catalytic activity and polymer properties were investigated. Furthermore, the effect of system between homopolymerization and copolymerization cause any change in activity and polymer properties was also discussed. The characteristics of supports and catalyst precursors using N₂ physisorption, X-ray diffraction (XRD), X-ray photoelectron spectroscopy (XPS), Scanning electron microscopy (SEM), Energy-dispersive x-ray spectrometer (EDX), and Thermogravimetric analysis (TGA) and obtained polymer using Differential scanning calorimetry (DSC) and ¹³C-nuclear magnetic resonance (¹³C –NMR) were further investigated.

Finally, conclusions of this work and some recommendations for future research work were provided in Chapter V.

CHAPTER II

LITERATURE REVIEW

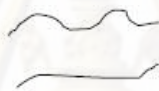
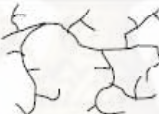

2.1 Background of polyolefin catalyst

Ethylene-based polyolefin polymers and copolymers can be produced either by free radical initiated polymerization or by transition metal catalysis chemistry such as Phillips catalysts, Ziegler-Natta catalysts and metallocene catalysts. One of the most excited discoveries in polymer science and catalysis during the last 40 years is the polymerization of olefins using transition metal-based catalysts. Karl Ziegler was the first to discover that transition metal halides such as TiCl_4 , TiCl_3 , ZrCl_4 and so on, in combination with alkylaluminum compounds convert ethylene to high molecular weight linear polyethylene [Srinivasa Raddy and Sivaram, 1995]. Later, Natta independently discovered stereoregular polymers of α -olefins such as propylene, 1-butene, and styrene. Ziegler and Natta shared the 1963 Nobel Prize for this unique contribution to chemistry and these catalysts have been most widely used because of their broad range application. However, they still occupy a dominant position in LLDPE manufacturing, but they suffer the disadvantage that the comonomer distribution in the polymer is non random as a result of the presence of different active species having different ethylene/ α -olefin reactivity ratios. Because of multiple active sites, copolymers produced with Ziegler-Natta catalyst exhibit broad molecular weight distribution (MWD) and chemical composition distribution (CCD).

The preferred catalysts for LLDPE are those that have a relatively uniform active center distribution, and for this reason, there has been a growing increase in the use of metallocene and related single-center catalysts, which give copolymers with narrow molecular weight and chemical composition distributions [Smit et al., 2006], so metallocene allowed the synthesis of polyolefins with very different properties from those made with Ziegler-Natta catalysts.

Normally, polyethylene is classified to three type according to its density and structure, high density polyethylene (HDPE), low density polyethylene (LDPE) and linear low density polyethylene (LLDPE). The numerous studies show that the global market of LLDPE was increased in very interesting rate about 10 % per annum [Richards, 1998].

Table 2.1 Density range, molecular structure, synthesis, and applications of various type polyethylenes [Richards, 1998]

Type of PE	Density (g/cm ³)	Molecular structure	Synthesis	Common uses
HDPE	0.945-0.965		Polymerization of ethylene on Philips, Ziegler-Natta and metallocene catalyst	Gas pipe, car gas tanks, bottles rope and fertilizer bag
LDPE	0.890-0.940		Free radical polymerization of ethylene at high temperature and high pressure	Packing film, bags, wire, sheathing, pipes, waterproof membrane
LLDPE (VLDPE,ULDPE)*	0.910-0.925		Copolymerization of ethylene with α -olefins on Ziegler-Natta and metallocene catalysts	Shopping bag, stretch wrap, greenhouse film

* A family of LLDPE with density of 0.87-0.915 g/cm³

Summarized characteristic of three type of polyethylene are listed in **Table 2.1**. The different in structure of polymer affects to the physical properties of polymer i.e. density of polymer and hence the application of polymer. HDPE is the polymer that has very less or does not have any branch in the polyethylene backbone. From this microstructure HDPE has very high crystalline phase in polymer morphology and highest density about 0.96 g/cm³. Polyethylenes which have many long and short chains branching formed by radical process are LDPE. The amount of long chain branching (LCB) and short chain branching (SCB) also affect the crystalline and others physical properties too. Normally, long chain branching has the main effect on the polymer viscosity and melt rheology due to the molecular size and shape. On the other hands, short chain branching has the influence to polymer morphology and solid state properties of polyethylene. LLDPE was produced by the

copolymerization of ethylene and α -olefins such as propylene, 1-butene, 1-hexene and 1-octene. Mostly, side chain in LLDPE distributed in short chain branching type by non-uniformly with linear microstructure of backbone polyethylene chain. The properties of LLDPE such as, thermal, physical and mechanical properties depend on the distribution of short chain in the copolymer and polymer microstructure (triad and dyad distribution). Thus, the several LLDPE grades are classified by the primarily result via microstructure of polymer and molecular weight of polymer

2.1.1 Metallocene catalysts

The evolution of single-site catalysts started when Breslow and Natta (1957) combined Cp_2TiCl_2 with alkylaluminum compounds, polymerizing ethylene with low activity and stability. Further studies on the above mentioned titanocene and analogous zirconocene systems demonstrated an enhancement in activity upon addition of water [Severn et al., 2005]. This serendipitous discovery led to a revolution in the early 1980s when Sinn and Kaminsky discovered new catalytic systems based on the combination of metallocene catalysts with methylaluminoxane (MAO), the latter proving to be a much more potent activator for single-site catalysts than traditional alkylaluminum complexes (Figure 2.1). Therefore, MAO plays a crucial part in the catalysis with metallocene. Since that time, homogeneous catalysis of olefin polymerization based on group IV metallocenes has been the subject of intensive research, leading, in recent years, to the development of a broad series of new metallocene complexes.

In comparison with conventional Ziegler-Natta system, metallocene-based catalysts are more attractive since it has many advantages in polymerization such as [Alt and Köppl, 2000]

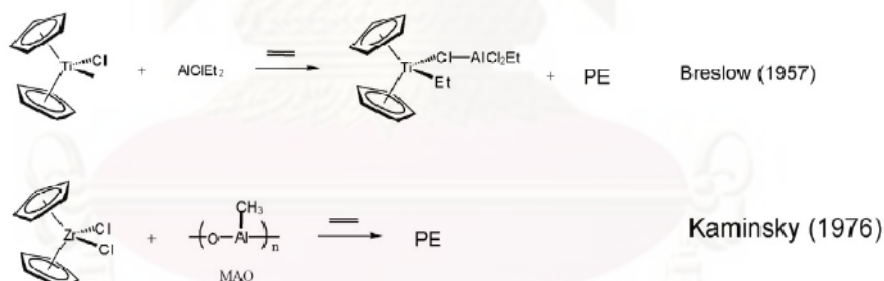
1. The homogeneous nature of these catalysts provides active sites for every molecule in solution and explains their enormous activity. Comparison to conventional Ziegler-Natta catalyst or Philips catalyst, it was found that metallocene complex gave the higher activity about 100 times.

2. Metallocene catalysts offer higher versatility and flexibility both for the synthesis and the control of the structures of polyolefins. For example, metallocene can be tailored to produce polyolefins with special stereoregularity and high degree of tacticity (isotactic, atactic, syndiotactic and hemitactic polypropylene).

3. According to the narrow molecular weight distribution of polymer about 1-2, we can call metallocene catalyst as single site catalysts.

4. Their potential for producing polyolefin with regularly distributed short and long chain branches in the polymer chain. These parameters determine the properties of new materials for applications i.e. LLDPE and thus generate new markets.

5. Heterogeneous catalysts provide different active sites than those in solution and can have an enormous effect on catalyst activity and the properties of the produced polyolefins in terms of molecular weights, branching and stereospecificity.



- Original Breslow catalyst had very low efficiency – academic interest only.
- Cocatalyst breakthrough by Kaminsky started a revolution in research into single-site olefin catalysts.

Figure 2.1 History of metallocene catalyst development

[Chum and Swogger, 2008]

2.1.2 Structure of Metallocene Catalyst

Metallocene catalysts are the organometallic coordination compounds in which one or two π -carbocyclic ligands such as cyclopentadienyl ring, substituted cyclopentadienyl ring, or derivative of cyclopentadienyl ring (such as fluorenyl and indenyl etc.) are bonded to central transition metal atom. The cyclopentadienyl ring of metallocene singly bonded to the ring-metal bond is not centered on any one of the five carbon atoms in the ring but equally on all of them [Gupta et al., 1994]. The typical structure of a metallocene catalyst is represented by Figure 2.2. The cyclopentadienyl ligands, halides and σ -homoleptic hydrocarbyl represent the three classes of ligands of the metallocene catalysts and variation of, and/or substitutions within some of these ligands could result in variation of the catalytic activity, polymer stereoregularity, and average molecular mass. In case of metallocene catalyst, which have only one π -carbocyclic ligand with a hetero atom that is attached to the bridging atom.



Where M = Groups 4B, 5B, or 6B transition metal,

normally group 4B (Ti, Zr and Hf).

A = An optional bridging atom usually Si or C atom.

R = A σ -homoleptic hydrocarbyl such as H, alkyl, or other hydrocarbon groups.

X = chlorine or other halogens from group 7A or an alkyl group.

Figure 2.2 Typical chemical structure of a metallocene catalyst [Gupta et al., 1994]

Single site catalysts can be separated into five main symmetry groups, which influence on the polymer architectures. Compositions and types of metallocene have several varieties. When the two cyclopentadienyl (Cp) rings on either side of the transition metal are unbridged, the metallocene is non-stereorigid and it is characterized by C_{2v} - symmetry. The Cp_2M (M = metal) fragment is bent back with

the centroid-metal-centroid angle θ about 140° due to the interaction with the other two σ bonding ligands. When the Cp rings are bridged (two Cp rings arranged in the chiral array and connected together with chemical bonds by a bridging group), the stereorigid metallocene, called ansa-metallocene, could be characterized by either a C_1 , C_2 or C_s symmetry depending upon the substitutions on two Cp rings and the structure of the bridging unit as schematically illustrated in the Figure 2.3.

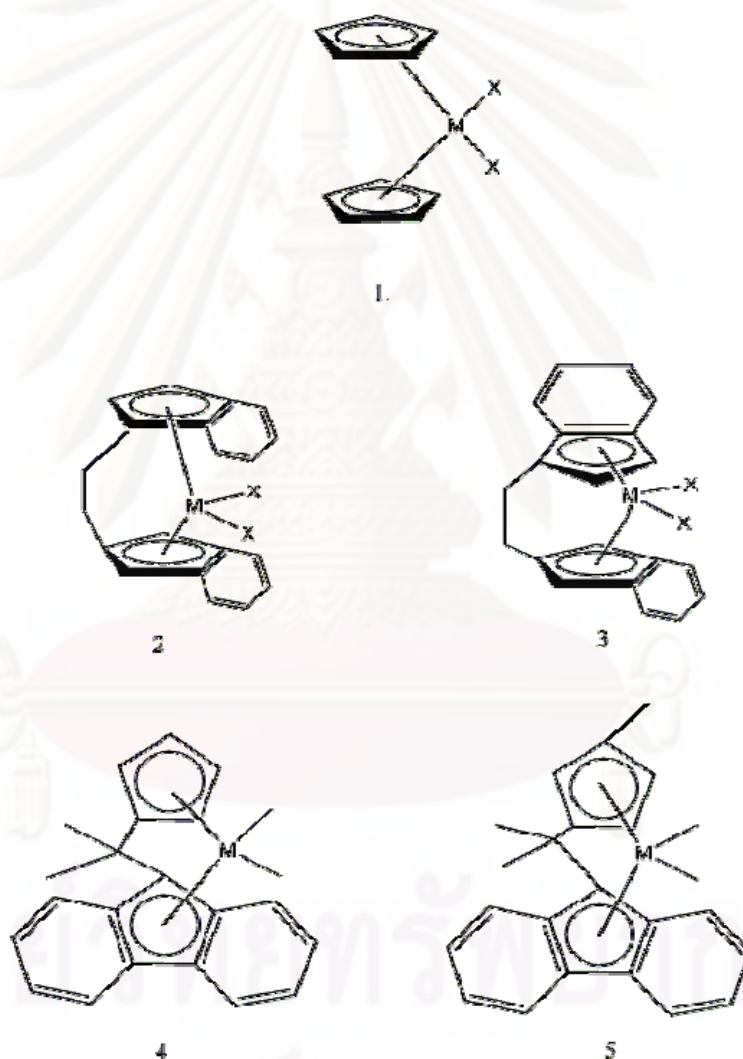


Figure 2.3 Schematic representations of metallocene symmetry (Type 1: C_{2v} -symmetric, Type 2: C_2 -Symmetric, Type 3 and Type 4: C_s -symmetric, Type 5: C_1 -symmetric) (*C*, italic. It is better to draw all the structures in a similar way) [Gupta et al., 1994]

2.1.3 Cocatalyst

MAO is the most important cocatalyst which activates the group 4B metallocenes in homogeneous Ziegler-Natta polymerization. Methylaluminoxane is a compound in which aluminum and oxygen atoms are arranged alternately and free valences are saturated by methyl substituents [Kaminsky and Laban, 2001]. Before the discovery of the MAO cocatalyst, the homogeneous Ziegler-Natta catalyst Cp_2TiCl_2 was activated with alkylaluminum chloride which led to poor catalyst activity. The use of MAO cocatalyst raised the catalyst activity by several orders of magnitude. There are some other alumoxanes which can also activate the metallocenes, such as ethylalumoxane (EAO), isobutylalumoxane (iBAO) and modified methylaluminoxane was employed to use as cocatalyst too, but MAO is much more effective than its ethyl and isobutyl analogues and is most preferred in practice [Huang and Rempel, 1995]. (Structure of MAO, EAO, iBAO and MMAO was shown in Figure 2.4)

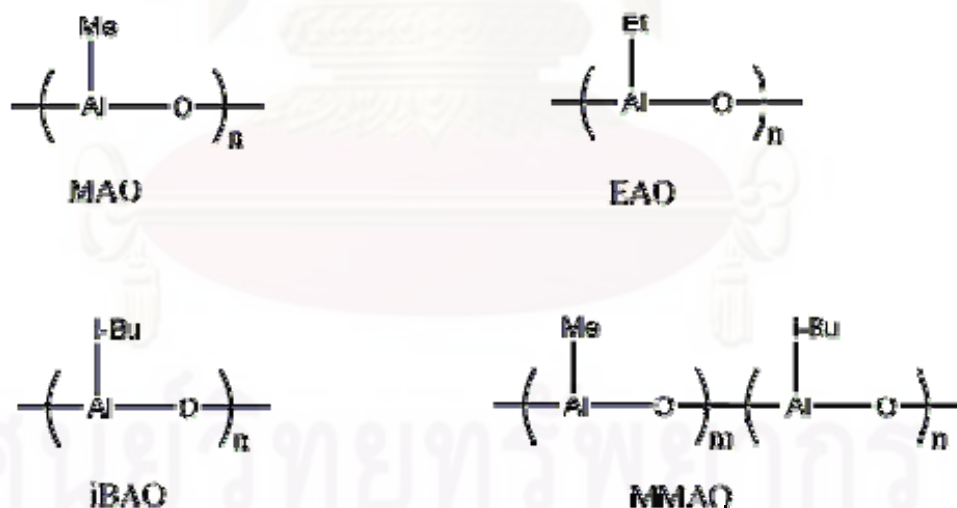


Figure 2.4 Several kinds of cocatalysts [Pasykiewicz, 1990]

Methylaluminoxane (MAO) is mostly used and synthesized by controlled hydrolysis of trimethyl aluminium. Several structures have been proposed for MAO: ring, clathrates and linear or branched chains [Soga and Shiono, 1997]. The structure of MAO is complex and might depend upon the synthesis conditions,

isolation methods, solvent used etc. In addition to uncertainty about the composition of MAO itself, the structure of MAO is further complicated by the presence of variable amounts of unreacted trimethylaluminum (TMA). More recently, Sinn *et al.* have reported that the MAO has crystalline structure as shown in Figure 2.5 which contains an unreacted TMA inside the ball. According to several reports, the role of MAO is generally proposed to be methylating agent for the generation of transition metal-alkyl adducts, a Lewis acid for anion abstraction from the complex generating an active cationic complex, and an impurity scavenger, particularly water in the olefin and solvent [Ciardelli *et al.*, 1998]. There are possible additional roles for MAO that reflect the large amount of it required for high activity and selectivity. The metallocene is probably surrounded by MAO even in the outer-sphere and thus prevents catalyst deactivation by bimolecular processes between two metallocenes, thus stabilizing the system [Huang and Rempel, 1995; Kaminsky and Arndt, 1997]. The activation steps of MAO cocatalyst are shown in Figure 2.6.

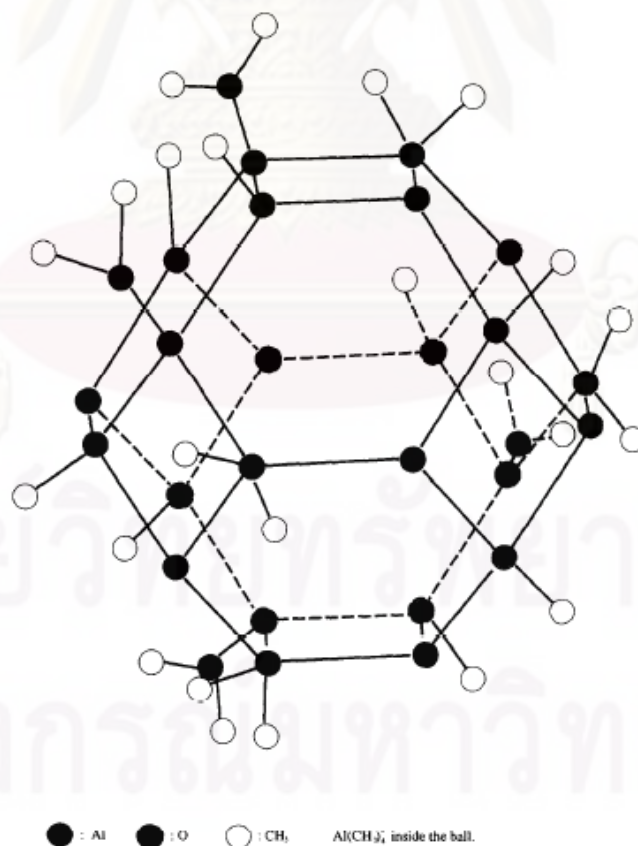
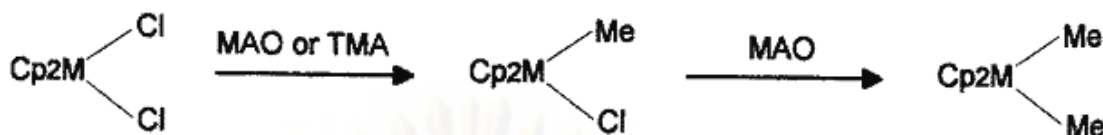


Figure 2.5 Structure of MAO proposed by Sinn *et al.* [Soga and Shiono, 1997].



MAO is the alkylation of halogenated metallocene complexes.



The MAO complex can seize a methyl anion, Cl^- anion or OR^- anion from the metallocene forming an AlL_4^- anion, and there is cationic $\text{L}_2\text{M}(\text{CH}_3)^+$ is the active center.

Figure 2.6 The activation step of MAO cocatalyst [Kaminsky and Arndt, 1997]

Cam and Giannini (1992) investigated the role of TMA present in MAO by a direct analysis of $\text{Cp}_2\text{ZrCl}_2/\text{MAO}$ solution in toluene- d_8 using $^1\text{H-NMR}$. They monitored the reaction at room temperature by slowly adding solid MAO into the toluene- d_8 solution of Cp_2ZrCl_2 . Their observation indicated that Cp_2ZrCl_2 is monoalkylated to give $\text{Cp}_2\text{Zr}(\text{Me})\text{Cl}$ by TMA contained in MAO and that the Cl of the resulting $\text{Cp}_2\text{Zr}(\text{Me})\text{Cl}$ is removed by MAO to form an active cation. However, in general it is believed that MAO is the key cocatalyst in polymerizations involving metallocene catalysts. The role of MAO included 1) alkylation of metallocene, thus forming catalyst active species, 2) scavenging impurities, 3) stabilizing the cationic center by ion-pair interaction and 4) preventing bimetallic deactivation of the active species [Cam and Gannini, 1992].

On the other hand, Tritto investigated the reactions of $\text{Cp}_2\text{Zr}(\text{Me})\text{Cl}$ and $\text{Cp}_2\text{Ti}(\text{Me})_2$ with TMA and MAO [Tritto et al., 1994]. The observation of the reaction between $\text{Cp}_2\text{Zr}(\text{Me})\text{Cl}$ and TMA by NMR revealed that the occurrence of the following equilibria and that complexation of TMA to $\text{Cp}_2\text{Zr}(\text{Me})\text{Cl}$ is very fast while the further methylation to Cp_2TiMe_2 is slow. However, the NMR spectra of the

reaction of $\text{Cp}_2\text{Ti}(\text{Me})\text{Cl}$ and MAO (containing 2% of TMA) indicated that $\text{Cp}_2\text{Ti}(\text{Me})\text{Cl}$ reacts rapidly with MAO to give Cp_2TiMe_2 . From these results together with some additional observations, the authors came to the conclusions that MAO is a better alkylating reagent of $\text{Cp}_2\text{Ti}(\text{Me})\text{Cl}$.

Hagimoto et al. (2004) have investigated the additive effect of trialkylaluminiums in the living polymerization of propylene proceeded by $[\text{ArN}(\text{CH}_2)_3\text{NAr}]\text{TiMe}_2$ MMAO/SiO₂ catalyst system by adding a similar amount of trialkylaluminiums present in MMAO. It was found that the activity and the molecular weight values in the presence of trialkylaluminiums were slightly smaller than that of the corresponding MMAO/SiO₂ system due to the induction period, AlMe_3 gave a longer induction period than $\text{Al}(i\text{Bu})_3$. Because of a small amount of trialkylaluminium hindered the initiation reaction [Hagimoto et al., 2004].

In the investigation of preparing condition of SiO₂ supported Cp_2ZrCl_2 catalyst on ethylene polymerization [Marques and Conte, 2002]. It was found that zirconocene content fixed on silica support was slightly lower when the support was pretreated with MAO but the increase on MAO concentration on pretreatment of silica promoted an enhancement of the catalytic activity. These results indicate that, even decreasing the amount of Zr fixed on the support, the presence of MAO seems to stabilize the active center and preserve the catalytic activity. Moreover the treatment used TMA instead of MAO in the support pretreatment exhibited amount of zirconium on the support treated with TMA was lower than that when MAO was first fixed. The catalyst activity was also lower, indicating that MAO acts to capture and stabilize Cp_2ZrCl_2 molecules.

2.1.4 Polymerization mechanism

The mechanism of catalyst activation is not clearly understood. However, alkylation and reduction of the metal site by a cocatalyst (generally alkyl aluminum or alkyl aluminoxane) is believed to generate the cationic active catalyst species.

First, in the polymerization, the initial mechanism started with formation of cationic species catalyst that is shown below.

Initiation



Propagation proceeds by coordination and insertion of new monomer unit in the metal carbon bond. Cossee mechanism is still one of the most generally accepted polymerization mechanism (Figure 2.7) [Castonguay and Rappe, 1992]. In the first step, monomer forms a complex with the vacant coordination site at the active catalyst center. Then through a four-centered transition state, bond between monomer and metal center and between monomer and polymer chain are formed, increasing the length of the polymer chain by one monomer unit and generating another vacant site.

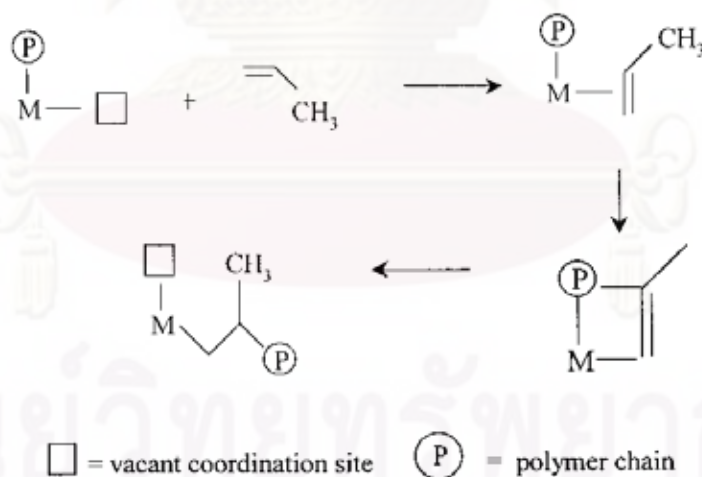


Figure 2.7 Cossee mechanism for Ziegler-Natta olefin polymerization
[Castonguay and Rappe, 1992]

The trigger mechanism (Figure 2.8) has been proposed for the polymerization of α -olefin with Ziegler-Natta catalysts [Kaminsky and Laban, 2001].

In this mechanism, two monomers interact with one active catalytic center in the transition state. A second monomer is required to form a new complex with the existing catalyst-monomer complex, thus trigger a chain propagation step. No vacant site is involved in this model. The trigger mechanism has been used to explain the rate enhancement effect observed when ethylene is copolymerized with α -olefins.

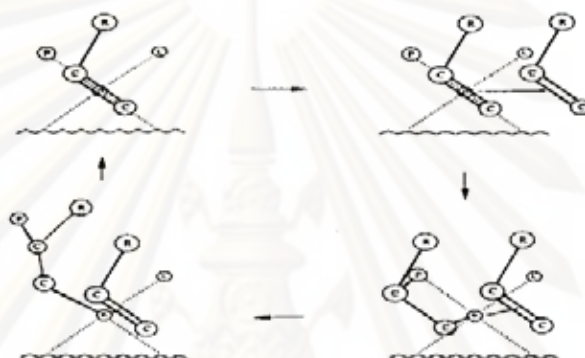


Figure 2.8 The propagation step according to the trigger mechanism
[Kaminsky and Laban, 2001]

After that, the propagation mechanism in polymerization shown in Figure 2.9

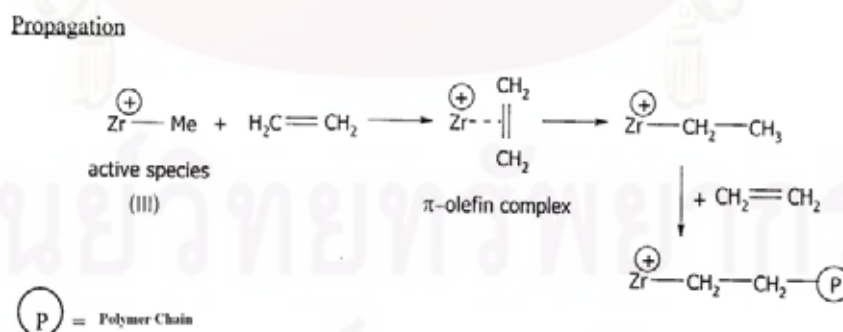


Figure 2.9 Propagation mechanism in polymerization [Kaminsky and Laban, 2001]

Finally, the termination of polymer chains can be formed by 1) chain transfer via β -H elimination, 2) chain transfer via β -Me elimination, 3) chain transfer to aluminum, 4) chain transfer to monomer, and 5) chain transfer to hydrogen (Figure 2.10-2.14) [Gupta et al., 1994]. The first two transfer reactions form the polymer chains containing terminal double bonds.

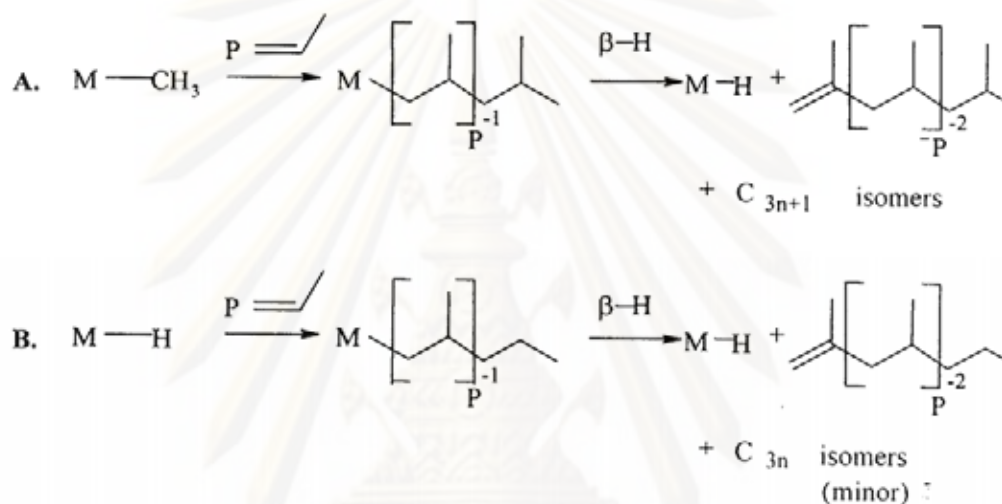


Figure 2.10 Chain transfer via β -H elimination [Gupta et al., 1994]

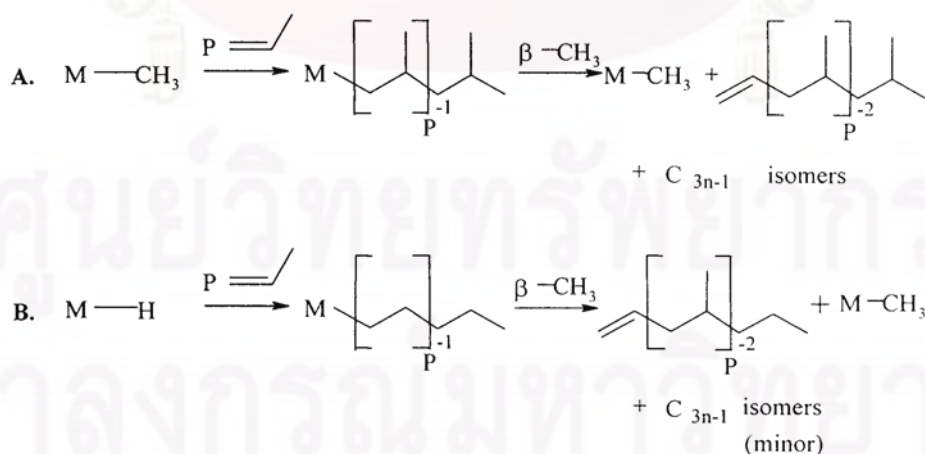


Figure 2.11 Chain transfer via β -CH₃ elimination [Gupta et al., 1994]

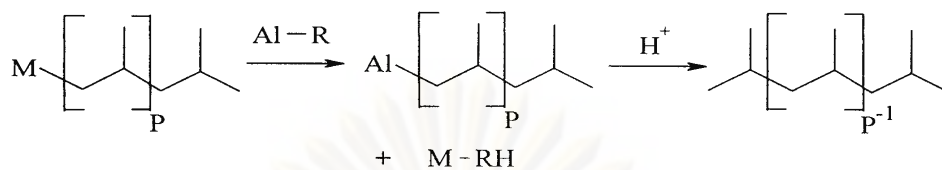


Figure 2.12 Chain transfer to aluminum [Gupta et al., 1994]

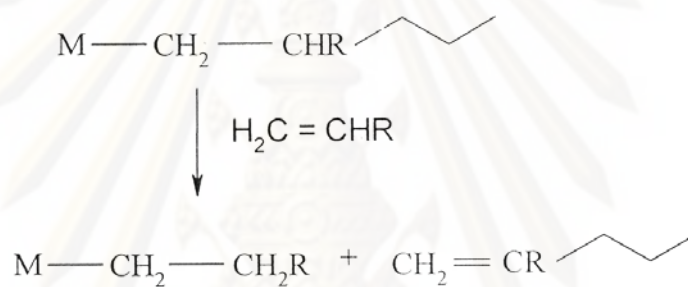


Figure 2.13 Chain transfer to monomer [Gupta et al., 1994]

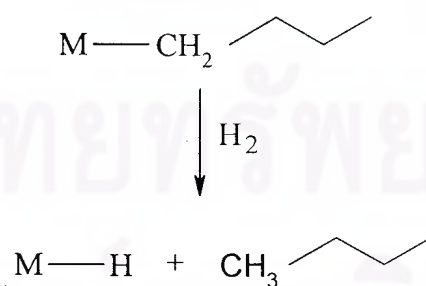


Figure 2.14 Chain transfer to hydrogen [Gupta et al., 1994]

2.1.5 Copolymerization

Metallocenes are highly useful for the copolymerization of ethane with other olefins. Propene, 1-butene, 1-pentene, 1-hexene, and 1-octene have been studied as comonomers, forming linear low density polyethylene (LLDPE). These copolymers have a great industrial potential and show a higher growth rate than the homopolymer. Due to the short branching from the incorporated α -olefin, the copolymers show a lower melting point, lower crystallinity, and a lower density, making films more flexible and more processible. Applications of the copolymers can be found in packaging, in shrink films with a low steam permeation, in elastic films using high comonomer concentration, in cable coatings in the medical field because of the low amount of extractables, and in foams, elastic fibers, adhesives, etc [Kaminsky and Arndt, 1997].

Under the same conditions, syndiospecific (C_s -symmetric) metallocenes are more effective for inserting α -olefins into an ethene-copolymer than isospecific working (C_2 -symmetric) metallocenes, or unbridged metallocenes.

On the other hand, enhancement of ethylene polymerization rate by α -olefin (comonomer) is a well-known phenomenon of considerable technological and scientist interest, called “comonomer effect”. Several possible causes had been proposed to explain this fact, but the most supported is the easier monomer diffusion due to crystallinity reduction of the polymer envelope when a small amount of comonomer is added. In ethylene homopolymerization, the monomer diffusion is very slow through the highly crystalline polymer formed around the catalyst particle until sufficient polymer has formed to allow particle fragmentation. The comonomer addition leads to less crystalline polymer formation, which makes the diffusion of ethylene easier, and thus favors extended particle fragmentation.

Monomer mass-transfer limitations can also contribute compositional heterogeneity in the copolymer (broad CCD), even with metallocene catalysts. Fink ascribed the compositional distribution of ethylene/1-hexene copolymers prepared

with a SiO_2 / methylaluminoxane (MAO) / zirconocene system to the formation, during the initial stages of polymerization, of a copolymer envelope around the catalyst particle [Przbyla et al., 1999]. The easier diffusion of the smaller monomer, ethylene, with respect to 1-hexene was proposed to lead to a polymer particle comprising an ethylene-rich center surrounded by an outer layer of the copolymer, thus giving a broad overall chemical composition distribution. The term “**filter effect**” was coined to describe this phenomenon.

Comonomer activation is less common in propylene polymerization, but Jüngling (1997) observed a threefold increase in activity when adding a small quantity of 1-octene to propylene polymerization catalyzed by a SiO_2 -supported metallocene and concluded that this was due to improved monomer mass transfer in the growing polymer particle [Jüngling et al., 1997].

The catalytic system $(n\text{BuCp})_2\text{ZrCl}_2/\text{MAO}$ immobilized over $\text{SiO}_2\text{-Al}_2\text{O}_3$ has been tested in ethylene/1-hexenecopolymerizations using different amounts of comonomer. Increasing in 1-hexene concentration, the catalytic activity increases reaching maximum values at 0.194 mol/L since larger amounts of 1-hexene lead to a decrease in activity. The average molecular weights of ethylene/1-hexene copolymers are lower than the one corresponding to the homopolymer because the comonomer promotes chain termination [Grieken et al., 2007].

Smit et al. (2006) investigated the particle fragmentation and growth characteristics, and molecular composition of ethylene homopolymers and copolymers, using MAO/[rac-Et(Ind) $_2$ ZrCl $_2$] catalyst on silica support [Smit et al., 2006]. Diffusion limitations can result in a broadening of the polymer molecular weight distribution and chemical composition distribution. Catalyst/support fragmentation during polymer particle growth is greatly accelerated by the presence of 1-hexene. The copolymer composition broadens with increasing polymerization time as a result of the gradual formation of an ethylene-rich fraction in addition to the main copolymer fraction, support Fink’s filter model.

The effect of 1-octene prepolymerization on the propene polymerization profile, used SiO₂-supported metallocene catalytic system, was investigated by Fink [Fink et al., 2000]. As illustrated in Figure 2.15, the amorphous poly(1-octene) layer on the particle which is generated by a prepolymerization of 1-octene causes a less significant diffusion limitation for the monomer gas compared to the one induced by a highly crystalline polypropene layer.

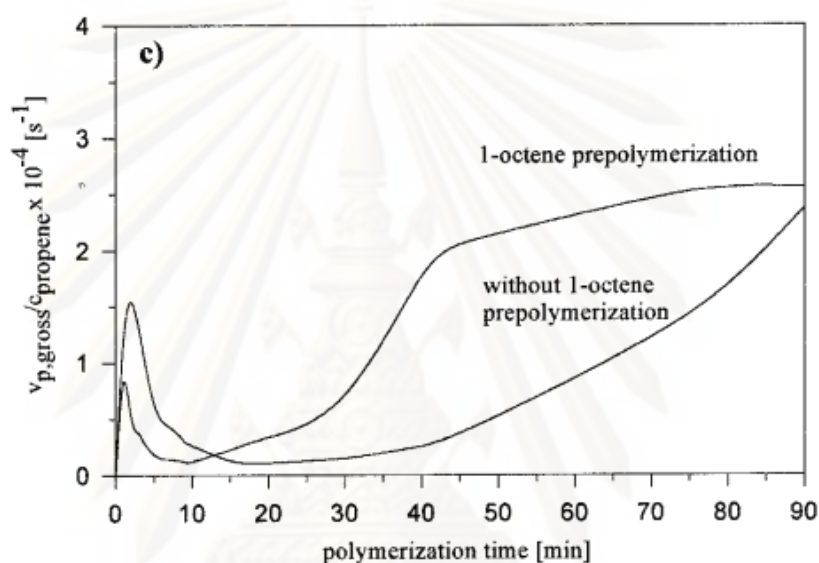


Figure 2.15 Propylene polymerization profile shows the comparison of activity profile between 1-octene prepolymerized catalyst and untreated system [Fink et al., 2000]

2.2 Supported metallocene catalysts

However, despite their numerous advantage of homogeneous catalyst, those systems still present disadvantages in regard to 1) their inability to be used in industrial application in polyolefin slurry or gas-phase processes because ill-defined morphologies of produced polymer cause reactor fouling and 2) the very large amount of methylaluminoxane needed to achieve maximum metallocene catalytic activity. One approach to overcome this problem is the immobilization of such catalyst system (metallocene/MAO) by physically or chemically supporting them on the surface of solid carrier. It is important to find a way to attach the metallocene to the support

without losing the performances of homogeneous catalyst (high catalytic activity, stereochemical control, ability to produce copolymers with statistical comonomer distribution, etc.) while improving the morphology of the polymers in order to meet the requirements for industrial applications. The development of supported metallocenes will enable their use in gas- and slurry-phase processes and prevent reactor-fouling problems [Ribeiro et al., 1997].

In general, when a metallocene catalyst is supported, its activity decreases because of steric hindrance around the active site caused by the large support surface, deactivation of catalytic sites, or inefficient production of active sites during the supporting process [Chu et al., 2000]. The nature of the support and the technique used for supporting metallocene have a crucial influence on catalytic activity and polymer properties. Inorganic oxides or other high surface area material have been employed as supports. The most commonly employed inorganic supports are silica (SiO_2), alumina (Al_2O_3), and magnesium chloride (MgCl_2). There are three basic methods of supporting aluminoxane-activated single-site catalyst as follow:

1. Supporting the aluminoxane first, and then reacting the aluminoxane-treated support with metallocene.
2. Supporting the metallocene first, and then reacting the metallocene-treated support with the aluminoxane.
3. Contacting the aluminoxane and the metallocene in solution before supporting and then adding this solution to the support.

The last method has advantages over the other two: it maximizes the number of active centers by activating the metallocene in solution, reduces the preparation time, and lowers solvent required for supporting [Hlatky, 2000]. On the other side, it was suggested that the cocatalyst should be first impregnated on the support and zirconocene was then injected into the solution in order to maintain high catalytic activity for the system [Jongsomjit et al., 2005].

The activity of silica-supported $\text{Et}(\text{Ind})_2\text{ZrCl}_2/\text{MAO}$ catalyst, produce ethylene copolymers, was affected by in situ- and ex situ- immobilized catalytic system

[Jongsomjit et al., 2004]. From this studied, it was observed that the MAO/SiO₂ in situ-immobilized catalytic system exhibited much higher activities for ethylene copolymerization than the ex situ one due to more active catalytic species present and molecular weight of copolymers produced from in situ catalytic system seemed to be low. Among α -olefin, ethylene/1-hexene copolymerization under both systems showed the highest activities due to shorter chain insertion preference.

2.2.1 Catalyst Chemistry

The nature of the active sites affects the polymer morphology, catalyst stability and activity, and the characteristics of the polymer produced. However, structure and chemistry of the active sites in supported catalysts are not clearly understood. Catalytic activities for supported metallocene are usually much lower than that of their counterpart homogeneous system. Formation of different active species, deactivation of catalyst during supporting procedure, and mass transfer resistance may contribute to decreased catalyst activity.

Tait et al. (1996) reported general effects of support type, treatment, supporting procedure, and type of diluents on reaction kinetics and physical properties of polymer produced. Although the activities of supported catalysts are much lower compared to homogeneous systems. The activity of catalysts increased slightly when o-dichlorobenzene was introduced in toluene [Tait et al., 1996].

The catalytic activities of supported catalyst depended on the percentage of the incorporated metallocene was reported [Quijada et al., 1997]. However, in the case of metallocenes supported on MAO pretreated silica, depending on how the surface bound MAO complex with the catalyst, the activity can be as high as that of homogeneous system. According to the experiment by Chein et al. (1995), if a single MAO is attached to silica, it would complex with zirconocene and lowers its activity [Chein et al., 1995]. On the other hand, if multiple MAOs are attached to the surface silanol, the supported zirconocene will not be further complexed with MAO and have activity.

2.2.2 Supporting Catalyst on Materials Treated with Alkylaluminum

When silica is pretreated with MAO, the supporting mechanism is different. The zirconocene is complexed to MAO supported on silica, which will make the catalyst similarly to a homogeneous system. The polymers produced in this way have lower molecular weights.

Hlatky and Upton [Hlatky and Upton, 1996] reported that supporting of the aluminum-alkyl free catalysts can form 2 complexes as shown in Figure 2.16, (a) deactivation through coordination of Lewis-basic surface oxides to the electrophilic metal center or (b) reaction of the ionic complex with residual surface hydroxyl groups.

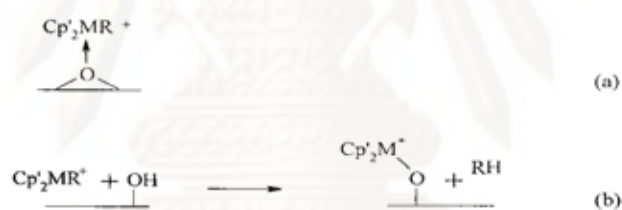


Figure 2.16 Effect of surface hydroxyl groups on ionic metallocene catalysts [Hlatky and Upton, 1996]

However, highly active supported ionic metallocene catalysts for olefin polymerization can be prepared by pretreating the support with scavenger. It is assumed that pretreatment of the support with a scavenger serves to activate the support and compatibilize it with the ionic metallocene complex.

Lee et al. used TMA pretreated-silica as the support for metallocene catalysts. The activity of supported catalysts showed dependency to H_2O content in silica, H_2O/TMA ratio, metallocene, and cocatalyst. The supported catalyst was also

able to polymerize ethylene in the absence of MAO when common alkyl aluminum was used as the cocatalyst [Lee et al., 1995].

The surface aluminum and metallocene loading was studied [Santos et al., 1997]. About 7 wt% of MAO can be supported on silica when the initial amount of MAO in mixture of silica was ca. 10 wt%. Depending on silica types, saturation of MAO supported on silica can occur at lower MAO contents.

Harrison et al. (1998) compared a variety of silica and alumina supports with different degrees of surface hydroxylation as the supports. It was shown that as the concentration of OH groups on the surface of the support increased, more MAO could be impregnated and thus catalyst with more metallocene content could be produced. The most obvious benefit of supported catalyst with more metallocene was increased activities compared to catalysts with lower concentration of surface hydroxyl groups (increased activities both in kg PE/mol Zr/hr and kg PE /g-support/h). However, at high polymerization temperatures, leaching of catalyst from the support was observed. In lower polymerization temperatures, leaching was less significant, however, the morphology and bulk density of the polymer formed were still unsuitable for use in gas-phase polymerization [Harrison et al., 1998].

For the case of propylene polymerization, a decrease in syndiotacticity was observed [Xu et al., 1998] when the metallocene catalyst was supported on pretreated silica.

2.2.3 Silica-supported catalytic system

Silica has been used as a support for α -olefin polymerization catalysts since the late 1950s. Although it is often referred to as an “inert” support, it is far from the “innocent bystander” that the term implies. In fact, it is one of the crucial components in a considerable number of heterogeneous single-site polymerization catalyst systems. Therefore, a deeper understanding of properties of the silica supports is important in making a good industrial catalyst. The key properties, which have a

major influence on a heterogeneous single-site polyolefin catalyst, are chemical composition [Severn and Chadwick, 2008]:

- Surface chemistry
- Particle size
- Particle morphology
- Physical properties (surface area, porosity)
- Attrition/mechanical properties

Amorphous and porous silica at present constitute the best support for metallocenes and MAO as cocatalyst because they possess a high surface area and porosity, have good mechanical properties, are stable and inert under reaction condition, and lead to good morphological features for polymer particles [Fink et al., 2000]. The unique characteristics of metallocene systems, combined with those of silica, facilitate the formation of uniform polymer particles with narrow particle size distributions and high bulk densities [Duchateau, 2002].

The effect of different catalyst particle diameter on the kinetics of propene polymerization which is promoted by SiO₂-supported metallocene catalyst has been reported in the review of Fink and coworker [Fink et al., 2000]. It was found that larger catalyst particle exhibited lower activity due to the longer induction period takes and the slower the reaction velocity increases as shown in Figure 2.17(a). They also observed that the increasing polymerization temperature lead to a rise of the total activity of catalyst system and a shift of the maximum activity to shorter reaction time (Figure 2.17(b)). This gain in activity leads to an increase of the velocity with which the individual stages of polymerization are passed.

Hagimoto et al. (2004) were investigated the relationship between the supporting effects of MMAO and compared the effects of supported MMAOs using alumina (Al₂O₃), magnesia (MgO) and silica gel (SiO₂) in propylene polymerization with [ArN(CH₂)₃NAr]TiMe₂. They found that propagation rate (k_p) value and the MWD value strongly depended on the metal oxide employed as a support [Hagimoto

et al., 2004]. (k_p : $\text{SiO}_2 > \text{Al}_2\text{O}_3 > \text{MgO} \approx$ homogeneous, MWD: $\text{MgO} > \text{Al}_2\text{O}_3 > \text{SiO}_2 >$ homogeneous)

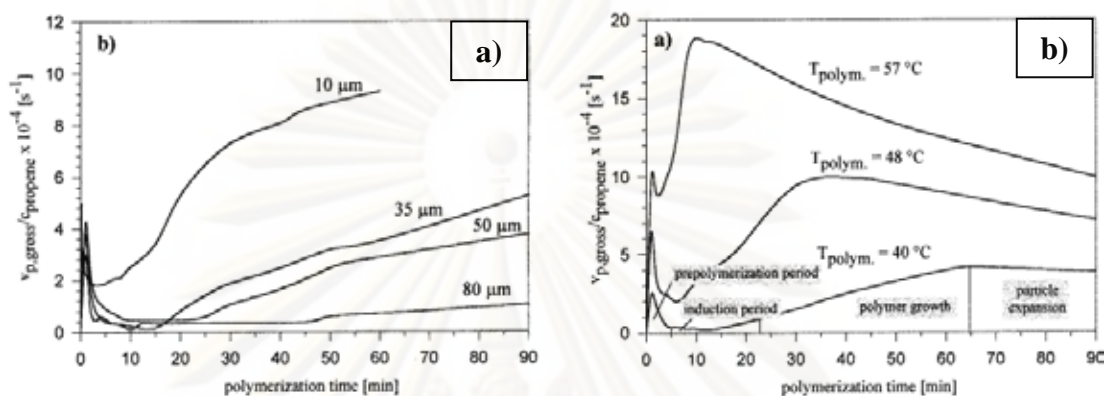


Figure 2.17 Propene polymerization profiles of a silica supported metallocene/MAO catalyst prepared by suspension impregnation [Fink et al., 2000]:

- (a) depending on particle size and polymerization time
- (b) depending on polymerization time and polymerization temperature.

Collins et al. reported that $\text{Et}(\text{Ind})_2\text{ZrCl}_2$, when supported on partially dehydrated silica, reacted with surface hydroxyl groups during adsorption to form inactive catalyst precursors and free ligands (Figure 2.18). Therefore, the activity is lower compared to the case of using dehydrated silica [Collins et al., 1992]. Figure 2.19 shows the proposed structure $\text{Et}(\text{Ind})_2\text{ZrCl}_2$ supported on alumina. For the case of alumina, the activity of catalyst supported on dehydrated alumina is lower than the one supported on partially dehydrated alumina. The high Lewis acidity of aluminum sites on dehydrated alumina facilitates the formation of Al-Cl bonds and Zr-O bonded species when the metallocene compound is adsorbed on these sites. However, the metal sites in this case remain inactive even after MAO addition.

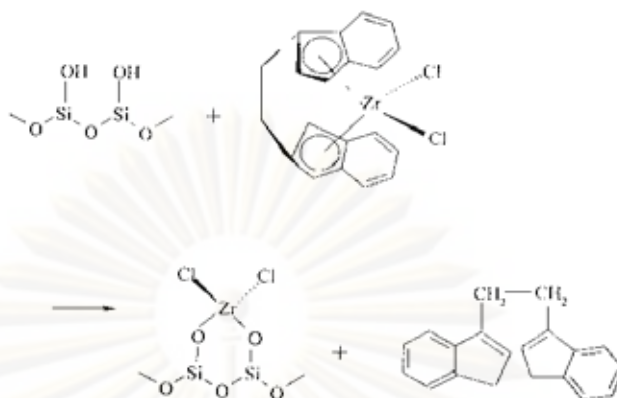


Figure 2.18 Structure of Et(Ind)₂ZrCl₂ supported on silica [Collins et al., 1992]

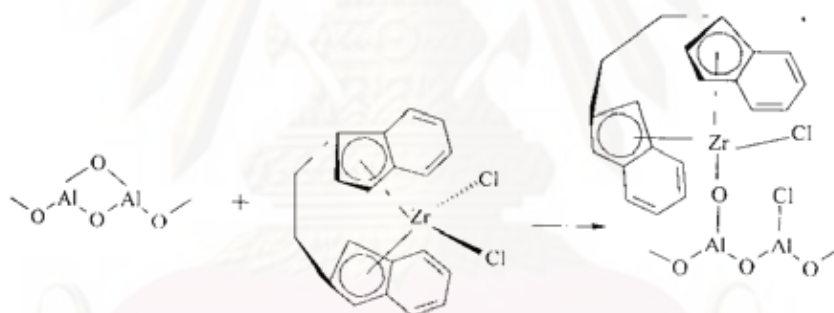


Figure 2.19 Structure of Et(Ind)₂ZrCl₂ supported on alumina [Collins et al., 1992]

It is known that nature of the support play important roles on catalytic activity and on the properties of polymers produced with supported metallocene. In the more recently work, the effect of different support types (commercial silica and silica-alumina, MCM-41, and SBA-15) on the microstructure of ethylene/1-hexene copolymers made with supported metallocene catalysts has been investigated through the analysis of MW and CCD using high temperature GPC and Crystaf. From this studied, it was observed that the copolymer samples obtained using commercial carriers (silica and silica-alumina) had narrow and unimodal chemical composition distributions, whereas MCM-41 and SBA-15 were used, MWD is still narrow but CCD can also become broad and bimodal with increasing 1-hexene content. This may

be related to the presence of two catalyst site type on the surface of support. Lower Crystaf temperature peaks (polymer populations with higher 1-hexene fractions) became more prominent with decreasing Si/Al ratio in MCM-41, and larger pore sizes of SBA-15 seemed to favour 1-hexene incorporation slightly [Paredes et al., 2007].

Zheng and coworker investigated the polymer particle growth in the early stages of olefin polymerization using metallocene /MAO/silica catalyst system. EDX analysis has been used to characterize the aluminum distribution in various MAO-impregnated supports, revealing that the homogeneity of the distribution is dependent on both calcinations temperature and the impregnation condition used. SEM studies of the polymer morphology and the fragmentation of the support reveal two kinds of fragmentation behaviors: a layer-by-layer fragmentation of the support in ethylene polymerization using a homogeneously immobilized catalyst, and main polymerization at the surface with instantaneous coarse fragmentation at the core of the support particles in the case of propylene polymerization and a heterogeneous (co)catalyst distribution [Zheng et al., 2005].

Similar to above studied, Zheng and Loos focus on the key parameters that affect the catalyst fragmentation and polymer particle morphology [Zheng and Loos, 2006]. Olefin homo- and copolymerizations were carried out in slurry by using $MgCl_2$ supported Ziegler Natta catalysts or silica supported metallocene/MAO catalysts under mild conditions. The active sites distribution on the catalyst particle is a prerequisite condition for a homogeneous fragmentation and good polymer morphology. For similar polymerization conditions, the porosity of the catalyst particle influence the way the catalyst fragment. Polymerization with less porous particles tends to take place only at the exterior of particle and then typical layer-by-layer fragmentation occurred, because the catalyst fragmentation starts at the outer surface of the particle and break-up gradually continues to the center. In contrast, the highly porous catalyst particles have large pores, therefore, the monomer diffuses easily into the pores of the catalyst particles and polymerization happens at the entire supported catalyst particle results in instantaneous fragmentation. The catalyst's

break-up progress is retarded in copolymerization, as the result of the high mobility of copolymer molecules.

In this study, it is focused on the morphology of polymer growth. It is important to have some understanding of how the catalyst particle produces a polymer particle, and also how that polymer particle grows. Ideally, a single catalyst particle of a certain shape should result in a single polymer particle of the same shape. As the polymerization proceeds, the initial catalyst support becomes fragmented and dispersed within the growing polymer matrix (Figure 2.20). When the supports are broken into irregular subparticles, the catalyst particle does not lose its overall integrity because the individual fragments are held together by the polymer formed. The morphology of the starting support is replicated in the final polymer, so that spherical supports will give spherical polymer morphology with increased particle size, dependent on the catalyst productivity [Zheng et al., 2005; Severn and Chadwick, 2008].

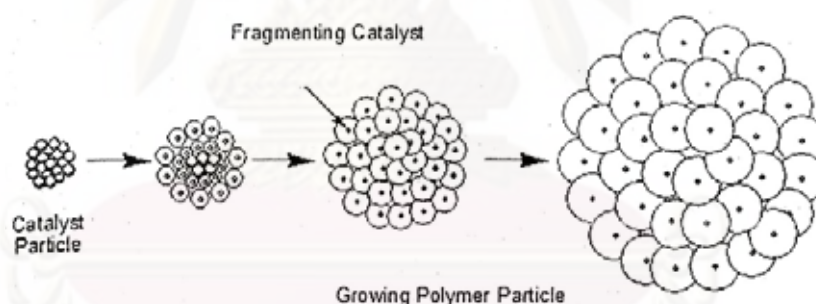


Figure 2.20 Schematic representation of a model for the growth of a single polymer particle [Severn and Chadwick, 2008]

The electron microscopic studies of polymer morphology and the fragmentation of the support lead to the clarification of the chronological course of a propene polymerization on SiO_2 -supported metallocene catalysts as shown in Figure 2.21 [Fink et al., 2000]. The polypropene growth on SiO_2 -supported metallocene catalysts can be described by a “**particle growth model**” which was developed by Fink et al.. From the schematic of particle growth model in Figure 2.21, the polymerization process can be divided into four different sections. The reaction starts with a short increase in activity, the “prepolymerization period”. During this stage the

polymer forms a regular thin layer around the particle, which partially continues to grow into the marginal areas of the support. After this, the layer of highly crystalline polypropene serves as a diffusion barrier for following propene and induces the “induction period” of very low activity. When enough monomer molecules have reached the inner polymerization active centers by diffusion through the polymer coating the third section starts. The polymerization rate rises again (“polymer growth”) and the polymer growth from the outside to the inside continues accompanied by a slowly beginning fragmentation of the support, produces new active centers. Finally, a plateau of maximum activity is reached (“particle expansion”) and the whole support is fragmented in the polymer [Fink et al., 2001].

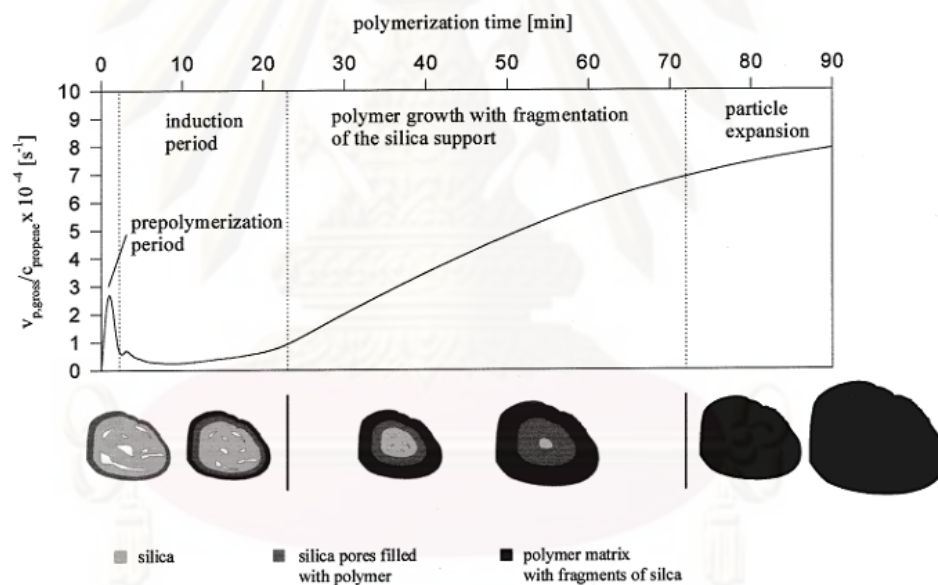


Figure 2.21 Schematic particle growth model for the propene polymerization of a silica-supported metallocene/MAO catalyst [Fink et al., 2001]

CHAPTER III

EXPERIMENTAL

3.1 Objectives of the Thesis

1. To investigate the effect of various sizes of spherical silica-supported metallocene catalyst for ethylene polymerization and ethylene/1-octene copolymerization regarding catalytic activities and polymer characteristics.
2. To compare the MAO impregnation methods between conventional ex situ and alternative in situ impregnation method.

3.2 Scopes of the Thesis

1. Preparation of spherical silica with different particle sizes that is submicron, 3, 5 and 10 μm .
2. Preparation of catalyst precursors by impregnation of silica support with Methylaluminoxane (MAO).
3. Characterization of spherical silica supports and catalyst precursors using N_2 physisorption, scanning electron microscopy (SEM), energy dispersive X-ray spectroscopy (EDX), X-ray diffraction (XRD), X-ray photoelectron spectroscopy (XPS) and thermal gravimetric analysis (TGA).
4. Polymerization reaction of ethylene and ethylene/1-octene via different sizes of spherical silica-supported metallocene catalyst at $T = 70^\circ\text{C}$, $P = 50$ psi, $[\text{Zr}]_{\text{cat}} = 5 \times 10^{-5}$ M, $[\text{Al}]_{\text{MAO}}/[\text{Zr}]_{\text{cat}} = 1135$ and $[\text{Al}]_{\text{TMA}}/[\text{Zr}]_{\text{cat}} = 2500$.
5. Study the effects of MAO impregnation method on catalytic and polymer properties during polymerization.
6. Study the effect of particle diameter of silica support on catalytic activity and copolymer properties characterized by scanning electron microscopy (SEM), differential scanning calorimetry (DSC), X-ray diffraction (XRD) and ^{13}C nuclear magnetic resonance (^{13}C NMR).

3.3 Research Methodology

The flow diagram of research methodology is show in **Figure 3.1** that is all reactions were conducted under argon atmosphere using Schlenk techniques and glove box.

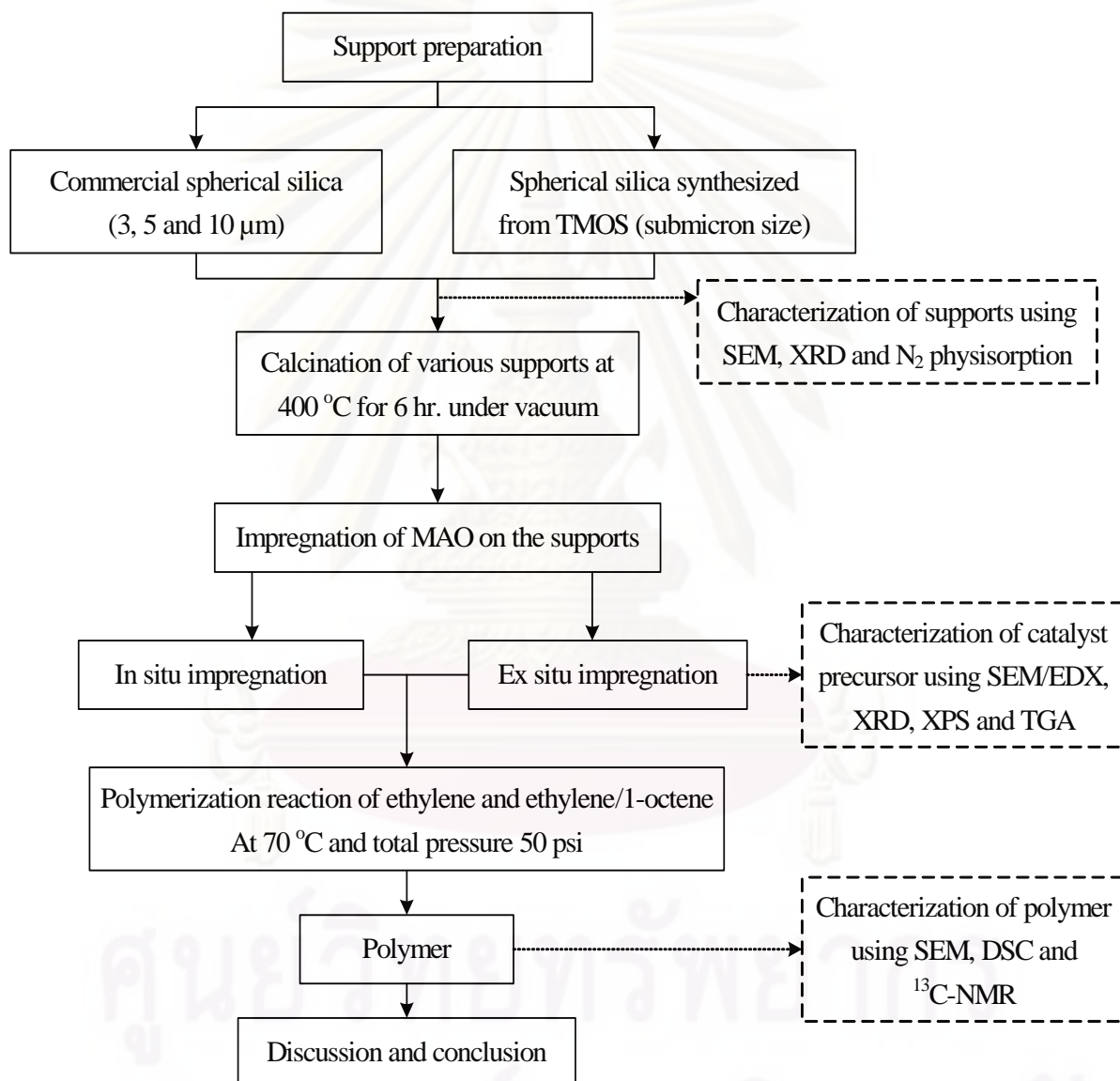


Figure 3.1 Flow diagram of research methodology

3.4 Experimental

3.4.1 Chemicals

The chemicals used in these experiments were analytical grade, but only major materials are specified as follows:

1. Tetramethyl orthosilicate for synthesis was purchased from Merck KGaA, Darmstadt, Germany and used as received.
2. Ethylene glycol ($\geq 99.5\%$) was purchased from Merck KGaA, Darmstadt, Germany and used as received.
3. Sodium hydroxide 1 mol/l was purchased from Merck KGaA, Darmstadt, Germany.
4. Dodecyltrimethylammonium bromide, $C_{12}TMABr$ (99%) was purchased from Aldrich Chemical Company, Inc. and used as received.
5. Spherical silica gel with various particle size (SiO_2 3, 5 and 10 μm) were purchased from Ligand Scientific Co.,Ltd.
6. *rac*-Ethylenebis(indenyl)zirconium dichloride (*rac*-Et(Ind) $_2$ ZrCl $_2$) was supplied from Aldrich Chemical Company, Inc. and used without further purification.
7. Ethylene gas (99.96%) was devotes from PTT Chemical Public Co., Ltd., Thailand and used as received.
8. 1-Hexene (99+%) was purchased from Aldrich Chemical Company, Inc. and purified by distilling over sodium under argon atmosphere before use.
9. 1-Octene (98%) was purchased from Aldrich Chemical Company, Inc. and purified by distilling over sodium under argon atmosphere before use.
10. Toluene was devotes from EXXON Chemical Ltd., Thailand. This solvent was dried over dehydrated CaCl $_2$ and distilled over sodium/benzophenone under argon atmosphere before use.
11. Methylaluminoxane (MAO) 20% in toluene was donated from PTT Public Co., Ltd., Thailand and used without further purification.
12. Trimethylaluminum (TMA) 2.0 M in toluene was supplied from Nippon aluminum Alkyls Ltd., Japan and used without further purification.

13. Hydrochloric acid (Fuming 36.7%) was supplied from Sigma and used as received.

14. Methanol (Commercial grade) was purchased from SR lab and used as received.

15. Sodium (99%) was purchased from Aldrich Chemical Company, Inc. and used as received.

16. Benzophenone (99%) was purchased from Fluka Chemie A.G. Switzerland and used as received.

17. Calciumhydride (99%) was purchased from Fluka Chemie A.G. Switzerland and used as received.

18. Ultra high purity argon gas (99.999%) was purchased from Thai Industrial Gas Co., Ltd., and further purified by passing through columns packed with molecular sieve 3A, BASF Catalyst R3-11G, sodium hydroxide (NaOH) and phosphorus pentoxide (P_2O_5) to remove traces of oxygen and moisture.

3.4.2 Equipments

Due to the metallocene system is extremely sensitive to the oxygen and moisture. Therefore, the special equipments were required to handle with the preparation and polymerization process. For example, glove box: equipped with the oxygen and moisture protection system will be used to produce the inert atmosphere. Schlenk techniques (Vacuum and Purge with inert gas) are the others set of the equipment will be used to handle air-sensitive product. All types of equipments used in the catalyst precursor preparation and polymerization are listed below:

3.4.2.1 Cooling system

The cooling system is in the solvent distillation in order to condense the freshly evaporated solvent.

3.4.2.2 Magnetic stirrer and heater

The magnetic stirrer and heater model RTC basis from IKA Labortechnik were used.

3.4.2.3 Vacuum pump

The vacuum pump model 195 from Labconco Corporation was used. A pressure of 10^{-1} to 10^{-3} mmHg is adequate for the vacuum supply to the vacuum line in the Schlenk line.

3.4.2.4 Inert gas supply

The inert gas (argon) was passed through columns of BASF catalyst R3-11G as oxygen scavenger, molecular sieve 3×10^{-10} m to remove moisture. The BASF catalyst will be regenerated by treatment with hydrogen at 300°C overnight before flowing the argon gas through all the above columns.

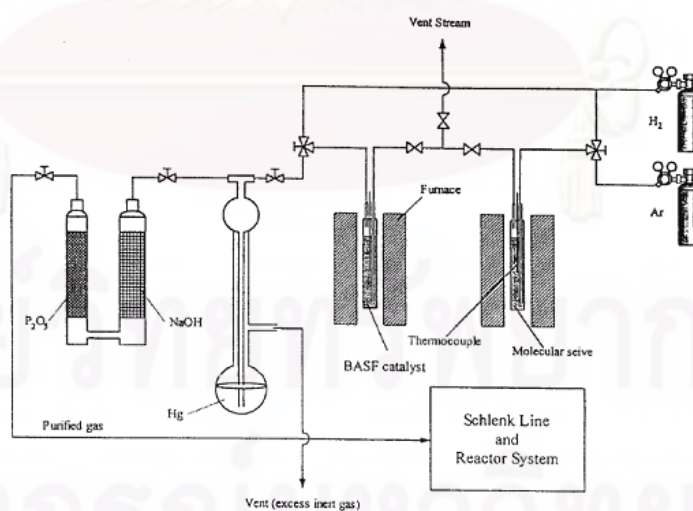


Figure 3.2 Inert gas supply system

3.4.2.5 Reactor

A 100 ml glass flask was connected with 3-ways valve was used as the copolymerization reactor for atmospheric pressure system and a 100 ml stainless steel autoclave was used as the copolymerization reactor for high pressure systems.

3.4.2.6 Schlenk line

Schlenk line consists of vacuum and argon lines. The vacuum line was equipped with the solvent trap and vacuum pump, respectively. The argon line was connected with the trap and the mercury bubbler that is a manometer tube and contains enough mercury to provide a seal from the atmosphere when argon line will be evacuated.

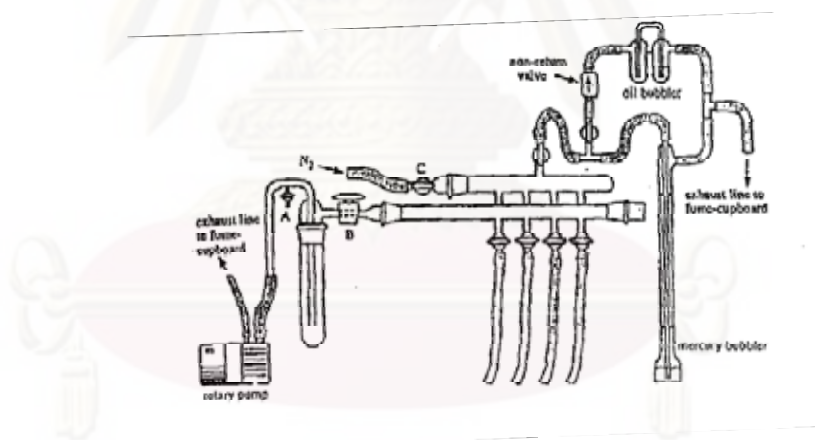


Figure 3.3 Schlenk line

3.4.2.7 Schlenk tube

A tube with a ground glass joint and side arm, which is three-way glass valve. Sizes of Schlenk tubes are 50, 100 and 200 ml. were used to prepare catalyst and store materials which are sensitive to oxygen and moisture.

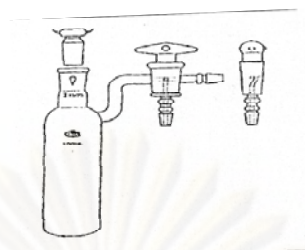


Figure 3.4 Schlenk tube

3.4.2.8 Polymerization line

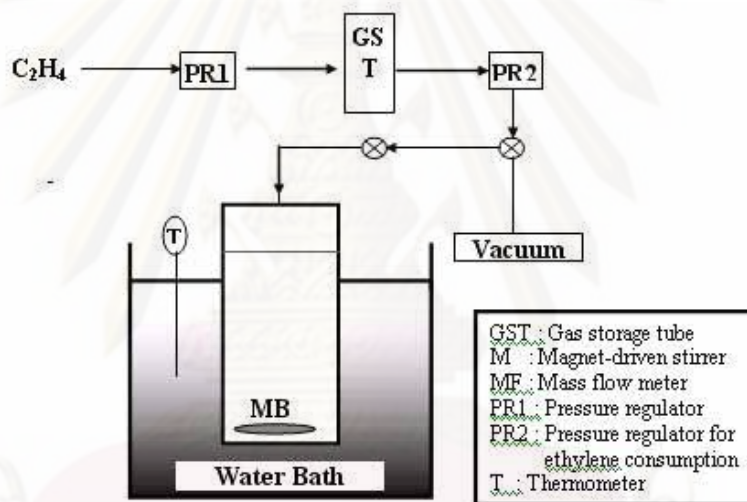


Figure 3.5 Diagram of system in slurry phase polymerization.

3.4.3 Supporting Procedure

3.4.3.1 Preparation of mesoporous silica sphere support

Mesoporous silica spheres were synthesized using n-dodecyltrimethylammonium bromide ($C_{12}TMABr$), tetramethoxysilane (TMOS), Sodium hydroxide solution (1 M) and ethylene glycol (99.5%) as reagent according to the following procedures described by Yamada and Yano [Yamada and Yano, 2006]. They were all used without further purification. In a typical synthesis procedure,

0.42 g of $C_{12}TMABr$ and 0.75 ml of 1 M sodium hydroxide solution were dissolved in 100 g of ethylene glycol/water (25/75 = w/w) solution (weight ratio of co-solvent: 0.25). Then 0.46 g of TMOS was added to the solution, with vigorous stirring at 293 K. The composition of the reaction mixture is $1SiO_2 : 0.45C_{12}TMABr : 0.25NaOH : 133$ ethylene glycol : $1392 H_2O$. Following the addition of TMOS, the clear solution suddenly turned opaque, resulting in a white precipitate. After 8 hours of continuous stirring the mixture was aged overnight. The white powder was filtered and washed with distilled water at least three times, and then dried at 318 K for 72 hours. The powder obtained was calcined in air at 823 K for 6 hours to remove the organic species.

3.4.3.2 Preparation of supported MAO (catalyst precursor)

1. Ex situ impregnation method

Commercial spherical silica and synthesized silica were heated under vacuum at 400 °C for 6 hours prior to used as support. After that MAO was impregnated onto the support, the method is described as follows. One gram of silica was reacted with the desired amount of MAO in toluene at room temperature and stirred for 30 min. The solvent was then removed from the mixture. About 20 ml of toluene was added into the obtained precipitate, stirred the mixture for 5 min, and then removed the solvent. This procedure was done for five times to ensure the removal of impurities. Then, the solid part was dried under vacuum at room temperature to obtain white powder of supported cocatalyst (MAO/support).

2. In situ impregnation method and polymerization

0.1 g of the silica supports was allowed to contact with 1.11 ml of MAO (10 %wt) for 30 min, in reactor with magnetic stirring. After this period of time, the suspension was mixed with desired amount of zirconocene and TMA ($[Al]_{TMA}/[Zr]_{cat} = 2500$) which stirred for 5 min aging. Then toluene (to make a total volume of 30 ml) was introduced in to reactor. The reactor was frozen in liquid

nitrogen to stop reaction and then the desired amount of 1-octene was injected into the reactor (in case of copolymerization). The reactor was evacuated to remove argon. Then, it was heated up to polymerization temperature (70°C) and the polymerization was started by feeding ethylene gas (total pressure 50 psi in the reactor) until the consumption of ethylene at 0.018 mol (6 psi was observed from the pressure gauge) was reached. The reaction of polymerization was completely terminated by addition of acidic methanol. The time of reaction was recorded for purpose of calculating the activity. The precipitated polymer was washed with methanol and dried at room temperature.

3.4.4 Ethylene and ethylene/1-octene polymerization procedure

The polymerization reaction was carried out in a 100 ml semi-batch stainless steel autoclave reactor equipped with magnetic stirrer. The autoclave and magnetic bar were dried in oven at 110 °C for 30 min and was purged with argon 5 times in glove box port before used. In the glove box, the desired amounts of *rac*-Et[Ind]₂ZrCl₂ (5×10^{-5} M) and TMA ($[Al]_{TMA}/[Zr]_{cat} = 2500$) were mixed and stirred for 5 min aging. Then, toluene (to make a total volume of 30 ml) and desired amount of MAO/support were introduced into the reactor. After that, the mixture of *rac*-Et[Ind]₂ZrCl₂ and TMA was injected into the reactor. From this point, the similar procedure as mentioned in 2 was conducted.

3.4.5 Characterization of supports and catalyst precursor

3.4.5.1 X-ray diffraction (XRD)

XRD was performed to determine the bulk phase of sample by SIEMENS D 5000 X-ray diffractometer connected with a computer with Diffract ZT version 3.3 program for fully control of the XRD analyzer. The experiments were carried out by using CuK_α radiation with Ni filter in the 2θ range of 20-80 degrees resolution 0.04°. The crystallite size was estimated from line broadening according to the Scherrer equation and α-Al₂O₃ was used as standard.

3.4.5.2 Scanning electron microscopy (SEM) and energy dispersive X-ray spectroscopy (EDX)

SEM observation with a JSM-5800 LV Scanning Microscope, Microspec WDX at Scientific Technological Research Equipment Center, Chulalongkorn University was employed to investigate the morphology of catalyst precursor and performed using Link Isis series 300 program for EDX analysis. Another JEOL JSM 6480 LV Scanning Microscope at Faculty of Science, Chulalongkorn University was employed to investigate the morphology of supports and polymer. The samples for SEM analysis will be coated with gold particles by ion sputtering device to provide electrical contact to the specimen.

3.4.5.3 N₂ physisorption

The BET surface areas, pore volumes, average pore diameters, and pore size distributions of catalysts were determined by N₂ physisorption using a Micromeritic ASAP 2000 automated system. Each sample was degassed in the Micromeritics ASAP 2000 at 200°C for 4 hours prior to N₂ physisorption.

3.4.5.4 Thermal gravimetric analysis (TGA)

TGA was performed to determine the interaction force of the supported MAO. It was conducted using TA Instruments SDT Q 600 analyzer. The samples of 10-20 mg and a temperature ramping from 25 to 600 °C at 2 °C /min were used in the operation. The carrier gas was N₂ UHP.

3.4.5.5 X-ray photoelectron spectroscopy (XPS)

XPS was used to determine the binding energies (BE) and the amount of Al on support surfaces. It was carried out using the Shimadzu AMICUS with VISION 2-control software. Spectra were recorded at room temperature in high-resolution mode (0.1 eV step, 23.5 eV pass energy) for Al 2p core-level region. The

samples were mounted on an adhesive carbon tape as pellets. The energies reference for Ag metal (368.0 eV for 3d_{5/2}) was used for this study.

3.4.6 Characterization of Polymer

3.4.6.1 Differential scanning calorimetry (DSC)

The melting temperature of polyethylene and ethylene/1-octene copolymer products were determined with a Perkin-Elmer diamond DSC from MEKTEC, at the Center of Excellence on Catalysis and Catalytic Reaction Engineering, Department of Chemical Engineering, Chulalongkorn University. The analyses were performed at the heating rate of 20 °C/ minutes in the temperature range of 50-150 °C. The heating cycle was run twice. In the first scan, samples were heated and then cooled to room temperature. In the second, samples were reheated at the same rate, but only the results of the second scan was reported because the first scan was influenced by the mechanical and thermal history of samples.

3.4.6.2 ¹³C NMR spectroscopy (¹³C NMR)

¹³C NMR spectroscopy was used to determine the α -olefin incorporation and copolymer microstructure. Chemical shift were referenced internally to the benzene-d₆ and calculated according to the method described by Randall [Randall,]. Sample solution was prepared by dissolving 50 mg of copolymer in 1,2,4-trichlorobenzene as solvent and benzene-d₆ for internal lock. ¹³C NMR spectra were taken at 60 °C using BRUKER A400 operating at 100 MHz with an acquisition time of 1.5 s and a delay time of 4 s.

CHAPTER IV

RESULTS AND DISCUSSIONS

The purpose of this study is to investigate and characterize the effect of different particle diameter of spherical silica supported zirconocene/MAO catalyst on catalytic activity and properties of copolymers during the copolymerization reaction of ethylene with 1-octene. Furthermore the “comonomer effect” on catalytic activity and polymer properties is also developed to get better understanding.

4.1 Characterization of supports and catalyst precursors

4.1.1 Characterization of supports with N₂ physisorption

Spherical silica were used in this study can be classified in two types; first is spherical silica gel with various particle sizes such as 3, 5 and 10 μm that were purchased from Ligand Scientific. Another was synthesized using tetramethoxysilane (TMOS) as silica source according to the method described by Yamada and Yano [Yamada and Yano, 2006]. After preparation of supports, the silica supports with different particle diameters were characterized before impregnation with MAO cocatalyst.

N₂ physisorption technique was performed to measure BET surface area, average pore diameter and pore size distribution of supports. The results of BET surface area and pore characteristics of various supports are summarized in **Table 4.1**. The synthesized spherical silica support denoted as SiO₂ (0.56 μm) having the average pore diameter of ca. 26.56 Å and surface area of 1202.2 m²/g which obviously showed that synthesized silica have the highest surface area among all of supports. However BET surface area for 3, 5 and 10 μm silica supports are in the same range (300-400 m²/g) and average pore diameter of these supports are 86.21, 56.20 and 88.07, respectively. It also revealed that the larger surface area silica is the smaller average pore diameter is evident. The pore size distribution of supports are

shown in **Figure 4.1**. This indicated that all of silica supports exhibited only unimodal pore size distribution. Moreover purchased silica supports evinced larger portion of the large pore than the synthesized silica support.

Table 4.1 BET surface area and pore characteristics of supports

Supports	BET surface area (m ² /g)	Average pore diameter (Å)	Pore volume (cm ³ /g)
SiO ₂ (0.56 μm)	1202.2	26.56	0.37
SiO ₂ (3 μm)	309.3	86.21	0.94
SiO ₂ (5 μm)	386.5	56.20	0.87
SiO ₂ (10 μm)	302.8	88.07	1.00

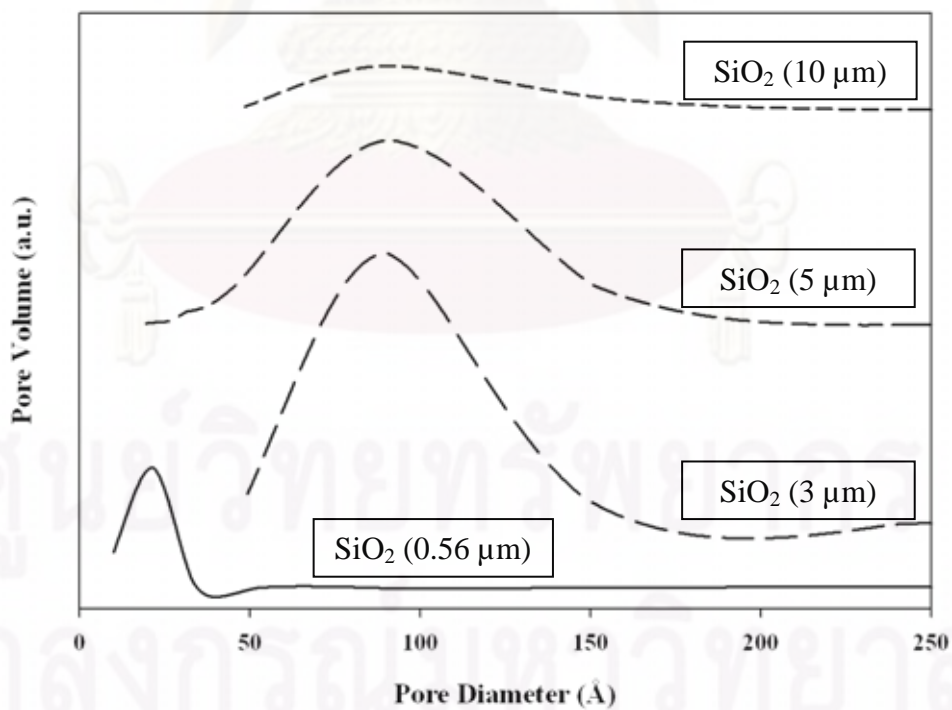


Figure 4.1 Pore size distribution of spherical silica supports

4.1.2 Characterization of supports and catalyst precursors with X-ray diffraction (XRD)

The various spherical silica supports with different particle size were characterized before and after impregnation with MAO. The XRD patterns of these supports are shown in **Figure 4.2**. It was observed that all silica supports exhibited the similar XRD patterns consisting of a broad peak between ca. $20^\circ - 30^\circ$ assigning to conventional amorphous silica. After impregnation with MAO, XRD patterns were almost identical with before impregnation that is no MAO peaks were detected. This was suggested that MAO was highly dispersed on the supports.

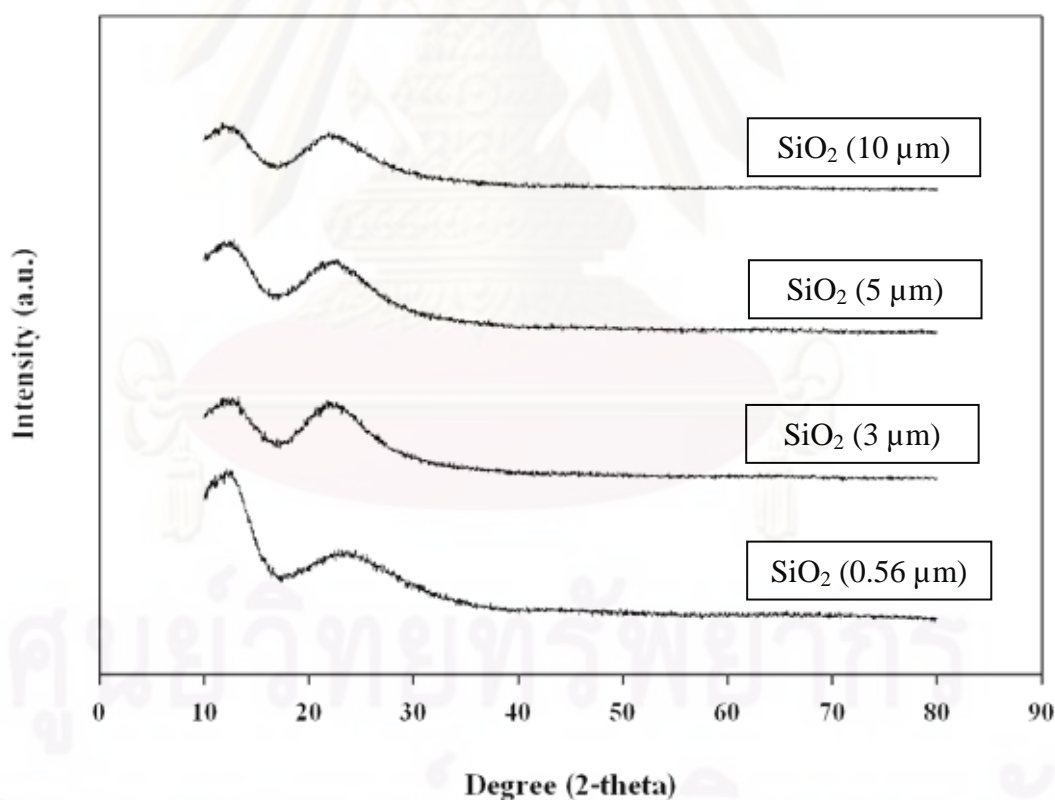


Figure 4.2 XRD patterns of different spherical silica supports

4.1.3 Characterization of catalyst precursors with X-ray photoelectron spectroscopy (XPS)

After impregnation of MAO on supports, XPS measurement was used to study the nature of $[Al]_{MAO}$ on various support surface which the binding energy (BE) for Al 2p core-level was extended. The typical XPS profile for all silica-supported MAO, shown in **Figure 4.3**, exhibited the identical BE for Al 2p of cocatalyst at 74.3-75.1 eV. These values were also in accordance with MAO and MMAO present on SiO_2 and TiO_2 supports as reported by Hagimoto *et al.*, Jongsomjit *et al.* and Ketloy *et al.*. This suggested that no significant change in oxidation state of $[Al]_{MAO}$ when presented on supports employed. XPS also measured the surface concentration of Al 2p on support as shown in **Table 4.2**. These result indicated that surface concentration of Al were around 30 wt% and $SiO_2(0.56 \mu m)$ gave the highest value due to its larger surface area among all supports. In addition, more bulk Al content and cocatalyst distribution on various supports should be performed.

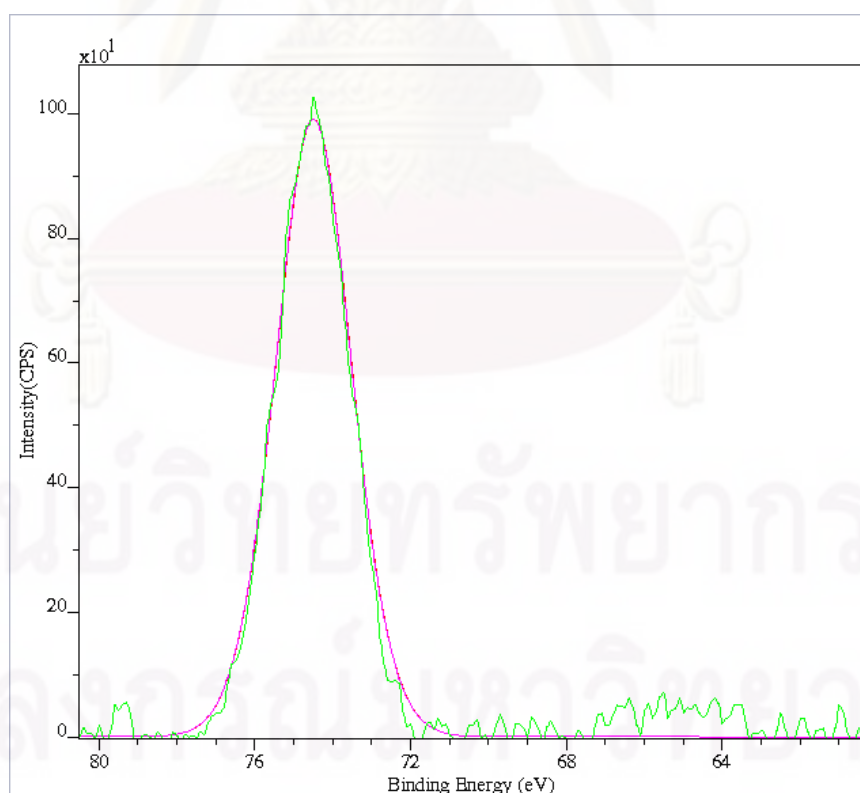


Figure 4.3 Typical XPS spectrum for Al 2p on various supports

Table 4.2 Binding energy and surface concentration for Al 2p obtained from XPS

Catalyst precursor	BE for Al 2p (eV)	Al mass concentration (wt%)
SiO ₂ (0.56 μm) / MAO	74.6	35.07
SiO ₂ (3 μm) / MAO	74.5	31.37
SiO ₂ (5 μm) / MAO	74.3	34.11
SiO ₂ (10 μm) / MAO	75.1	28.42

4.1.4 Characterization of supports and catalyst precursors with scanning electron microscope (SEM) and energy dispersive X-ray spectroscopy (EDX)

SEM and EDX were performed to determine the $[Al]_{MAO}$ content, elemental distributions and morphologies of supports before and after impregnation. From **Figure 4.4**, the SEM micrographs show that all silica supports have spherical shape and various particle sizes in the range of submicron, 3, 5, and 10 μm, respectively. The SEM micrographs of supports after impregnation with MAO are shown in **Figure 4.5** indicating similar result as before MAO impregnation. In addition, the surfaces of spherical silica supports have more roughness by being attached with cocatalyst on the covering face.

The EDX mapping images of catalyst precursors in **Figure 4.6** can provide more information about elemental distribution on support surface. The distribution of all elements (Al, Si, and O) was similar in all samples suggesting good distribution of MAO, as seen from Al distribution mapping on each support, without any change in support morphology. Besides the Al distribution on supports, the consideration of $[Al]_{MAO}$ content in the supports was another important point. From the measurement curve for the quantitative analysis using EDX (as shown in appendix B) can be seen that the amount of $[Al]_{MAO}$ in various supports were altered due to surface area and adsorption ability of each support. The data from these curves were in accordance with amounts of $[Al]_{MAO}$ in various catalyst precursors as listed in **Table 4.3**. It revealed that $[Al]_{MAO}$ contents were in order of SiO₂ (0.56 μm) > SiO₂ (3μm) > SiO₂ (5 μm) > SiO₂ (10 μm). The higher amount of $[Al]_{MAO}$ presented on

silica supports can be probably attributed to the smaller particle size, which have larger external surface area.

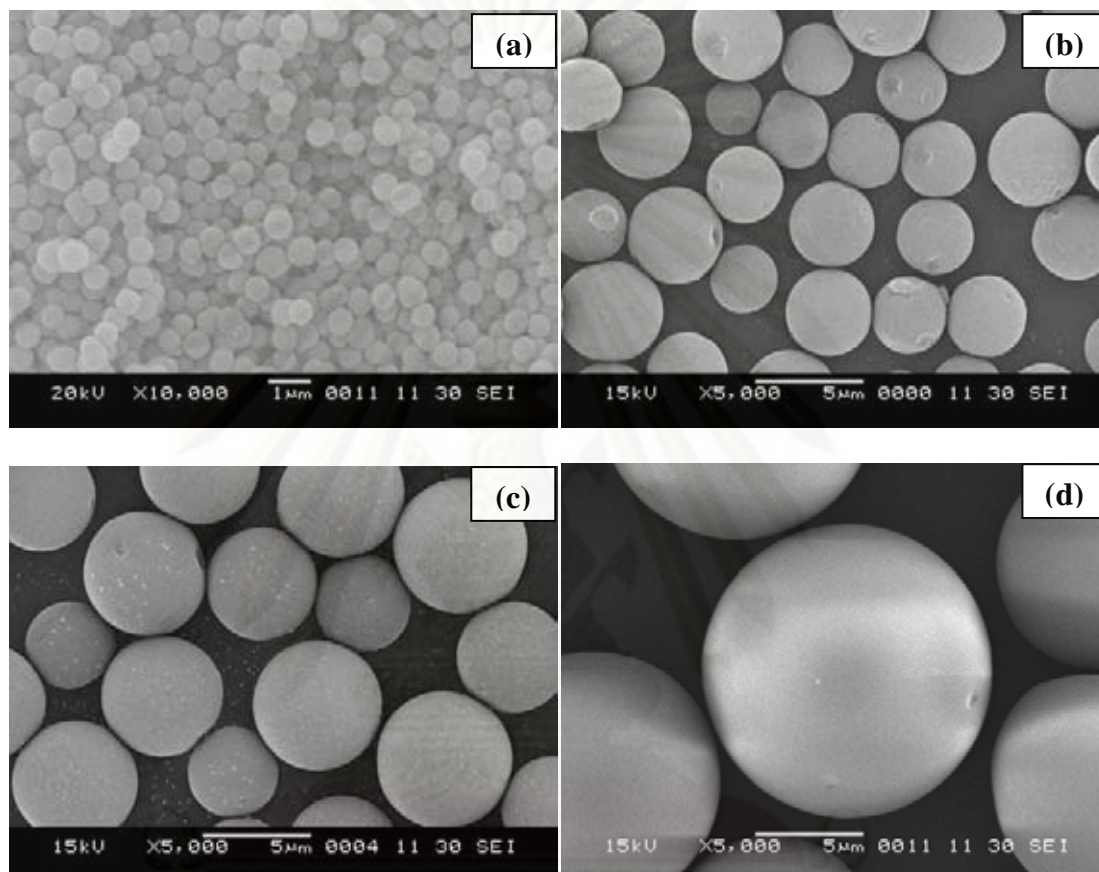


Figure 4.4 SEM micrographs of various spherical silica supports before MAO impregnation; (a) SiO_2 (0.56 μm), (b) SiO_2 (3 μm), (c) SiO_2 (5 μm) and (d) SiO_2 (10 μm)

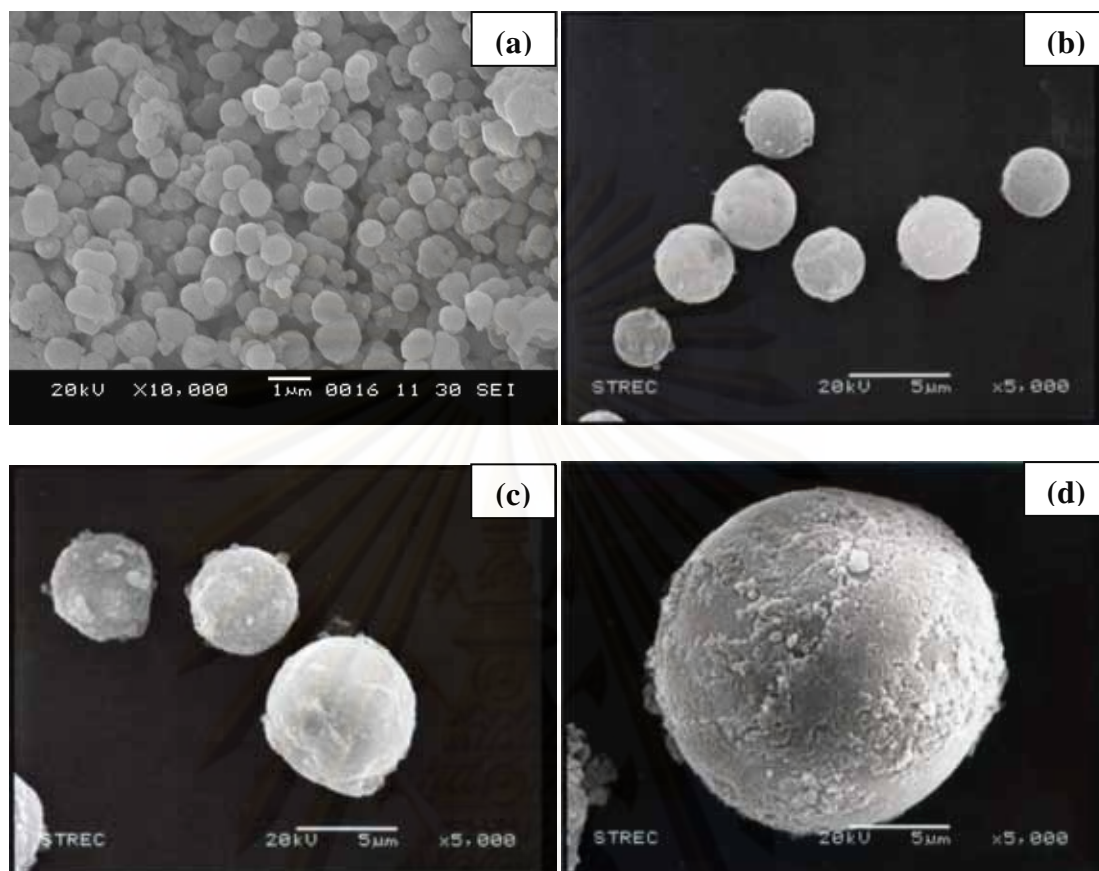


Figure 4.5 SEM micrographs of various spherical silica supports after MAO ex situ impregnation; (a) SiO_2 (0.56 μm), (b) SiO_2 (3 μm), (c) SiO_2 (5 μm) and (d) SiO_2 (10 μm)

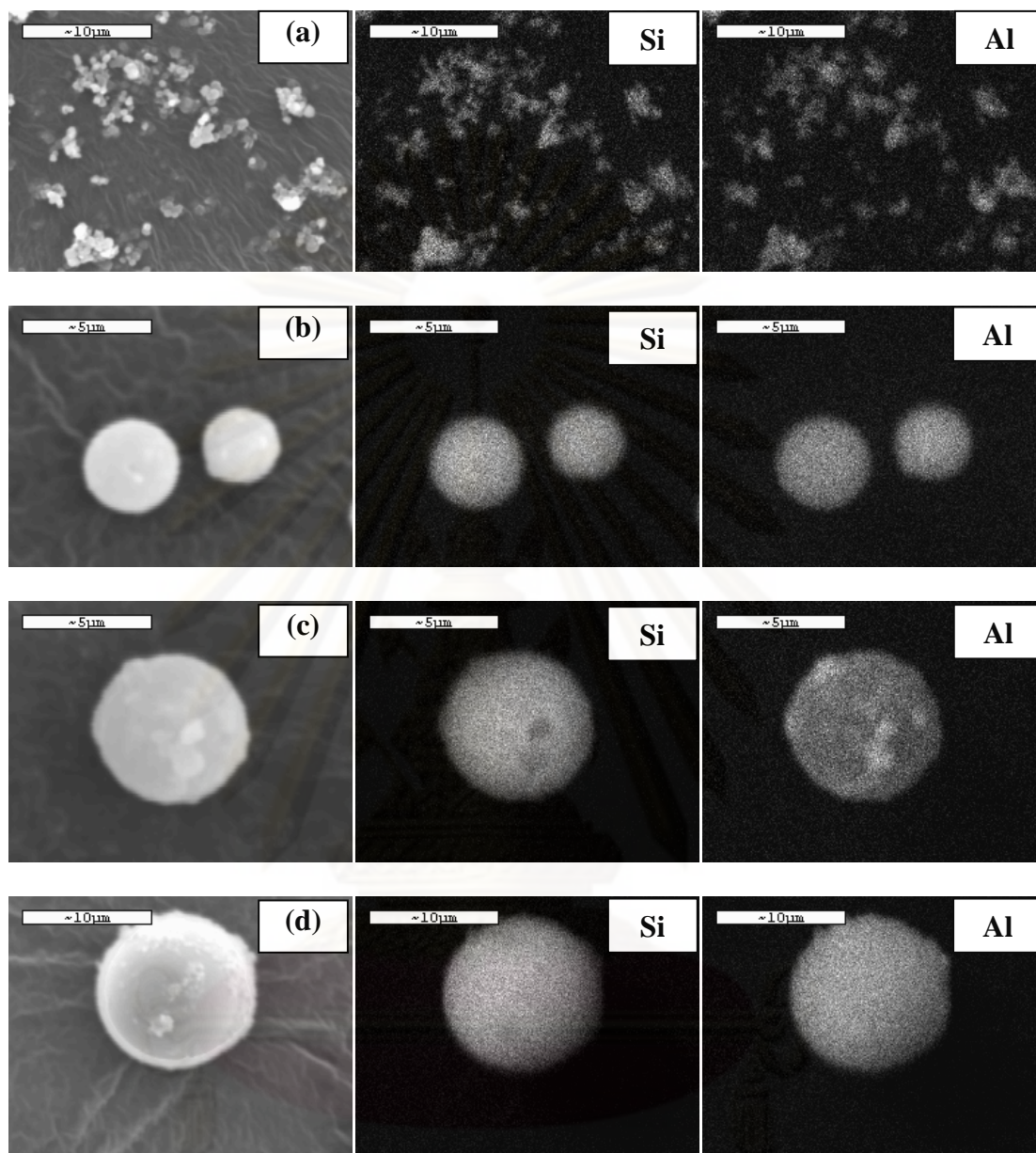


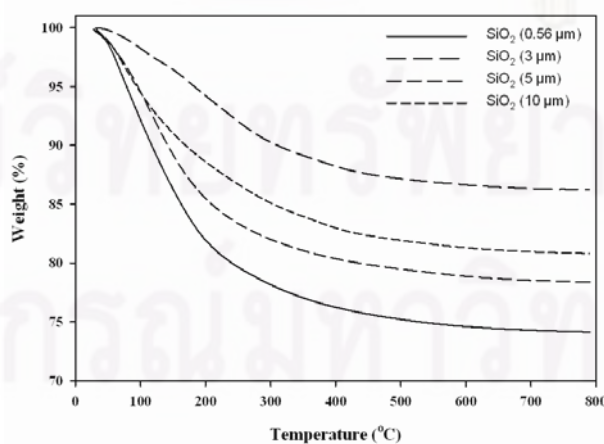
Figure 4.6 Si and Al mapping of silica/MAO particles with ex situ impregnation; (a) $\text{SiO}_2(0.56 \mu\text{m})$, (b) $\text{SiO}_2(3 \mu\text{m})$, (c) $\text{SiO}_2(5 \mu\text{m})$ and (d) $\text{SiO}_2(10 \mu\text{m})$

Table 4.3 The average $[Al]_{MAO}$ content on various spherical silica supports

Catalyst precursor	$[Al]_{MAO}$ (wt%) in catalyst precursor
SiO ₂ (0.56 μm) / MAO	26.04
SiO ₂ (3 μm) / MAO	23.42
SiO ₂ (5 μm) / MAO	22.77
SiO ₂ (10 μm) / MAO	21.42

4.1.5 Characterization of supports and catalyst precursors with thermogravimetric analysis (TGA)

In this study, the TGA measurement was performed to determine the interaction between cocatalyst (MAO) and support. The TGA provide information on the degree of interaction for the MAO bound to the support in terms of weight loss and removal temperature. The TGA profiles of $[Al]_{MAO}$ on various supports are shown in **Figure 4.7** indicating the similar profiles for various supports. The species was removed from the supports at ca. 69, 174, 110 and 70°C for SiO₂(0.56 μm), SiO₂(3 μm), SiO₂ (5 μm) and SiO₂(10 μm), respectively. It was observed that the weight loss of $[Al]_{MAO}$ present on various supports were in the order of SiO₂(0.56 μm) 25.85% > SiO₂(5μm) 21.60% > SiO₂(10μm) 19.17% > SiO₂(3μm) 13.74%. This indicated that $[Al]_{MAO}$ present on SiO₂(3 μm) support had the strongest interaction.

**Figure 4.7** TGA profiles of supported MAO on spherical silica supports

4.2 Characteristics and catalytic properties of ethylene and ethylene/1-octene polymerization which catalyst precursors prepared by in situ impregnation.

In this study, the various spherical silica supports after impregnation with MAO (in situ impregnation) were employed and studied for catalytic activities. Ethylene polymerization using silica supported zirconocene/MAO catalyst was performed to determine the characteristics and catalytic properties of polymer influence by various supports. For a comparative study, ethylene/1-octene copolymerization was also conducted in order to investigate the comonomer effect for this catalytic system. Methylaluminoxane was used as cocatalyst with $[Al]_{MAO}/[Zr]_{cat}$ was 1135 and zirconium concentration 5.0×10^{-5} mol, which $[Al]_{MAO}$ was calculated based on EDX measurement. The copolymerization was performed in toluene solvent at 70°C using ethylene consumption of 0.018 mol, 1-octene 0.018 mol and 0.1 g of support with reaction total volume of 30 ml.

4.2.1 The effect of particle size of spherical silica supports and comonomer on the catalytic activity

The catalytic activities from ethylene and ethylene/1-octene polymerization via various supports are listed in **Table 4.4**.

The ethylene polymerization with *rac*-Et[Ind]₂ZrCl₂ catalyst was performed for a comparative study of the catalytic activities derived from different size of spherical supports. The polymerization activity of homogeneous catalytic system was highest due to the supporting effect of heterogeneous system as mentioned by many authors [Jongsomjit et al., 2004; Jongsomjit et al., 2005; Jiamwijitkul et al., 2007]. Considering the catalytic activity for heterogeneous catalytic system, it was found that catalytic activities were in the order of SiO₂(3µm) > SiO₂(5µm) > SiO₂(10µm) > SiO₂(0.56 µm). The polymerization activity obtain from SiO₂ (0.56 µm) was the lowest. In additional the lower activity may be attributed to the SiO₂ (0.56 µm) particle, which particle size is too small, and causes of more steric hindrance than the larger particle [Chaichana et al., 2007]. The micron

size supports are 3, 5, and 10 μm exhibited the smaller particle caused the higher activity. This may be suggested that the larger the particle diameter is, the longer the induction period takes and then the reaction velocity slowly increases as described by Fink [Fink et al., 2000].

Table 4.4 Catalytic activity of various silica-supported MAO during ethylene (E) and ethylene/1-octene (EO) polymerization (In situ impregnation)

System	Polymerization	Polymerization time (sec)	Polymer yield ^a (g)	Catalytic Activity ^b (kg Pol.mol.Zr ⁻¹ ·h ⁻¹)
homogeneous	E	75	0.7318	23,418
SiO ₂ (0.56 μm)	E	143	0.4949	8,306
SiO ₂ (3 μm)	E	109	0.5756	12,674
SiO ₂ (5 μm)	E	114	0.5425	11,421
SiO ₂ (10 μm)	E	120	0.5526	11,052
homogeneous	EO	101	1.95	46,344
SiO ₂ (0.56 μm)	EO	155	1.81	27,972
SiO ₂ (3 μm)	EO	80	1.89	56,643
SiO ₂ (5 μm)	EO	86	1.65	45,913
SiO ₂ (10 μm)	EO	153	1.80	28,281

^a The polymer yield was fixed limited by 0.018 mol of ethylene consumption.

^b Measurement at polymerization temperature of 70°C, [Ethylene] = 0.018 mole, [1-octene] = 0.018 mole, [Zr]_{cat} = 5×10^{-5} M, [Al]_{MAO} / [Zr]_{cat} = 1135, [Al]_{TMA} / [Zr]_{cat} = 2500 in toluene with total volume = 30 ml.

For a comparative study of ethylene and ethylene/1-octene polymerization, the catalytic activities were measured. The activities for ethylene/1-octene polymerization are also shown in **Table 4.4**. The similar trends from supported system as seen in ethylene polymerization were also evident. The homogeneous catalytic system should provide the highest activity due to the absence of support interaction but catalytic activity of SiO₂(3 μm) was higher than homogeneous system. This result was presumably because both the heterogeneous system exhibited higher bulk density than homogeneous system which improved distribution of active site and the smaller particles have less support interaction. However it clearly illustrated that the activities of polymerization dramatically increased with the insertion of α -olefin

monomer (1-octene). These phenomena are commonly well known as the comonomer effect in copolymerization behavior [Grieken et al., 2007]. Several possible causes had been proposed to explain this fact, but the most reasonable reason is the easier monomer diffusion due to crystallinity reduction of the growing polymer when a small amount of comonomer is added. In ethylene homopolymerization, the monomer diffusion is very slow through the highly crystalline polymer formed around the catalyst particle. The comonomer addition leads to less crystalline polymer formation, which makes the diffusion of ethylene easier, and thus the activity increases.

4.2.2 The effect of particle size of spherical silica supports on the polymer microstructure

Table 4.5 ^{13}C NMR analysis of and ethylene/1-octene copolymer
(In situ impregnation)

System	Triad distribution of copolymer						1-octene insertion (mol %)
	OOO	EOO	EOE	EEE	OEO	OEE	
Homogeneous	0	0	0.212	0.550	0.071	0.167	21.209
SiO ₂ (0.56 μm)	0	0	0.030	0.909	0	0.061	3.030
SiO ₂ (3μm)	0	0	0.209	0.560	0	0.230	20.942
SiO ₂ (5μm)	0	0	0.256	0.464	0.067	0.213	25.625
SiO ₂ (10μm)	0.103	0	0.271	0.444	0.145	0.038	37.301

E refers to ethylene monomer and O refers to 1-octene comonomer

^{13}C NMR is one of the most powerful techniques to identify the comonomer incorporation and polymer microstructure. The resulted ^{13}C NMR spectra (Appendix C) for all copolymers were similar. The quantitative analysis of triad distribution for all copolymer has been conducted based on the method described by Randall [Randall, 1989]. The triad distributions for all copolymers are shown in **Table 4.5**. All copolymers synthesized from each support exhibited similar triad distribution having the majority of EEE. The OOO distribution occurred in only 10 μm of SiO₂. It implied that the size of each supports hardly cause the effect on

polymer microstructure except the largest particle. Moreover the insertion of comonomer can be calculated [Galland et al., 1996], it was observed that the larger particle size resulted in increased 1-octene insertion. This may be probably due to less steric hindrance. For ^{13}C NMR spectra of polyethylene, the NMR peak cannot be noticed because there is no comonomer incorporation in polymer chain.

4.2.3 The effect of particle size of spherical silica supports on the polyethylene crystallinity

The XRD technique was used to confirm that obtained polymers were polyethylene due to polyethylene (homopolymer) cannot be checked with ^{13}C NMR spectra. The XRD patterns of polyethylene from homogeneous and supported system are shown in **Figure 4.8**. XRD patterns showed two characteristics peaks at 2θ are 21.8° and 24.3° corresponding to crystalline form of polyethylene [Kuo et al., 2003]. It exhibited that the polyethylene retains crystalline structure although the silica supports are incorporated into the polymer matrix.

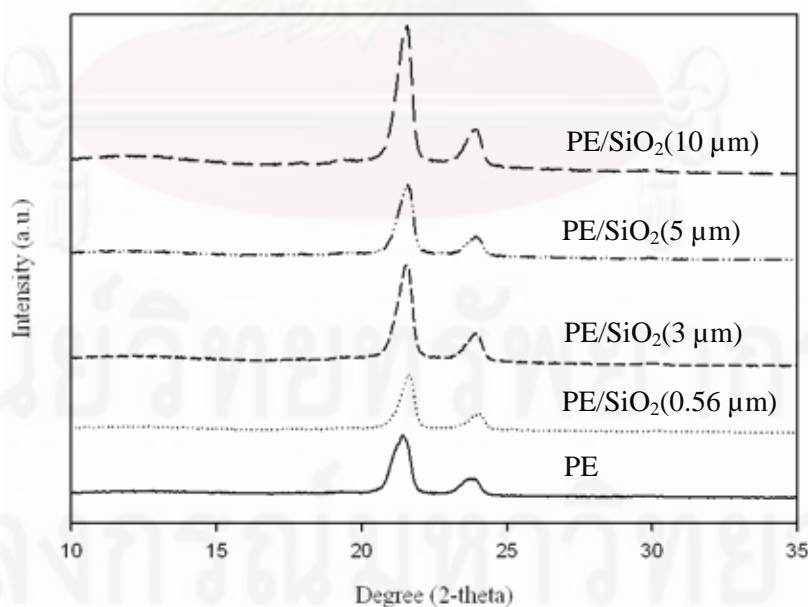


Figure 4.8 XRD patterns of polyethylene (in situ impregnation)

4.3 Characteristics and catalytic properties of ethylene and ethylene/1-octene polymerization which catalyst precursors prepared by ex situ impregnation.

Then the various spherical silica supports after ex situ impregnation with MAO were employed and studied for catalytic activities. The catalyst precursors were characterized by EDX to examine the Al concentration on support surface. Ethylene polymerization using silica supported zirconocene/MAO catalyst was performed to determine the characteristics and catalytic properties of polymer influence by various supports. For a comparative study, ethylene/1-octene copolymerization was also conducted in order to investigate the comonomer effect for this catalytic system. Methylaluminoxane was used as cocatalyst with $[Al]_{MAO}/[Zr]_{cat}$ was 1135 and zirconium concentration 5.0×10^{-5} mol, which $[Al]_{MAO}$ was calculated based on EDX measurement. The copolymerization was performed in toluene solvent at 70°C using ethylene consumption of 0.018 mol, 1-octene 0.018 mol (~ 0.71 ml) and desired amount of catalyst precursors with reaction total volume of 30 ml.

4.3.1 The effect of particle size of spherical silica supports and comonomer on the catalytic activity

The catalytic activities towards the ethylene and ethylene/1-octene polymerization upon various supports were measured. The polymerization activities of the homogeneous system and various supports are shown in **Table 4.6**.

The effect of support size on polymerization reaction prepared by ex situ impregnation method was investigated. Consider the activities for different particle sizes of spherical silica supports, the polymerization activities were in the order of homogeneous system > SiO₂ (5 μm) > SiO₂ (10 μm) > SiO₂ (3 μm) > SiO₂ (0.56 μm) for both ethylene and ethylene/1-octene polymerization. Generally, the supported system exhibited lower activity than the homogeneous one due to the supporting effect. This should be due to a loss of active species by support interaction and/or steric hindrance arising from the support.

Table 4.6 Catalytic activity of various silica-supported MAO during ethylene (E) and ethylene/1-octene (EO) polymerization (Ex situ impregnation)

System	Polymerization	Polymerization time (sec)	Polymer yield ^a (g)	Catalytic Activity ^b (kg Pol.mol.Zr ⁻¹ .h ⁻¹)
homogeneous	E	75	0.7318	23,418
SiO ₂ (0.56 μm)	E	148	0.5199	8,432
SiO ₂ (3 μm)	E	105	0.6275	14,343
SiO ₂ (5 μm)	E	72	0.6245	20,816
SiO ₂ (10 μm)	E	87	0.7406	20,431
homogeneous	EO	71	1.086	36,710
SiO ₂ (0.56 μm)	EO	131	0.9114	16,697
SiO ₂ (3 μm)	EO	113	1.1091	23,556
SiO ₂ (5 μm)	EO	94	1.1328	28,922
SiO ₂ (10 μm)	EO	84	0.9427	26,935

^a The polymer yield was fixed limited by 0.018 mol of ethylene consumption.

^b Measurement at polymerization temperature of 70°C, [Ethylene] = 0.018 mole, [1-octene] = 0.0045 mole, [Zr]_{cat} = 5×10⁻⁵ M, [Al]_{MAO} / [Zr]_{cat} = 1135, [Al]_{TMA} / [Zr]_{cat} = 2500 in toluene with total volume = 30 ml.

In supported system, the polymerization activity obtain from SiO₂ (0.56 μm) was the lowest whereas the surface concentration of [Al]_{MAO} was the highest. In fact, the greater amount of [Al]_{MAO} should result in more active species present during polymerization [Chaichana et al., 2007; Wongwaiwattanakul and Jongsomjit, 2008]. The lower activity may be attributed to the SiO₂ (0.56 μm) particle, which particle size is too small, and causes of more steric hindrance than the larger particle [Chaichana et al., 2007]. Besides the steric hindrance effect and surface concentration of [Al]_{MAO}, the interaction between support and [Al]_{MAO} was substantially important. In fact, the interaction in this study was referred to the interaction between the support and cocatalyst(MAO). In order to give more explanation about relationship between support interaction and polymerization activity, the interaction of support and dMMAO can be proposed based on the review paper by Severn [Severn et al., 2005]. They explain the connection of the support and cocatalyst occurred via the O_{support}~Al_{cocatalyst} linkage. In particular, the TGA can only provide useful information on the degree of interaction for [Al]_{MAO} bound to the

support. The stronger interaction can result in being more difficult for the MAO bound to the support to react with the metallocene complex during activation process leading to lower catalytic activity for polymerization. In contrast, the leaching of $[Al]_{MAO}$ can occur due to very weak interaction resulting in low activity as well. So the optimum interaction is crucial. As mentioned above, the SiO_2 (0.56 μm) support had the weakest interaction with MAO being present on it and thus the lowest activity was observed.

Considering only the micron size support, the activity of SiO_2 (5 μm) was the highest because of the higher surface area and weaker interaction among these three supports. SiO_2 (3 μm) and SiO_2 (10 μm) showed the lower activity than SiO_2 (5 μm). Indeed, the amounts of Al over the surface of every size of SiO_2 have similar value. The change in activity upon various support were mainly attributed to both amounts of $[Al]_{MAO}$ present and its interaction with support as described above. Based on our results, these may be attributed to the stronger interaction between MAO and support as seen by TGA results. It was suggested that the strong interaction can result in more difficult for MAO react with catalyst in reaction medium, thus the lower polymerization activity was observed in SiO_2 (3 μm).

For a comparative study of ethylene and ethylene/1-octene polymerization, the copolymerization activity was higher than purely ethylene polymerization as described in 4.2.1.

4.3.2 The effect of particle size of spherical silica supports and comonomer on morphologies of polymers.

Morphology of polyethylene and LLDPE that synthesized by ex situ impregnation method were also investigated. It indicated that there was no significant change in polymer morphologies upon various supports used. From **Figures 4.9** and **4.10**, we observed the leaching of support from both polymers and copolymers matrix. This observation pointed that the smoother surface of support affected to

surface tension and attachment of support with the synthesized polymer. In fact, there are no surface tensions to help polymer attachment.

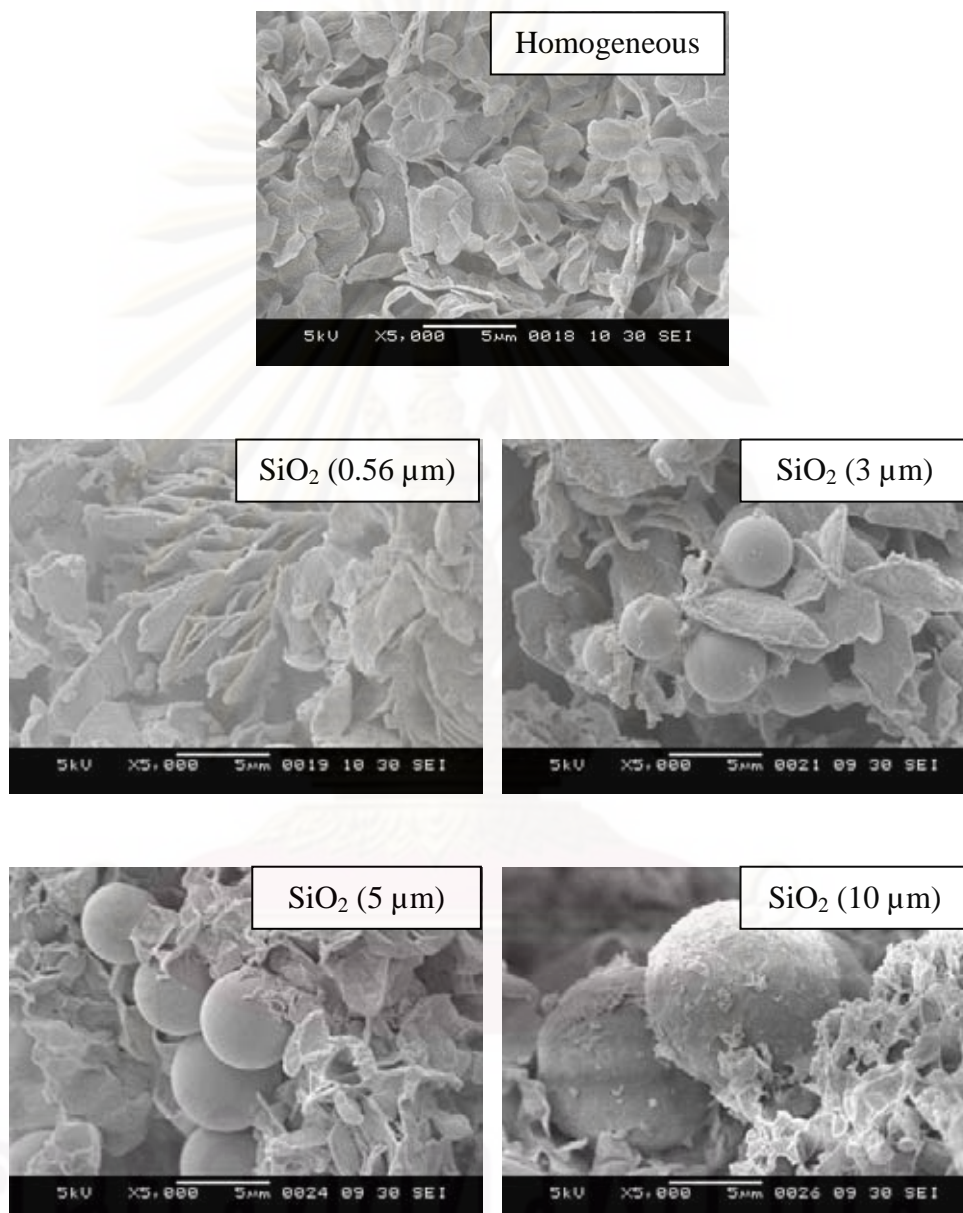


Figure 4.9 SEM micrographs of polyethylene obtained with various spherical silica supports

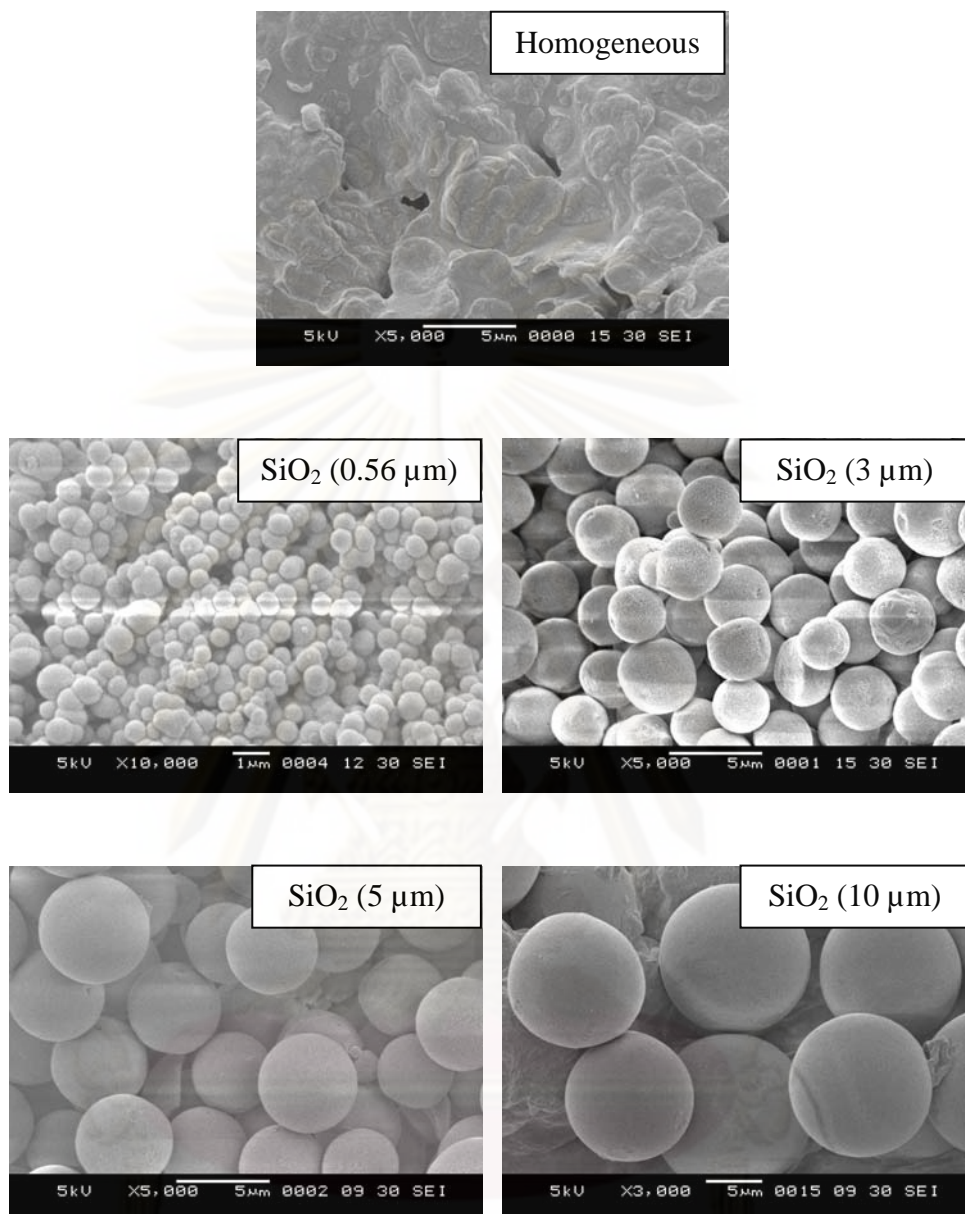


Figure 4.10 SEM micrographs of copolymers obtained with various spherical silica supports

4.3.3 The effect of particle size of spherical silica supports and comonomer on polymers microstructure

^{13}C NMR spectroscopy was used to determine comonomer incorporation and polymer microstructure. The quantitative analysis of triad distribution for all copolymers was calculated. The triad distributions of all copolymers from ex situ impregnation method are shown in **Table 4.7**. The characteristics of ^{13}C NMR spectra (as shown in appendix C) for all copolymers were similar indicating the copolymer of ethylene/1-octene. There are no ^{13}C NMR spectra for polyethylene because it has no insertion of comonomer in polymer chain.

Table 4.7 ^{13}C NMR analysis of and ethylene/1-octene copolymer
(Ex situ impregnation)

System	Triad distribution of copolymer						1-octene insertion (mol %)
	OOO	EOO	EOE	EEE	OEO	OEE	
Homogeneous	0	0	0.085	0.751	0	0.163	8.526
SiO ₂ (0.56 μm)	0	0	0.122	0.743	0	0.135	12.232
SiO ₂ (3μm)	0	0	0.118	0.672	0	0.209	11.812
SiO ₂ (5μm)	0	0	0.128	0.706	0	0.166	12.830
SiO ₂ (10μm)	0	0	0.305	0.124	0	0.571	30.476

E refers to ethylene monomer and O refers to 1-octene comonomer

For all copolymers synthesized from each support exhibited similar triad distribution having the majority of EEE. No triad distribution of EOO and OOO in the copolymers was found. Because the comonomer has the bigger size than the ethylene, which the reaction of the comonomer occurs harder than usual. It implied that the size of each supports did not cause the effect on polymer microstructure. Only the random copolymers can be produced in all systems. Comonomer incorporation increased with the larger particle size. This may be probably due to less steric hindrance. In addition, the 1-octene incorporations in all supported systems were between 11 to 30 mol%, which was higher than the homogeneous system.

4.3.4 The effect of particle size of spherical silica supports on the polyethylene crystallinity

The XRD patterns (**Figure 4.11**) of polyethylene from homogeneous and supported system, which prepared by ex situ impregnation, were showed to confirm that polymers were polyethylene due to polyethylene (homopolymer) cannot be verified with ^{13}C NMR spectra. XRD patterns showed two characteristics peaks at 2θ are 21.8° and 24.3° corresponding to crystalline form of polyethylene [Kuo et al., 2003]. It exhibited that the polyethylene retains crystalline structure although the silica supports are incorporated into the polymer matrix.

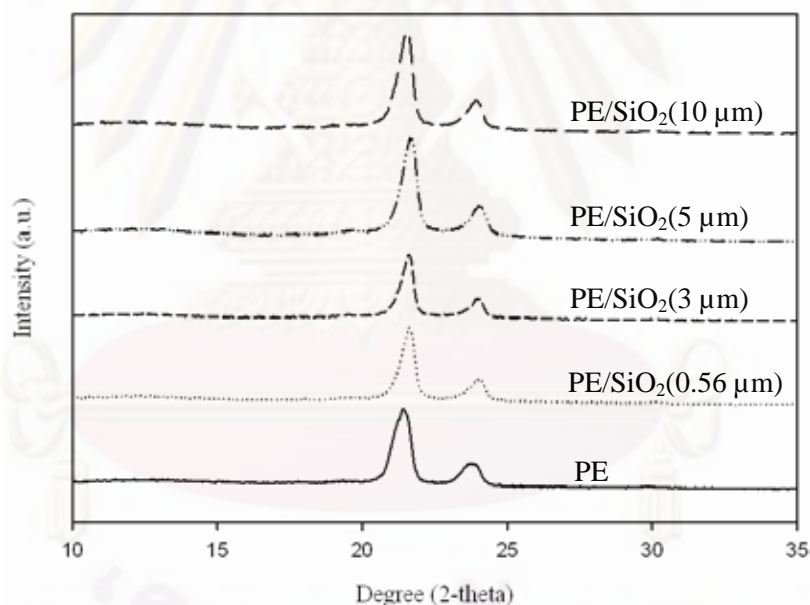


Figure 4.11 XRD patterns of polyethylene (ex situ impregnation)

4.3.5 The effect of particle size of spherical silica supports on melting temperature of polymers

The melting temperatures (T_m) of polymer and copolymer were evaluated by the differential scanning calorimeter (DSC) are shown in **Table 4.8**. DSC curves of the copolymer are also shown in Appendix D.

Table 4.8 Melting temperatures of polymers obtained various silica supports
(Ex situ impregnation)

System	Polymer	T _m (°C)	T _c (°C)	Crystallinity (%)
Homogeneous	E	131.36	115.51	68.81
SiO ₂ (0.56μm)	E	132.72	116.53	53.63
SiO ₂ (3μm)	E	132.42	116.88	52.27
SiO ₂ (5μm)	E	134.79	115.87	48.16
SiO ₂ (10μm)	E	132.47	116.57	46.87
Homogeneous	EO	117.41	98.89	4.70
SiO ₂ (0.56μm)	EO	111.73	95.30	1.85
SiO ₂ (3μm)	EO	113.27	98.67	1.99
SiO ₂ (5μm)	EO	111.68	95.22	1.79
SiO ₂ (10μm)	EO	113.98	99.44	3.18

n.o. refers to not observe, E refers to polyethylene and EO refers to copolymer

Based on DSC measurement of polymer and copolymer in **Table 4.8**, the melting temperature (T_m) for ethylene polymerization had a value in ranged of about 130°C. These indicated that the support type did not significantly effect to T_m of polyethylene. On the other hand, the larger support size reduced the polymer crystallinity because the amount of using catalyst precursor was not equal in each experiment, the amount of using was SiO₂ (10μm) > SiO₂ (5μm) > SiO₂ (3μm) > SiO₂ (0.56μm). It implied that the quantity of supports influenced the crystallization of polymer but not affect to melting temperature. For EO copolymer, it was found that the increased comonomer incorporation basically decreased the crystallization of polymer and melting temperature is proportional to polymer crystallinity. Thus ¹³C NMR and DSC results were in agreement. However, the system of SiO₂(10μm) exhibited the distinct result from the others. In supported system, the highest crystallization for SiO₂(10μm) was observed although it had the highest 1-octene incorporation. This should be suggested that besides the effect of 1-octene insertion on T_m and crystallinity, and the SiO₂ particle size also affect the T_m of polymer. It was reported that the particles in polymer matrix can act as nucleating agent which increase the crystallinity of polymer. When the particles are too small, they may locate themselves in the interlamellar spaces, which leave little room for additional

crystallization [Chaichana et al., 2007]. So, the presence of small particles may even inhibit crystallization. As known, the polyethylene obviously showed the higher melting temperature than EO copolymer since the comonomer insertion in copolymer decrease the crystallization.

4.4 Comparison of catalytic activity between in situ and ex situ impregnation method

Table 4.9 shows the comparison of polymerization activities of polyethylene synthesized by in situ impregnation and ex situ impregnation method.

Table 4.9 Ethylene polymerization activities from various silica-supported MAO prepared by in situ and ex situ impregnation method

System	Impregnation method	Polymerization time (sec)	Polymer yield ^a (g)	Catalytic Activity ^b (kg Pol.mol.Zr ⁻¹ .h ⁻¹)
SiO ₂ (3 μm)	In situ	109	0.5756	12,674
SiO ₂ (5 μm)	In situ	114	0.5425	11,421
SiO ₂ (10 μm)	In situ	120	0.5526	11,052
SiO ₂ (3 μm)	Ex situ	105	0.6275	14,343
SiO ₂ (5 μm)	Ex situ	72	0.6245	20,816
SiO ₂ (10 μm)	Ex situ	87	0.7406	20,431

^a The polymer yield was fixed limited by 0.018 mol of ethylene consumption.

^b Measurement at polymerization temperature of 70°C, [Ethylene] = 0.018 mole, [Zr]_{cat} = 5×10⁻⁵ M, [Al]_{MAO}/[Zr]_{cat} = 1135, [Al]_{TMA}/[Zr]_{cat} = 2500 in toluene with total volume = 30 ml.

It was found that silica-supported MAO prepared by ex situ impregnation method exhibited higher activities than in situ impregnation method. The different trend from each system is occurred although the values from these two systems look like similar. The polymerization activities obtained from in situ impregnation method was in the order of SiO₂ (3 μm) > SiO₂ (5 μm) > SiO₂ (10 μm), but ex situ impregnation method was SiO₂ (5 μm) > SiO₂ (10 μm) > SiO₂ (3 μm). These results were attributed to that the in situ impregnation method did not have the completely

impregnation, which caused the mainly MAO still attached only at the outer surface area of supports. Furthermore, the main cause that influence to the activity is only outer surface area of supports. Another reason is active site thoroughly present in reaction medium not only on the support, so catalytic activities from in situ impregnation were no significant difference. On the other hand, the silica supports were really impregnated with MAO and dried under vacuum before used as catalyst precursors in ex situ impregnation method. Therefore, the interaction between $[Al]_{MAO}$ and supports, proved by TGA measurement, directly affected to the polymerization activities of supported system.



ศูนย์วิจัยทรัพยากร
จุฬาลงกรณ์มหาวิทยาลัย

CHAPTER V

CONCLUSIONS & RECOMMENDATIONS

5.1 CONCLUSIONS

The experiment presented in this thesis aimed to investigate the effect of particle diameter of spherical silica-supported metallocene catalyst on the catalytic activity and polymer characteristic via ethylene and ethylene/1-octene polymerization. The experiment was divided into two parts which different in the impregnation method (In situ and Ex situ impregnation). In the first part, the polymerization reaction was performed using a zirconocene/MAO catalyst, which prepared by in situ impregnation method. It was found that the activities of the supported system were lower than the homogeneous one due to the supporting effect. Among the supported system for both homo- and copolymerization, the catalytic activity obtained from the smaller spherical silica was the highest among the others [$\text{SiO}_2(3\mu\text{m}) > \text{SiO}_2(5\mu\text{m}) > \text{SiO}_2(10\mu\text{m})$] attributed to larger outer surface area, which enhanced the distribution of active sites on supports. On the other hand, $\text{SiO}_2(0.56\mu\text{m})$ exhibited the lowest activity because of higher steric hindrance. The ethylene/1-octene copolymerization gave higher activity than ethylene polymerization due to comonomer effect in copolymerization. It was obviously seen that all copolymers had the similar triad distribution. The larger particle size rendered the higher 1-octene incorporation.

The second part was similar to first part but catalyst precursors prepared by ex situ impregnation method. For ethylene polymerization, the activities of the supported system were also lower than the homogeneous one. In the supported system, the slight difference in the polymerization activities was apparently found. $\text{SiO}_2(0.56\mu\text{m})$ with submicron size showed the lowest activity due to more steric hindrance of small particle. For the micron-sized support, the catalytic activities were in the order of $\text{SiO}_2(5\mu\text{m}) > \text{SiO}_2(10\mu\text{m}) > \text{SiO}_2(3\mu\text{m})$. The stronger interaction of support and MAO caused the lower in catalytic activity. The result in term of comonomer effect is similar to the first part. Considering the polymer microstructure, only the random

copolymers can be produced in all systems. Comonomer incorporation increased with the larger particle size.

5.2 RECOMMENDATIONS

- Polymer from in situ impregnation method should be characterized with DSC and SEM.
- ICP should be used to examine the amount of $[Al]_{MAO}$ on catalyst precursor because ICP is bulk technique.
- The larger particle size of spherical silica supports should be investigated.
- The modification of support surface should be further studied to improve surface tension.
- Synthesis of spherical silica, TEOS should be used as silica source instead of TMOS, which is expensive and unavailable.

REFERENCES

- Alt, H. G., and Köppl, A. Effect of the nature of metallocene complexes of group IV metals on their performance in catalytic ethylene and propylene polymerization. **Chemical Reviews** 100 (2000): 1205-1221.
- Britto, M. L., Galland, G. B., dos Santos, J. H. Z., and Forte, M.C. Copolymerization of ethylene and 1-hexene with $\text{Et}(\text{Ind})_2\text{ZrCl}_2$ in hexane. **Polymer** 42 (2001): 6355-6361.
- Bunchongturakarn, S., Jongsomjit, B., and Praserttham, P. Impact of bimodal pore MCM-41-supported zirconocene/dMMAO catalyst on copolymerization of ethylene/1-octene. **Catalysis Communications** 9 (2008): 789-795.
- Cam, D., Giannini, U. Concerning the reaction of zirconocene dichloride and methylalumoxane: Homogeneous Ziegler-Natta catalytic system for olefin polymerization. **Makromolekulare Chemie** 193 (1992): 1049-1055.
- Castonguay, L.A. and Rappe, A.K. Ziegler-Natta catalysis. A theoretical study of the isotactic polymerization of propylene. **Journal of the American Chemical Society** 114 (1992): 5832-5842
- Chaichana, E., Jongsomjit, B., and Praserttham, P. Effect of nano-SiO₂ particle size on the formation of LLDPE/SiO₂ nanocomposite synthesized via in situ polymerization with metallocene catalyst. **Chemical Engineering Science** 62 (2007): 899-905.
- Chen, Y.X., Rausch, M.D., and Chein, J.C.W. Heptane-Soluble Homogenous Zirconocene Catalyst – Synthesis of a Single Diastereomer, Polymerization Catalysis, and Effect of Silica Supports. **Journal of Polymer Science Part A: Polymer Chemistry** 33 (1995): 2093-2108
- Chu, K.-J., Soares, J. B. P., and Penlidis, A. Polymerization mechanism for in situ supported metallocene catalysts. **Journal of Polymer Science Part A: Polymer Chemistry** 38 (2000): 462-468.
- Chum, P. S., and Swogger, K. W. Olefin polymer technologies-History and recent progress at The Dow Chemical Company. **Progress in Polymer Science** 33 (2008): 797-819.
- Ciardelli, F., Altomare, A., and Michelotti, M. From homogeneous to supported metallocene catalysts. **Catalysis Today** 41 (1998): 149-157.

- Collins, S., Kelly, W. M., and Holden, D.A. Polymerization of propylene using supported, chiral, ansa-metallocene catalysts: Production of polypropylene with narrow molecular weight distributions. **Macromolecules** 25 (1992): 1780-1785.
- De Marques, M. F. V., and Conte, A. The influence of the preparing conditions of SiO₂ supported Cp₂ZrCl₂ catalyst on ethylene polymerization. **Journal of Applied Polymer Science** 86 (2002): 2054-2061.
- Dos Santos, J.H.Z., Dorneles, S., Stedile, F., Dupont, J., Forte, M.M.C., and Baumovl, I.J.R. Silica supported zirconocenes and Al-based cocatalysts: Surface metal loading and catalytic activity. **Macromolecular Chemistry and Physics** 198 (1997): 3529-3537
- Duchateau, R. Incompletely condensed silsesquioxanes: Versatile tools in developing silica-supported olefin polymerization catalysts. **Chemical Reviews** 102 (2002): 3525-3542.
- Fink, G., Steinmetz, B., Zechlin, J., Przybyla, C., and Tesche, B. Propene polymerization with silica-supported metallocene/MAO catalysts. **Chemical Reviews** 100 (2000): 1377-1390.
- Fink, G., Tesche, B., Korber, F., and Knoke, S. The particle-forming process of SiO₂-supported metallocene catalysts. **Macromolecular Symposia** 173 (2001): 77-87.
- Galland, G.B., Quijada, P., Mauler, R.S., and De Menezes, S.C. Determination of reactivity ratios for ethylene/ α -olefin copolymerization catalysed by the C₂H₄[Ind]₂ZrCl₂/methylaluminoxane system. **Macromolecular Rapid Communications** 17 (1996): 607-613.
- Galli, P., and Vecellio, G. Technology: Driving force behind innovation and growth of polyolefins. **Progress in Polymer Science** 26 (2001): 1287-1336.
- Gupta, V. K., Satish, S., and Bhardwaj, I.S. Metallocene complexes of group 4 elements in the polymerization of monoolefins. **Journal of Macromolecular Science - Reviews in Macromolecular Chemistry and Physics** C34 (1994): 439-514.
- Hagimoto, H., Shiono, T., and Ikeda, T. Supporting effect of methylaluminoxane on the living polymerization of propylene with a chelating (diamide)dimethyltitanium complex. **Macromolecular Chemistry and Physics** 205 (2004): 19-26.

- Harrison, D., Coulter, I.M., Wang, S., Nistala, S., Kuntz, B.A., Pigeon, M., Tian, J., and Collins, S. Olefin polymerization using supported metallocene catalysts: Development of high activity catalysts for use in slurry and gas phase ethylene polymerizations. **Journal of Molecular Catalysis A: Chemical** 128 (1998): 65-77
- Hlatky, G. G. Heterogeneous single-site catalysts for olefin polymerization. **Chemical Reviews** 100 (2000): 1347-1376.
- Hlatky, G.G. and Upton, D.J. Supported ionic metallocene polymerization catalysts. **Macromolecules** 29 (1996): 8019-8020
- Huang, J., and Rempel, G. L. Ziegler-Natta catalysts for olefin polymerization: Mechanistic insights from metallocene systems. **Progress in Polymer Science** 20 (1995): 459-526.
- James, C., Randall. A review of high resolution liquid ^{13}C nuclear magnetic resonance characterization of ethylene-based polymers. **Macromolecular Chemistry and Physics** C29 (1989): 201.
- Jiamwijitkul, S., Jongsomjit, B., and Prasertthdam, P. Effect of boron-modified MCM-41-supported dMMAO/zirconocene catalyst on copolymerization of ethylene/1-octene for LLDPE synthesis. **Iranian Polymer Journal** 16 (2007): 549-559.
- Jongsomjit, B., Kaewkrajang, P., and Prasertthdam, P. Effect of silane-modified silica/MAO-supported $\text{Et}[\text{Ind}]_2\text{ZrCl}_2$ metallocene catalyst on copolymerization of ethylene. **European Polymer Journal** 40 (2004): 2813-2817.
- Jongsomjit, B., Kaewkrajang, P., Wanke, S.E., and Prasertthdam, P. A comparative study of ethylene/ α -olefin copolymerization with silane-modified silica-supported MAO using zirconocene catalysts. **Catalysis Letters** 94 (2004): 205-208.
- Jongsomjit, B., Ngamposri, S., and Prasertthdam, P. Application of silica/titania mixed oxide-supported zirconocene catalyst for synthesis of linear low-density polyethylene. **Industrial and Engineering Chemistry Research** 44 (2005): 9059-9063.
- Jongsomjit, B., Ngamposri, S., and Prasertthdam, P. Catalytic activity during copolymerization of ethylene and 1-hexene via mixed $\text{TiO}_2/\text{SiO}_2$ -supported MAO with $\text{rac-Et}[\text{Ind}]_2\text{ZrCl}_2$ metallocene catalyst. **Molecules** 10 (2005): 672-678.

- Jongsomjit, B., Praserttham, P., and Kaewkrajang, P. A comparative study on supporting effect during copolymerization of ethylene/1-olefins with silica-supported zirconocene/MAO catalyst. **Materials Chemistry and Physics** 86 (2004): 243-246.
- Jüngling, S., Koltzenburg, S., and Mülhaupt, R. Propene homo- and copolymerization using homogeneous and supported metallocene catalysts based on MeSi(2-Me-Benz[e]Ind)ZrCl. **Journal of Polymer Science Part A: Polymer Chemistry** 35 (1997): 1-8.
- Kaminsky, W., and Arndt, M. Metallocenes for Polymer Catalysis. **Advances in Polymer Science** 127 (1997): 143-187.
- Kaminsky, W., and Laban A. Metallocene catalysis. **Applied Catalysis A: General** 222 (2001): 47-61.
- Klapper, M., Nenov, S., Diesing, T., and Müllen, K. Morphology control in metallocene polymerization; organic supports vs. non-aqueous emulsion polymerization. **Macromolecular Symposia** 260 (2007): 90-97.
- Kuo, S.-W., Huang, W.-J., Huang, S.-B., Kao, H.-C., and Chang, F.-C. Syntheses and characterization of in situ blended metallocene polyethylene/clay nanocomposites. **Polymer** 44 (2003): 7709-7719.
- Lee, D.H., Shin, S.Y., and Lee, D.H. Ethylene polymerization with metallocene and trimethylaluminum-treated silica. **Macromolecular Symposia** 97 (1995): 195-203
- Liu, S., Yu, G., and Huang, B. Polymerization of ethylene by zirconocene $B(C_6F_5)_3$ catalysts with aluminum compounds. **Journal of applied polymer science** 66 (1997): 1715-1720
- Marques, M. D. F. V., da Silva, O. F. C., Coutinho, A. C. S. L. S., and de Araujo, A.S. Ethylene polymerization catalyzed by metallocene supported on mesoporous materials. **Polymer Bulletin** 61 (2008): 415-423.
- Paredes, B., Soares, J. B. P., Van Grieken, R., Carrero, A., and Suarez, I. Characterization of ethylene-1-hexene copolymers made with supported metallocene catalysts: Influence of support type. **Macromolecular Symposia** 257 (2007): 103-111.
- Pasynkiewicz, S. Aluminoxanes: Synthesis, structures, complexes and reactions. **Polyhedron** 9 (1990): 429-453.

- Pothirat, T., Jongsomjit, B., and Prasertthdam, P. A comparative study of SiO₂- and ZrO₂-supported zirconocene/MAO catalysts on ethylene/1-olefin copolymerization. **Catalysis Communications** 9 (2008): 1426-1431.
- Przbyla, C., Tesche, B., and Fink, G. Ethylene/hexene copolymerization with the heterogeneous catalyst system SiO₂/MAO/rac-MeSi[2-Me-4-Ph-Ind]ZrCl: The filter effect. **Macromolecular Rapid Communications** 20 (1999): 328-332.
- Pullukat, T. J., and Hu, Y. Effect of silica supports on olefin polymerization catalyst performance. **Current Achievements on Heterogeneous Olefin Polymerization Catalysts** (2004): 57.
- Quijadal, R., Rojas, R., Alzamora, L., Retuert, J., and Rabagliati, F.M. Study of metallocene supported on porous and nonporous silica for the polymerization of ethylene. **Catalysis letters** 46 (1997):107-112.
- Ribeiro, M. R., Deffieux, A., and Portela, M.F. Supported metallocene complexes for ethylene and propylene polymerizations: preparation and activity. **Industrial and Engineering Chemistry Research** 36 (1997): 1224-1237.
- Richards, C.T. Plastic Rubber Composites **Processing and Applications** 27 (1) (1998): 3-7.
- Roscoe, S. B., Fréchet, J. M. J., Walzer, J. F., and Dias, A. J. Polyolefin spheres from metallocenes supported on noninteracting polystyrene. **Science** 280 (1998): 270-273.
- Sarzotti, D. M., Soares J. B. P., and Penlidis A. Ethylene/1-hexene copolymers synthesized with a single-site catalyst: Crystallization analysis fractionation, modeling, and reactivity ratio estimation. **Journal of Polymer Science Part B: Polymer Physics** 40 (2002): 2595-2611.
- Schumacher, J. W., and Borruso A. V. **Chemical Economics Handbook, SRI International** (2002) 580.
- Severn, J. R., and Chadwick J. C. **Tailor-Made Polymers via immobilization of alpha-olefin polymerization catalysts**, Weinheim, WILEY-VCH Verlag GmbH & Co., 2008.
- Severn, J. R., Chadwick, J. C., Duchateau, R., and Friederichs, N. "Bound but not gagged" Immobilizing single-site α -olefin polymerization catalysts. **Chemical Reviews** 105 (2005): 4073-4147.

- Silva, A. L. S. S., Costa, Marcos A. S., de Santa Maria, L. C., Menezes, Sonia M. C., and Coutinho, Fernanda M. B. Copolymerization of ethylene with high α -olefins by biscyclopentadienylzirconium dichloride. **Progress and Development of Catalytic Olefin Polymerization** (2000): 204.
- Smit, M., Zheng, X., Brüll, R., Loos, J., Chadwick, J. C., and Koning, C. E. Effect of 1-hexene comonomer on polyethylene particle growth and copolymer chemical composition distribution. **Journal of Polymer Science Part A: Polymer Chemistry** 44 (2006): 2883-2890.
- Soga, K., and Shiono, T. Ziegler-Natta catalysts for olefin polymerizations. **Progress in Polymer Science** 22 (1997): 1503-1546.
- Srinivasa Reddy, S., and Sivaram, S. Homogeneous metallocene-methylaluminoxane catalyst systems for ethylene polymerization. **Progress in Polymer Science** 20 (1995): 309-367.
- Tait, P.J.T. and Monterio, M.G.K. **Mecton'96** (June 1996)
- Tritto, I., Sacchi, M. C., and Li, S. NMR study of the reactions in $\text{Cp}_2\text{TiMeCl}/\text{AlMe}_3$ and $\text{Cp}_2\text{TiMeCl}/\text{methylaluminoxane}$ systems, catalysts for olefin polymerization. **Macromolecular Rapid Communications** 15 (1994): 217-223.
- Van Grieken, R., Carrero, A., Suarez, I., and Paredes, B. Effect of 1-hexene comonomer on polyethylene particle growth and kinetic profiles. **Macromolecular Symposia** 259 (2007): 243-252.
- Wongwaiwattanakul, P., and Jongsomjit, B. Copolymerization of ethylene/1-octene via different pore sized silica-based-supported zirconocene/dMMAO catalysts. **Catalysis Communication** 10 (2008): 118-122.
- Xu, J., Deng, Y., Feng, L., Cui, C., and Chen, W. Temperature rising elution fractionation of syndiotactic polypropylene prepared by homogeneous and supported metallocene catalysts **Polymer Journal** 30 (1998): 824-827
- Yamada, Y. and Yano, K. Synthesis of monodispersed super-microporous/mesoporous silica spheres with diameters in the low submicron range. **Microporous and Mesoporous Materials** 93 (2006): 190-198.
- Zhang, Z., Yang, L., Wang, Y., Luo, G., and Dai, Y. Morphology controlling of micrometer-sized mesoporous silica spheres assisted by polymers of polyethylene-glycol and methyl cellulose. **Microporous and Mesoporous Materials** 115 (2008): 447-453.

Zheng, X., and Loos, J. Morphology evolution in the early stages of olefin polymerization. **Macromolecular Symposia** 236 (2006): 249-258.

Zheng, X., Smit, M., Chadwick, J. C., and Loos, J. Fragmentation behavior of silica-supported metallocene/MAO catalyst in the early stages of olefin polymerization. **Macromolecules** 38 (2005): 4673-4678.

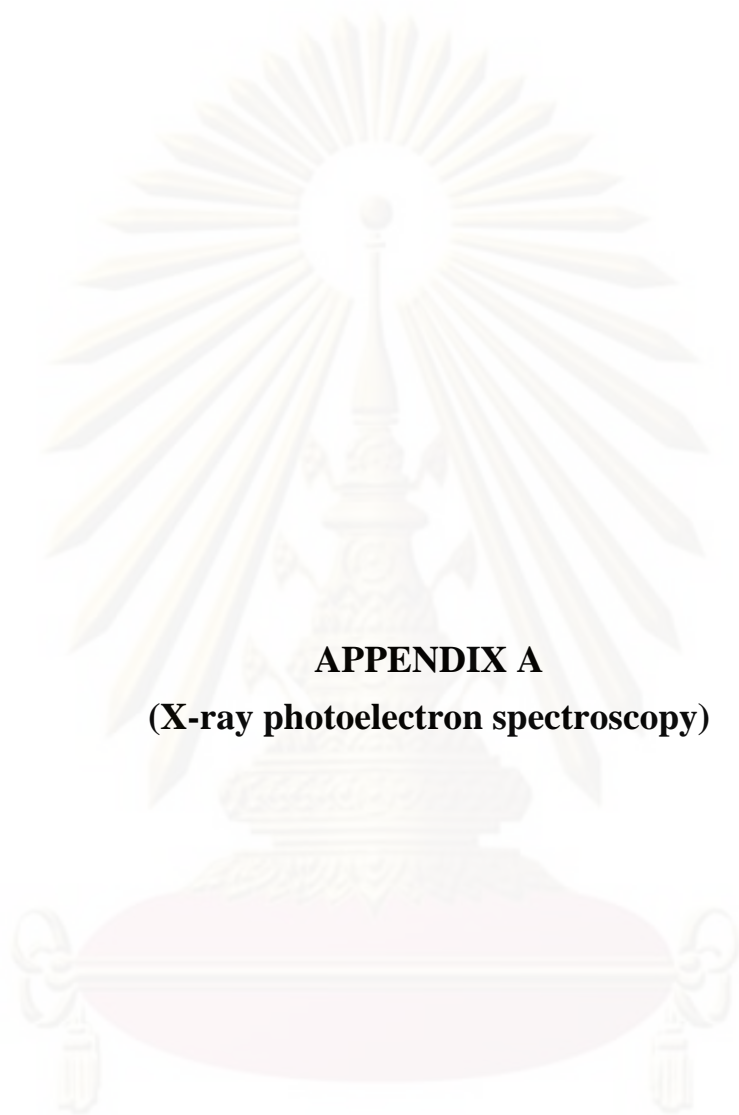


ศูนย์วิจัยทรัพยากร
จุฬาลงกรณ์มหาวิทยาลัย



APPENDICES

ศูนย์วิทยทรัพยากร
จุฬาลงกรณ์มหาวิทยาลัย



APPENDIX A
(X-ray photoelectron spectroscopy)

ศูนย์วิจัยทรัพยากร
จุฬาลงกรณ์มหาวิทยาลัย

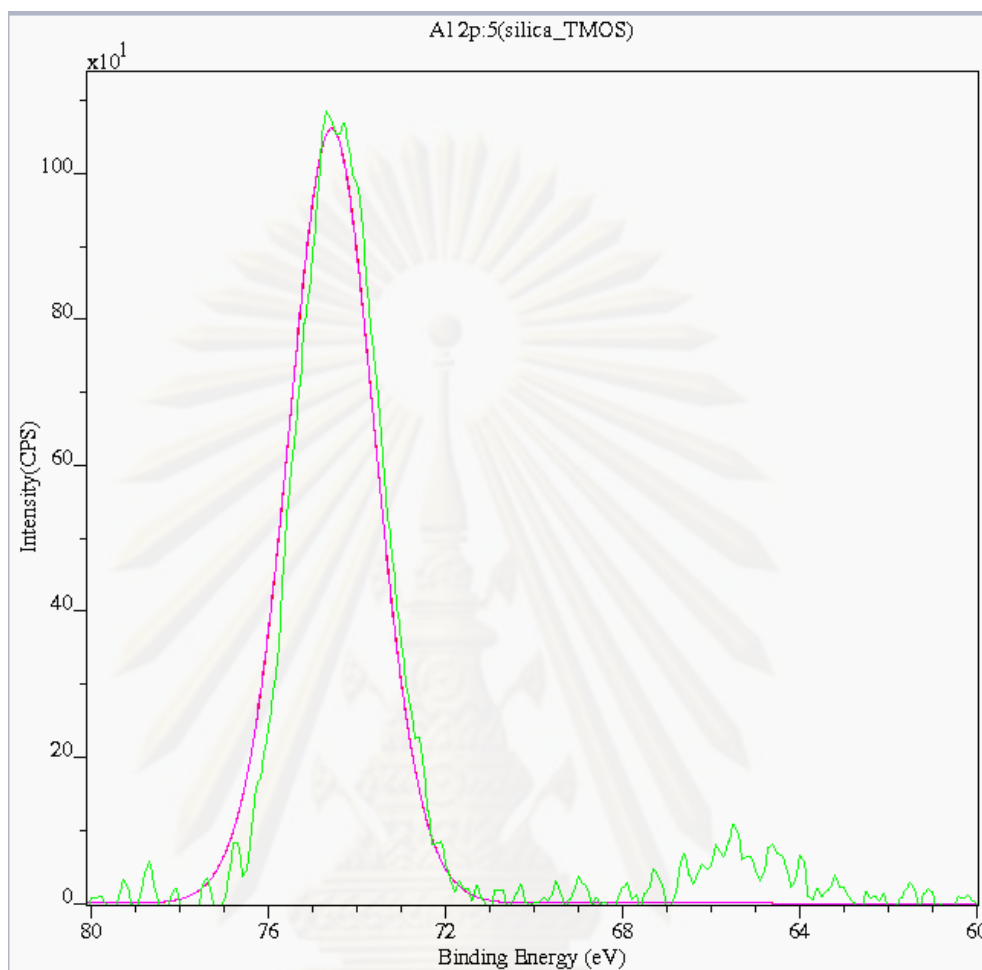


Figure A-1 The XPS profile of Al_{2p} on SiO₂ (0.56μm) support

Table A-1 Binding energy (BE) and % mass concentration of SiO₂ (0.56μm)

Peak	Position BE (ev)	FWHM (ev)	Atomic Mass	Atomic Conc %	Mass Conc %
O _{1s}	531.0	3.132	15.999	61.57	53.95
C _{1s}	285.0	2.393	12.011	13.22	8.70
Si _{2p}	101.0	1.893	28.086	1.48	2.28
Al _{2p}	74.6	2.271	26.982	23.73	35.07

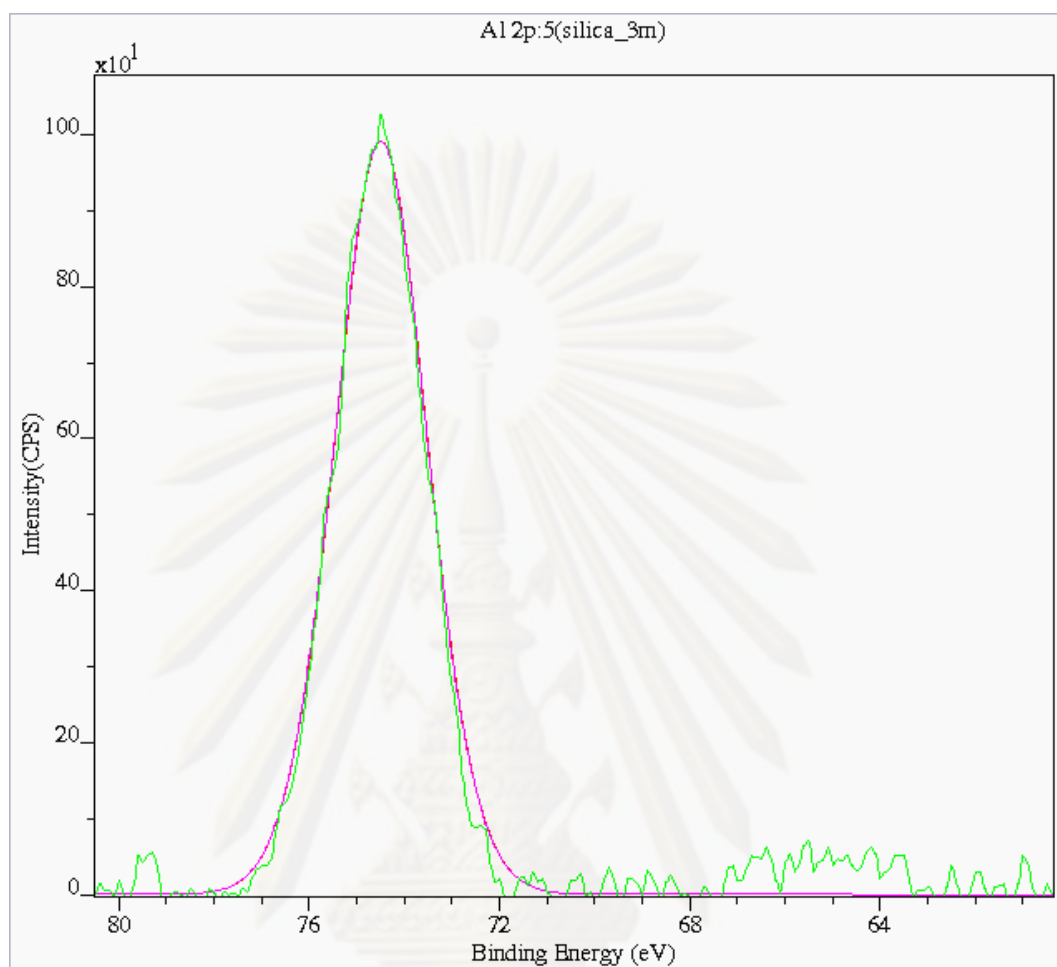


Figure A-2 The XPS profile of Al_{2p} on SiO₂ (3 μm) support

Table A-2 Binding energy (BE) and % mass concentration of SiO₂ (3 μm)

Peak	Position BE (ev)	FWHM (ev)	Atomic Mass	Atomic Conc %	Mass Conc %
O _{1s}	532.2	3.005	15.999	59.47	52.78
C _{1s}	285.0	2.688	12.011	16.44	10.95
Si _{2p}	103.0	2.480	28.086	3.14	4.90
Al _{2p}	74.5	2.265	26.982	20.95	31.37

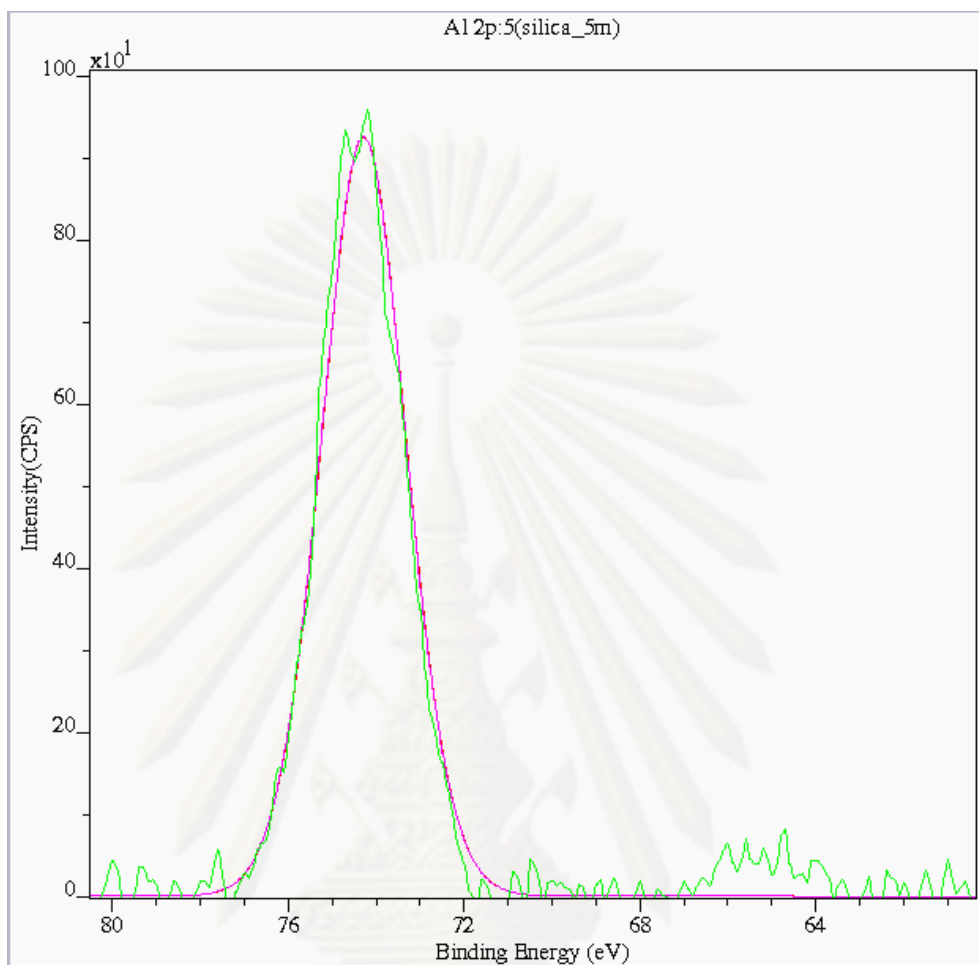


Figure A-3 The XPS profile of Al_{2p} on SiO₂ (5 μm) support

Table A-3 Binding energy (BE) and % mass concentration of SiO₂ (5 μm)

Peak	Position BE (ev)	FWHM (ev)	Atomic Mass	Atomic Conc %	Mass Conc %
O _{1s}	532.0	3.018	15.999	57.27	51.60
C _{1s}	285.0	2.567	12.011	19.66	13.30
Si _{2p}	101.3	1.234	28.086	0.63	0.99
Al _{2p}	74.3	2.234	26.982	22.45	34.11

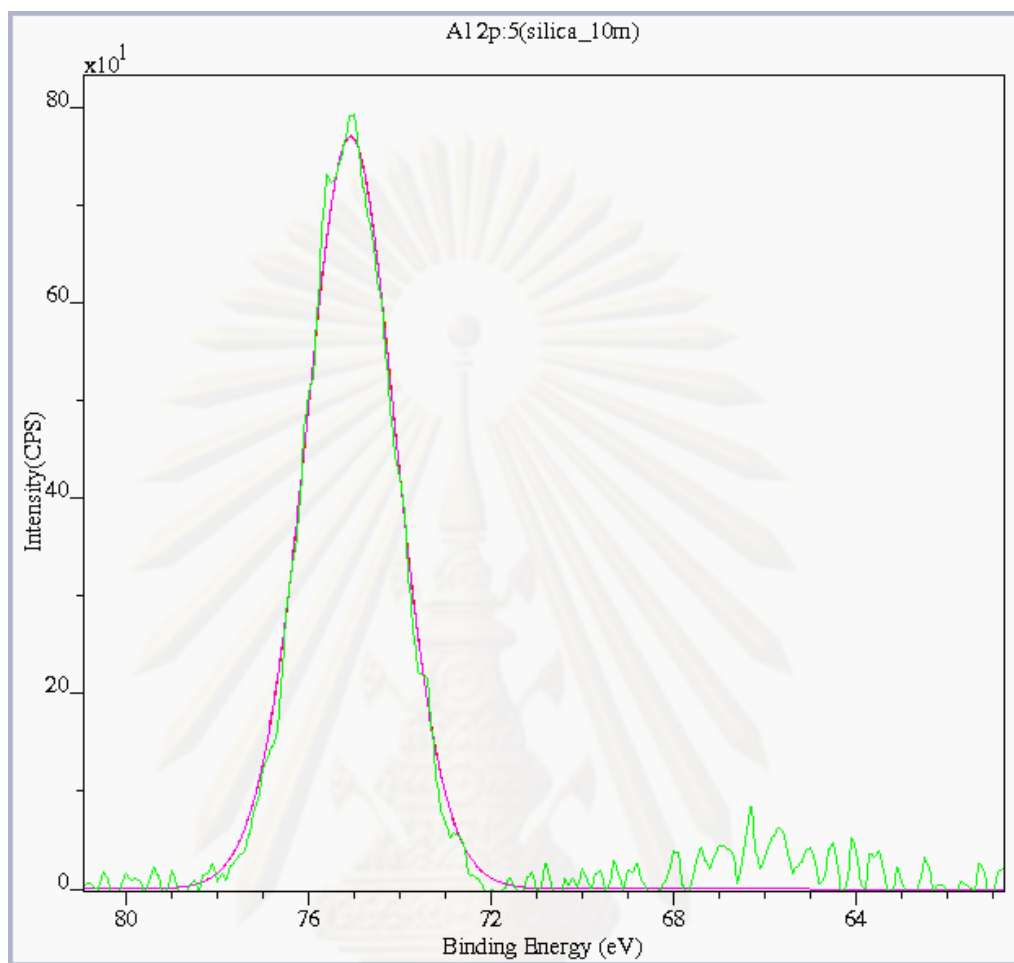
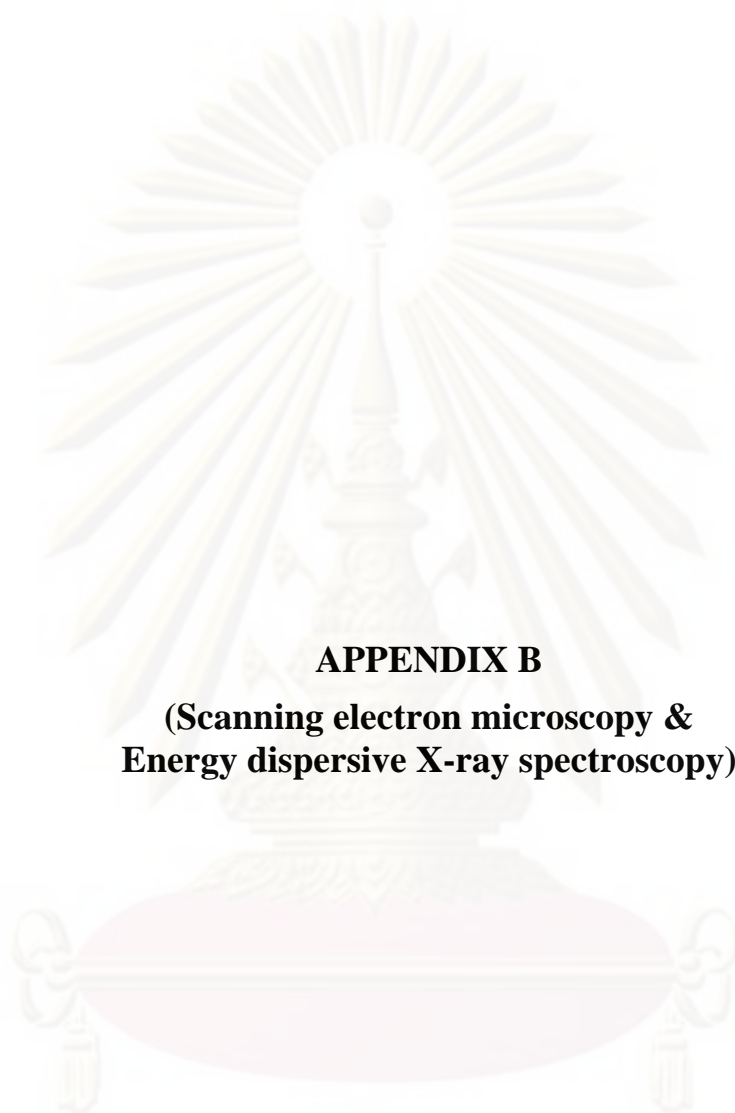


Figure A-4 The XPS profile of Al_{2p} on SiO₂ (10 μm) support

Table A-4 Binding energy (BE) and % mass concentration of SiO₂ (10 μm)

Peak	Position BE (ev)	FWHM (ev)	Atomic Mass	Atomic Conc %	Mass Conc %
O _{1s}	532.7	3.188	15.999	56.56	50.19
C _{1s}	285.0	2.536	12.011	18.73	12.48
Si _{2p}	102.6	3.199	28.086	5.72	8.91
Al _{2p}	75.1	2.292	26.982	18.99	28.42



APPENDIX B

**(Scanning electron microscopy &
Energy dispersive X-ray spectroscopy)**

ศูนย์วิจัยทรัพยากร
จุฬาลงกรณ์มหาวิทยาลัย

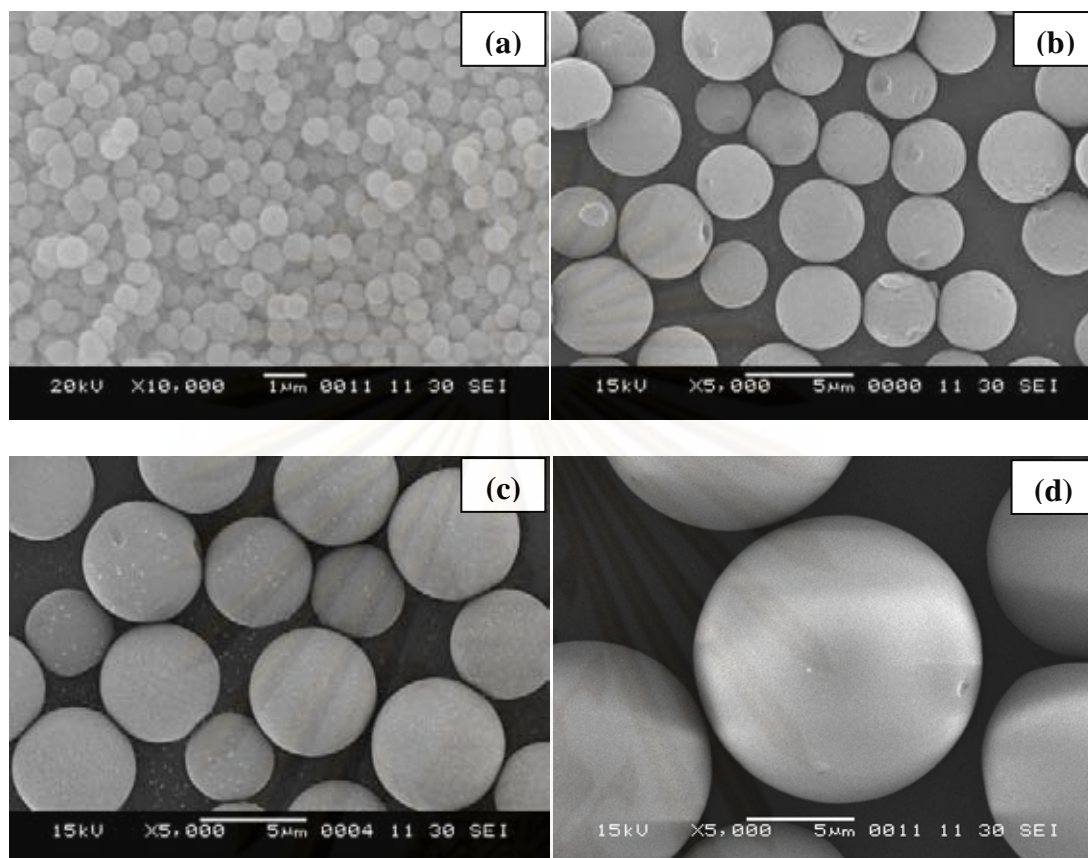


Figure B-1 SEM micrographs of various spherical silica supports before MAO impregnation; (a) $\text{SiO}_2(0.56 \mu\text{m})$, (b) $\text{SiO}_2(3 \mu\text{m})$, (c) $\text{SiO}_2(5 \mu\text{m})$ and (d) $\text{SiO}_2(10 \mu\text{m})$

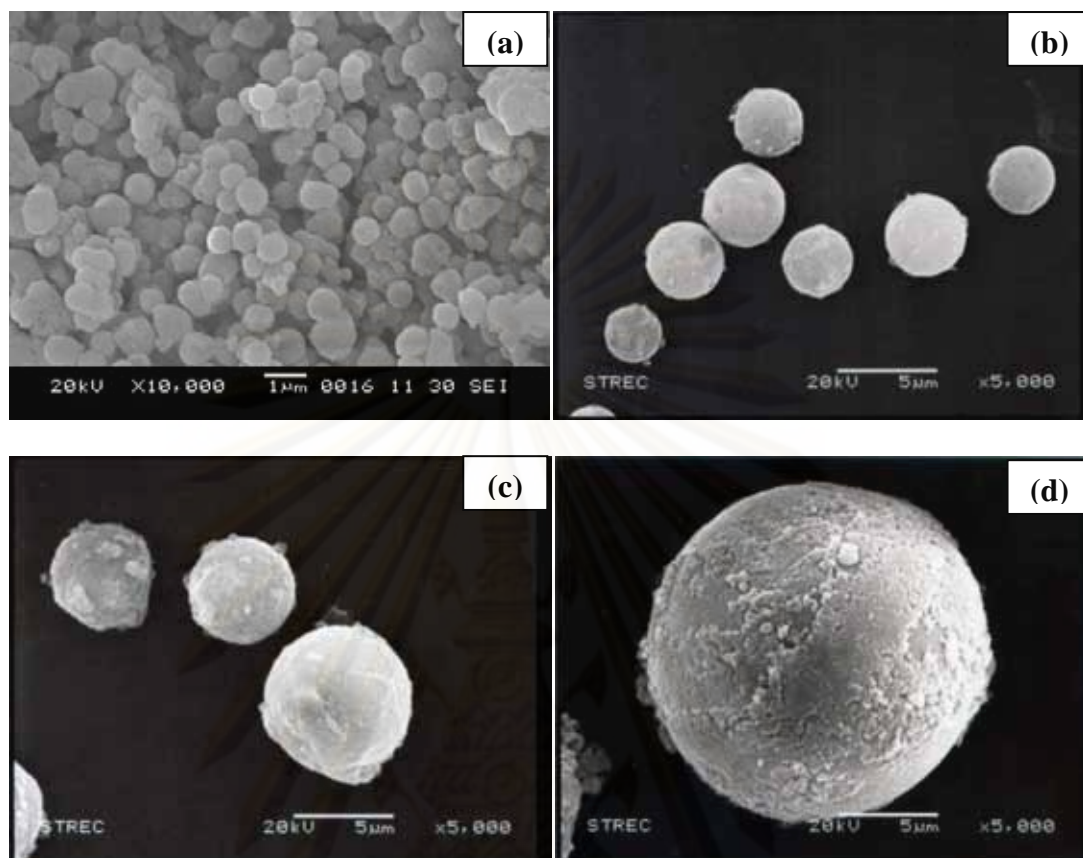


Figure B-2 SEM micrographs of various spherical silica supports after MAO ex situ impregnation; (a) SiO_2 (0.56 μm), (b) SiO_2 (3 μm), (c) SiO_2 (5 μm) and (d) SiO_2 (10 μm)

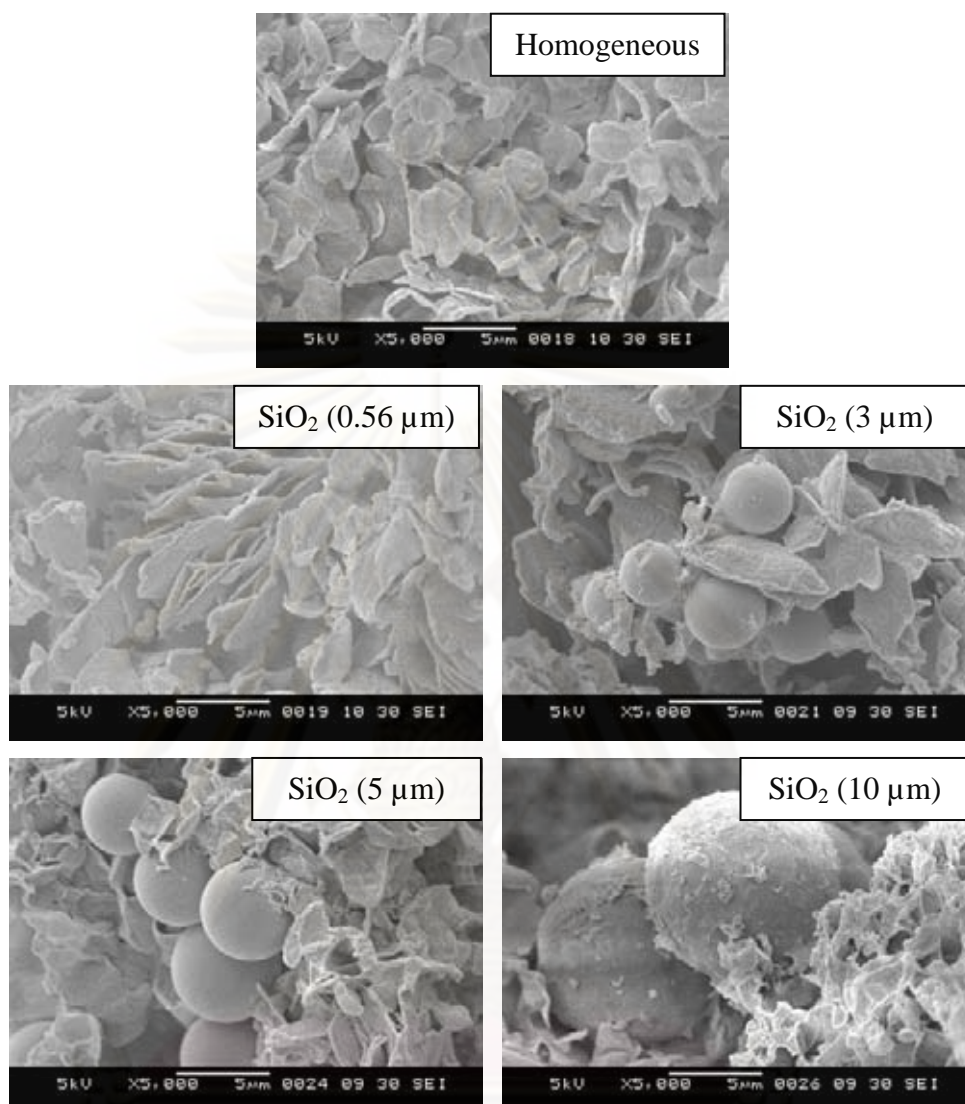


Figure B-3 SEM micrographs of polyethylene obtained with various spherical silica supports

ศูนย์วิทยทรัพยากร
จุฬาลงกรณ์มหาวิทยาลัย

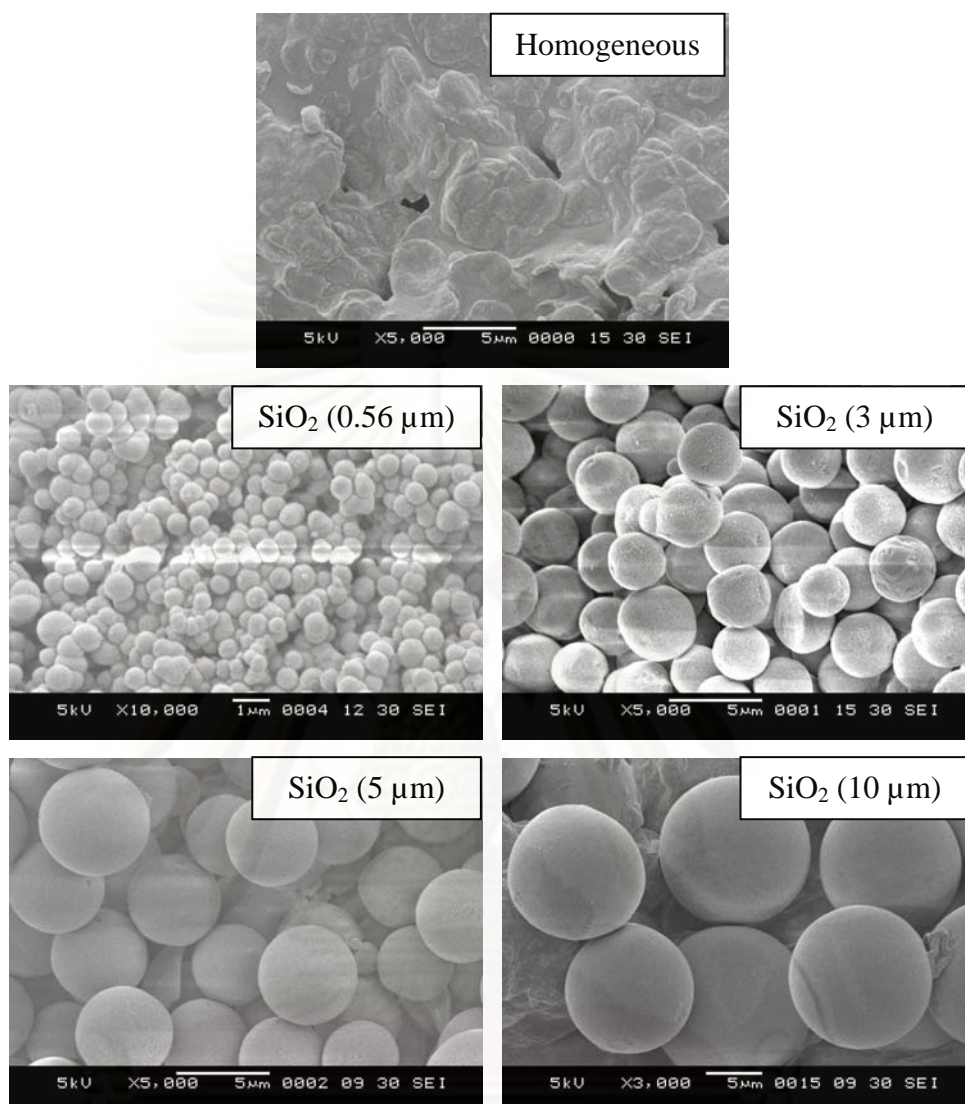


Figure B-4 SEM micrographs of copolymers obtained with various spherical silica supports

ศูนย์วิทยทรัพยากร
จุฬาลงกรณ์มหาวิทยาลัย

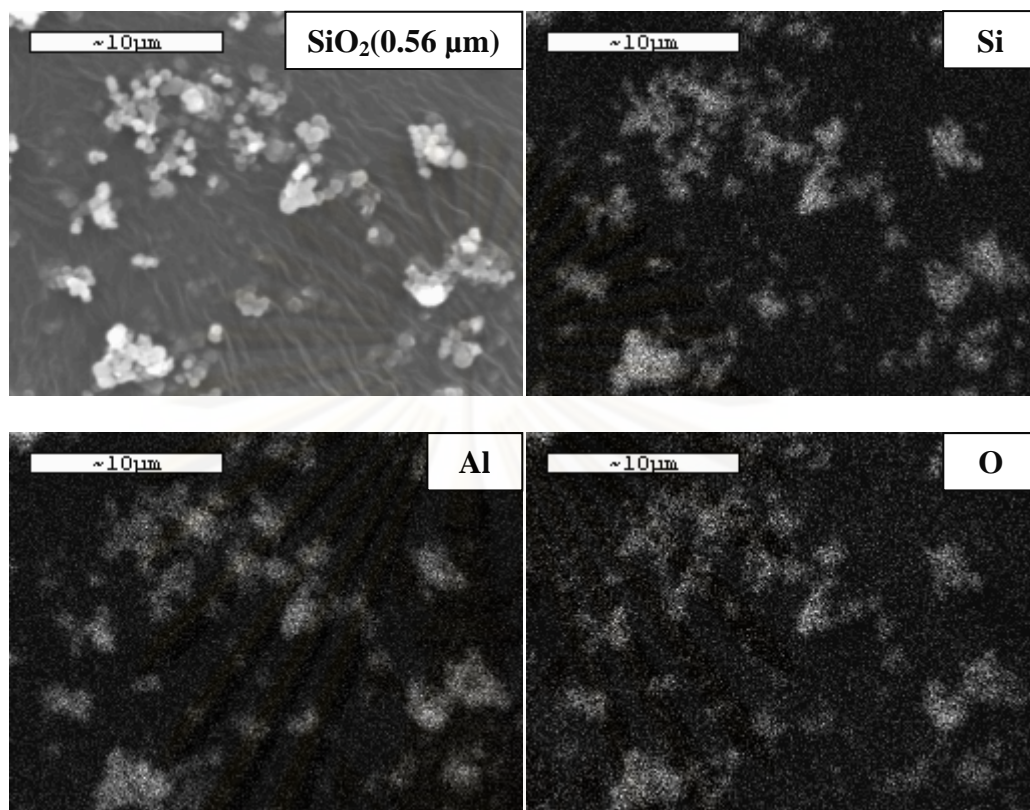


Figure B-5 EDX mapping of $\text{SiO}_2(0.56 \mu\text{m})$ supports after MAO impregnation.

ศูนย์วิจัยทรัพยากร
จุฬาลงกรณ์มหาวิทยาลัย

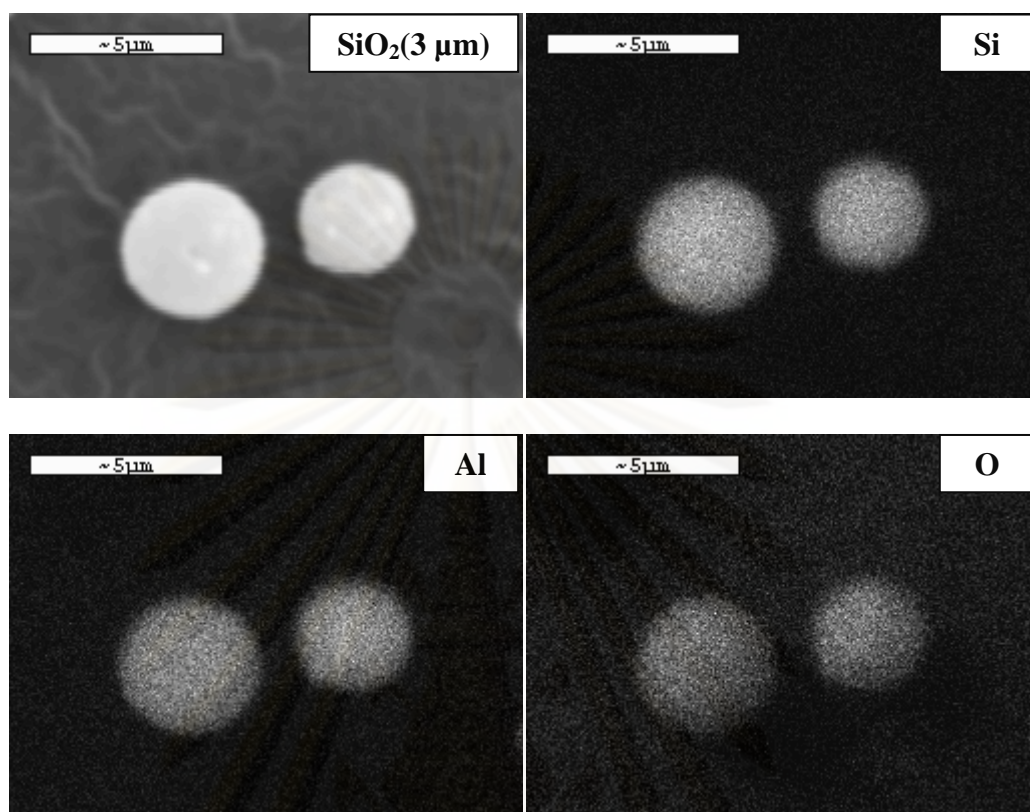


Figure B-6 EDX mapping of SiO₂(3 μm) supports after MAO impregnation.

ศูนย์วิจัยทรัพยากร
จุฬาลงกรณ์มหาวิทยาลัย

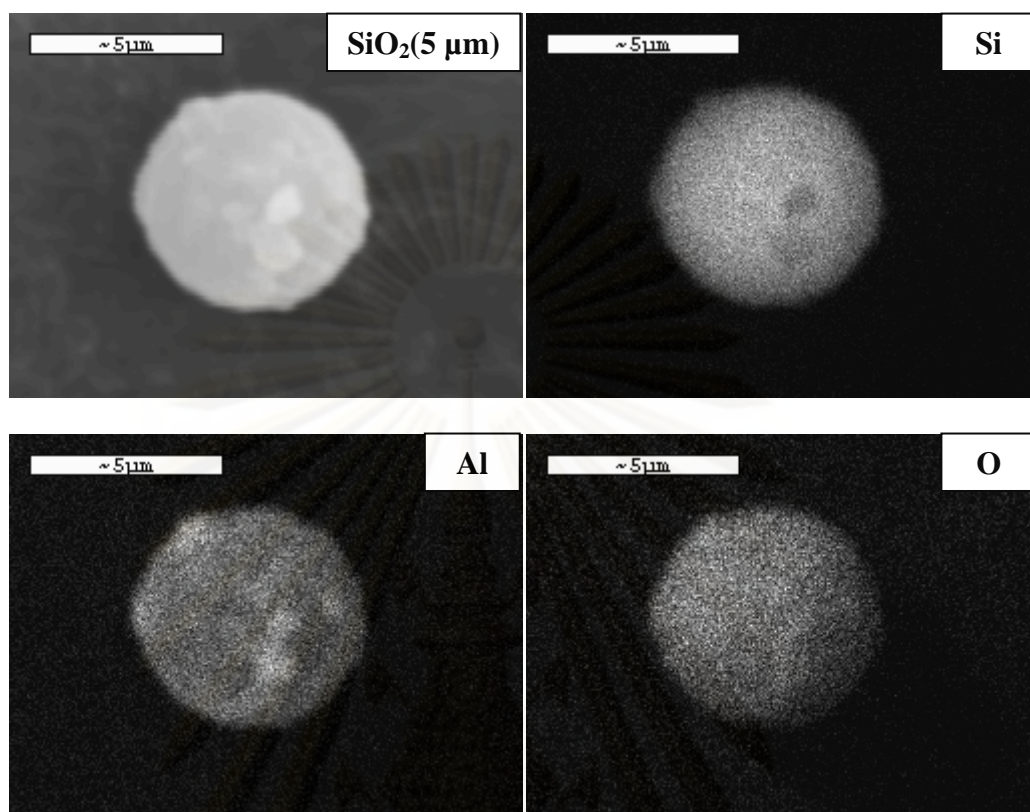


Figure B-7 EDX mapping of SiO₂(5 μm) supports after MAO impregnation.

ศูนย์วิจัยทรัพยากร
จุฬาลงกรณ์มหาวิทยาลัย

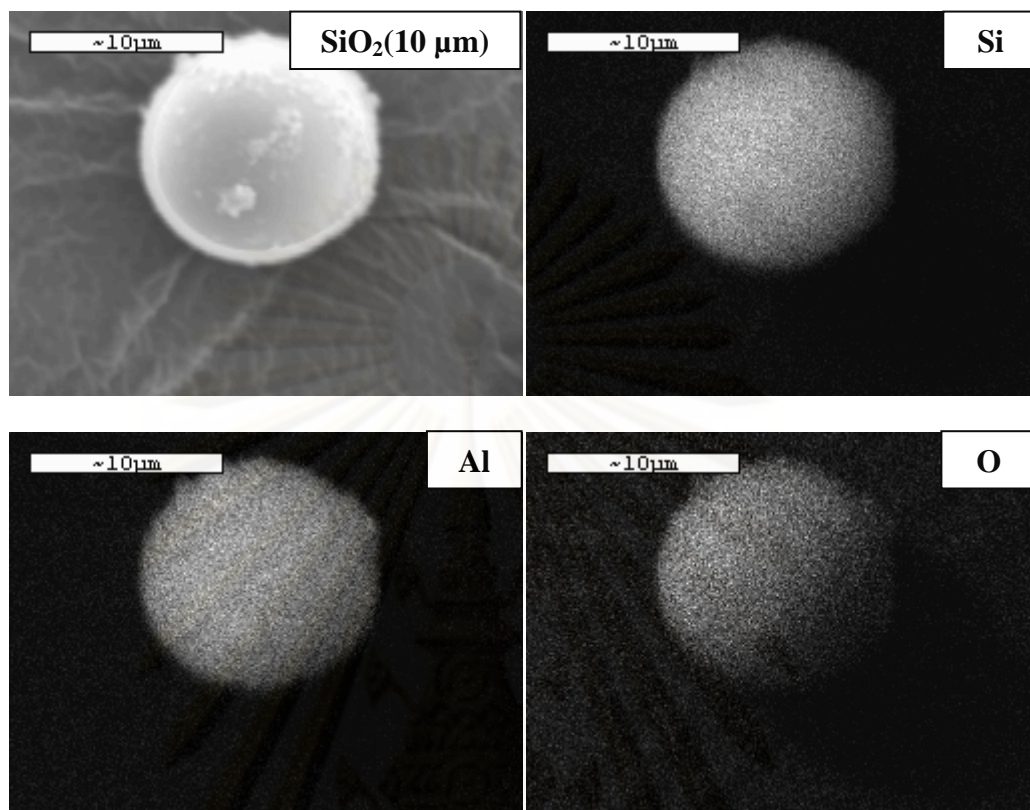


Figure B-8 EDX mapping of SiO₂(10 μm) supports after MAO impregnation.

ศูนย์วิทยทรัพยากร
จุฬาลงกรณ์มหาวิทยาลัย

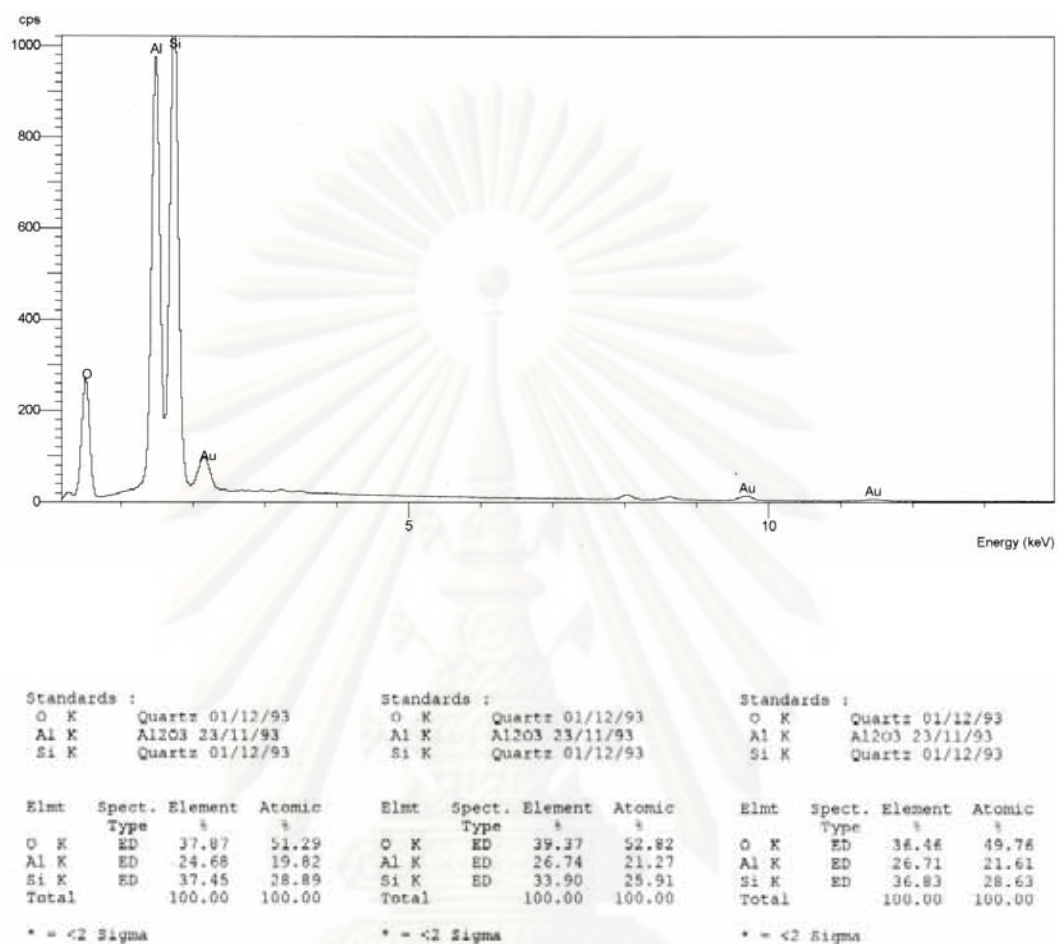


Figure B-9 EDX profile of [Al]_{MAO} on SiO₂ (0.56 μm)

ศูนย์วิทยทรัพยากร
จุฬาลงกรณ์มหาวิทยาลัย

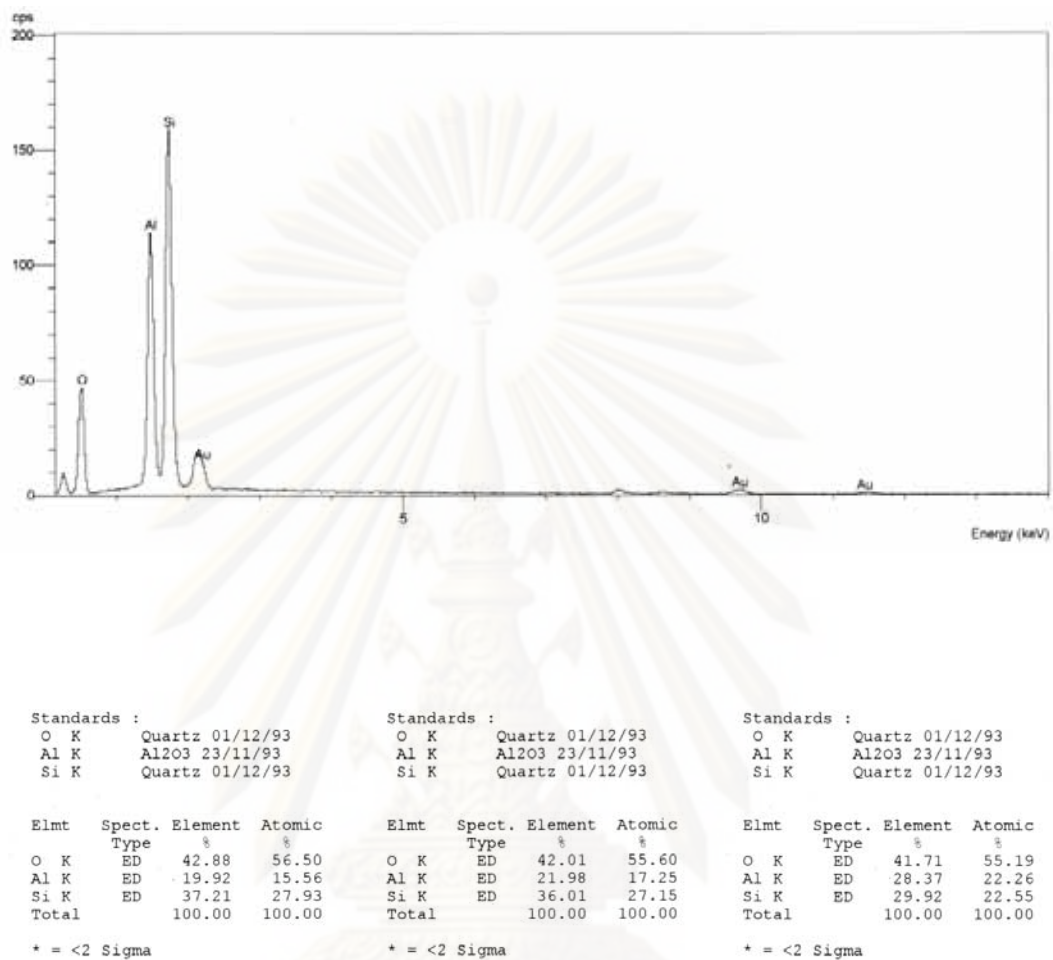
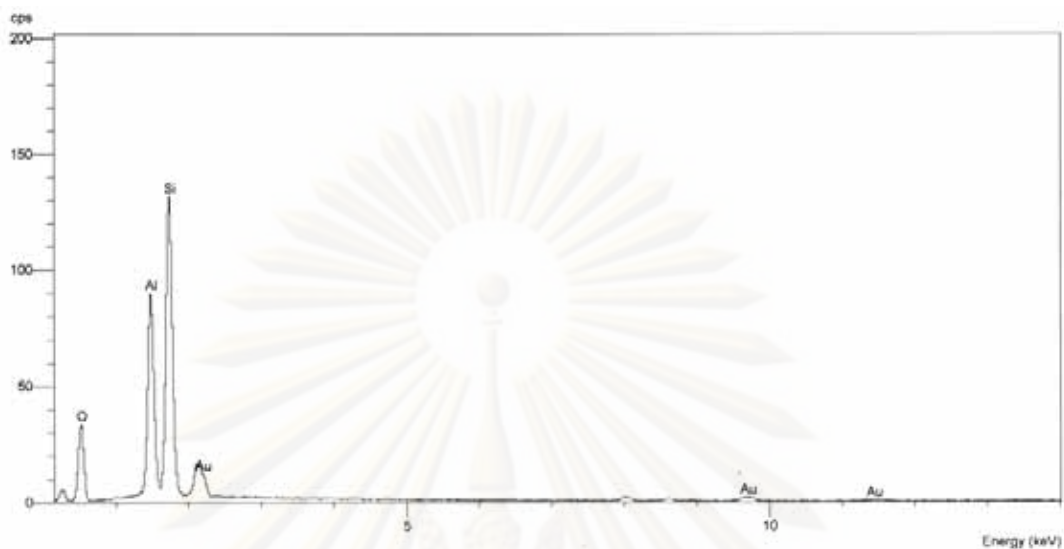


Figure B-10 EDX profile of $[Al]_{MAO}$ on SiO_2 (3 μm)

ศูนย์วิทยทรัพยากร
จุฬาลงกรณ์มหาวิทยาลัย



Standards :
 O K Quartz 01/12/93
 Al K Al2O3 23/11/93
 Si K Quartz 01/12/93

Standards :
 O K Quartz 01/12/93
 Al K Al2O3 23/11/93
 Si K Quartz 01/12/93

Standards :
 O K Quartz 01/12/93
 Al K Al2O3 23/11/93
 Si K Quartz 01/12/93

Elmt	Spect. Type	Element %	Atomic %
O K	ED	40.55	54.07
Al K	ED	24.83	19.63
Si K	ED	34.62	26.29
Total		100.00	100.00

Elmt	Spect. Type	Element %	Atomic %
O K	ED	41.62	55.18
Al K	ED	23.56	18.52
Si K	ED	34.83	26.30
Total		100.00	100.00

Elmt	Spect. Type	Element %	Atomic %
O K	ED	40.44	54.04
Al K	ED	19.93	15.79
Si K	ED	39.63	30.16
Total		100.00	100.00

* = <2 Sigma

* = <2 Sigma

* = <2 Sigma

Figure B-11 EDX profile of [Al]_{MAO} on SiO₂ (5 μm)

ศูนย์วิทยทรัพยากร
 จุฬาลงกรณ์มหาวิทยาลัย

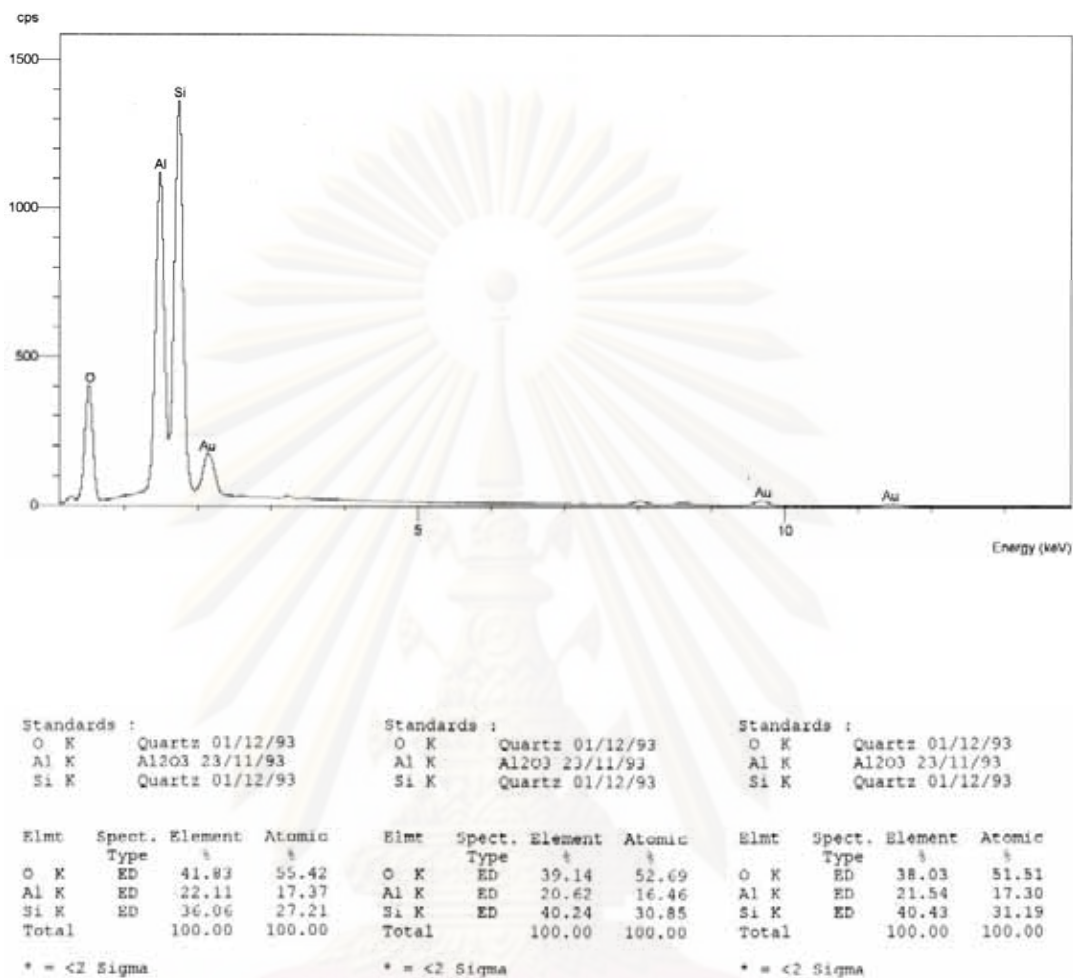
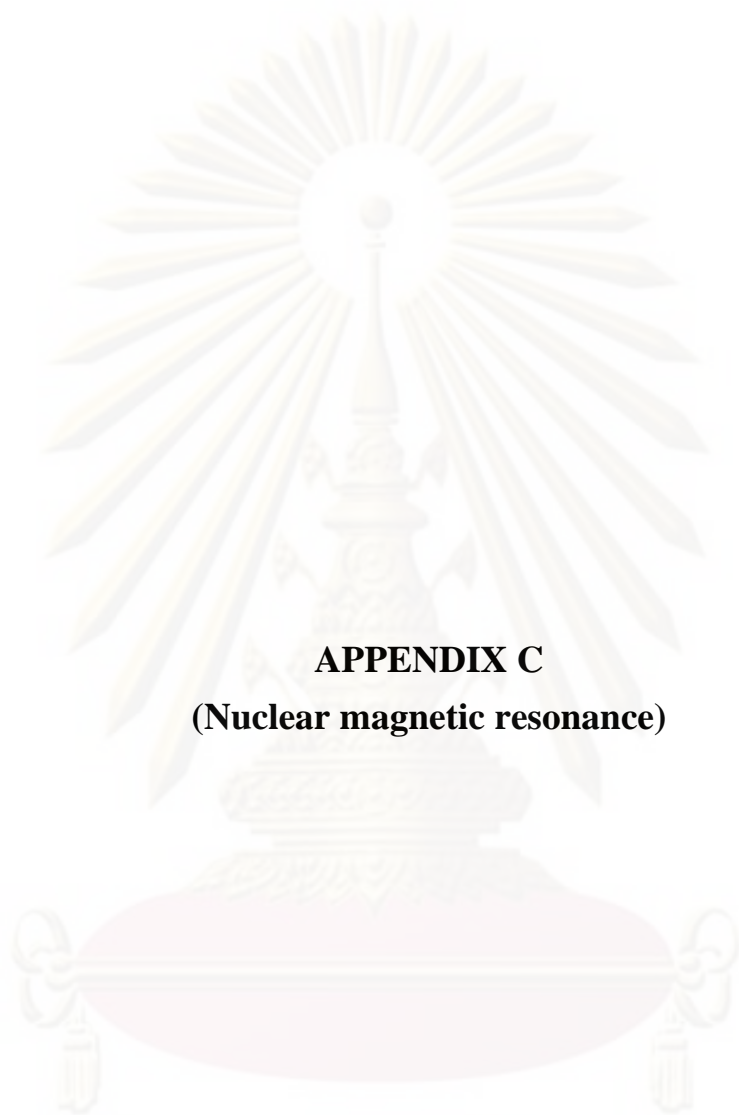


Figure B-12 EDX profile of [Al]_{MAO} on SiO₂ (10 μm)

ศูนย์วิทยทรัพยากร
จุฬาลงกรณ์มหาวิทยาลัย



APPENDIX C
(Nuclear magnetic resonance)

ศูนย์วิทยุทรัพยากร
จุฬาลงกรณ์มหาวิทยาลัย

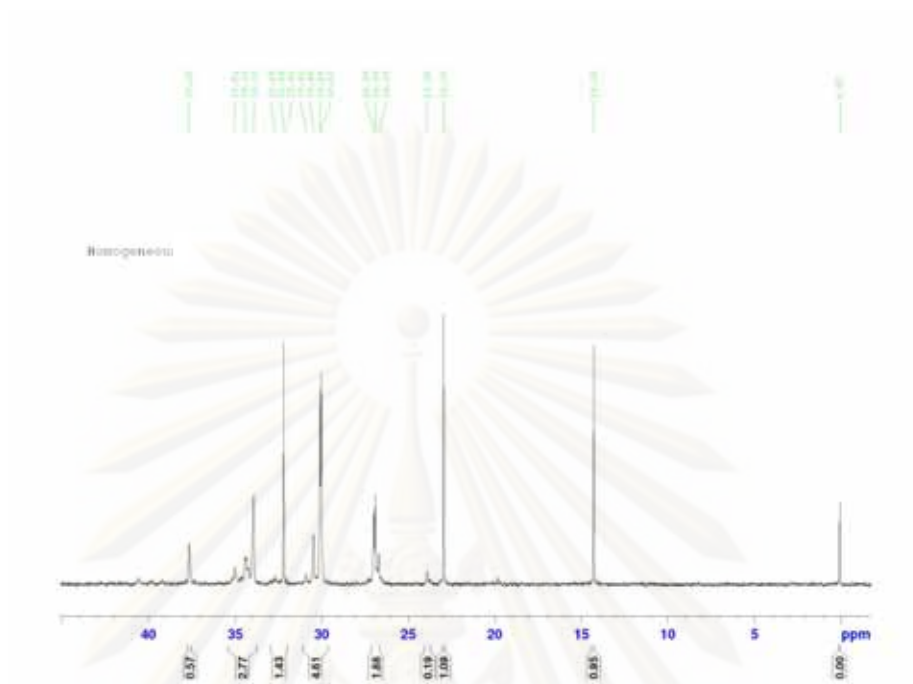


Figure C-1 ^{13}C NMR spectrum of ethylene/1-octene copolymer
(Homogenous by in situ impregnation)

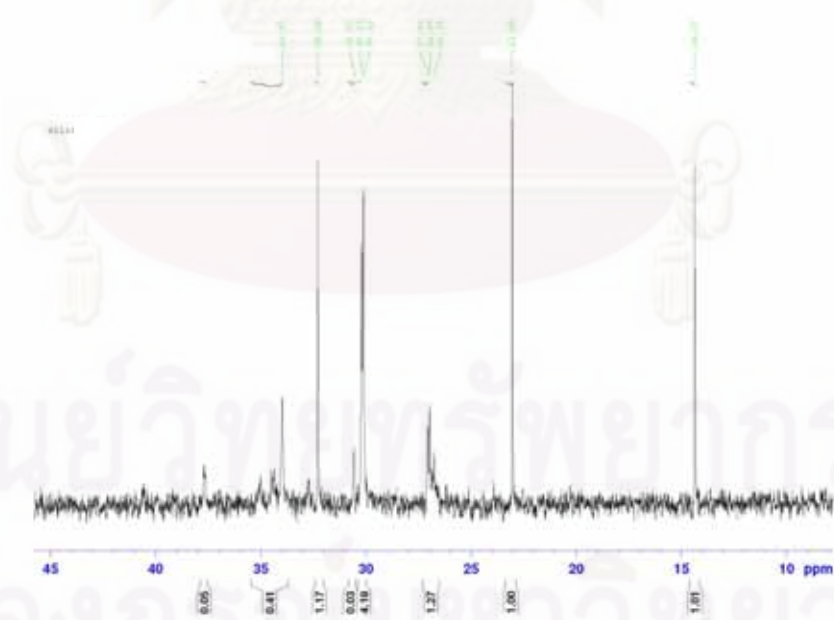


Figure C-2 ^{13}C NMR spectrum of ethylene/1-octene copolymer
(SiO_2 -0.56 μm by in situ impregnation)

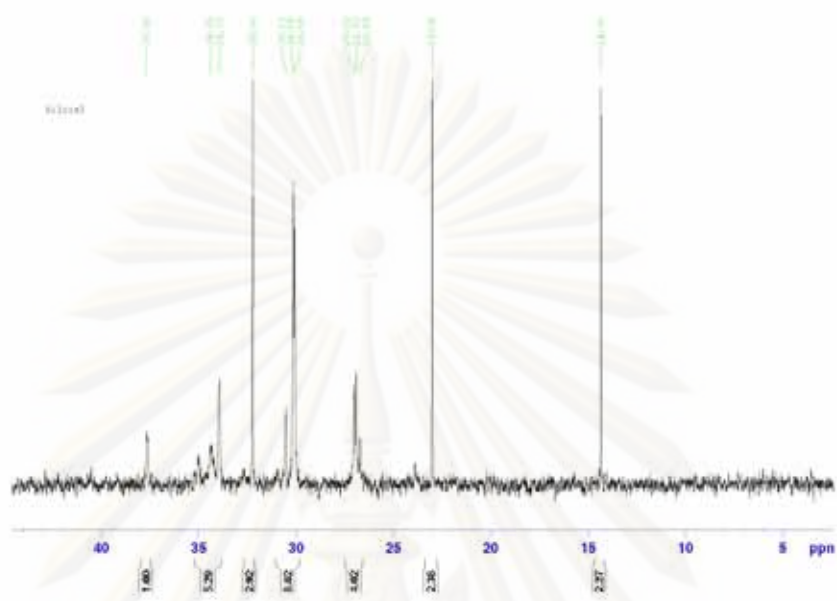


Figure C-3 ^{13}C NMR spectrum of ethylene/1-octene copolymer
(SiO_2 -3 μm by in situ impregnation)

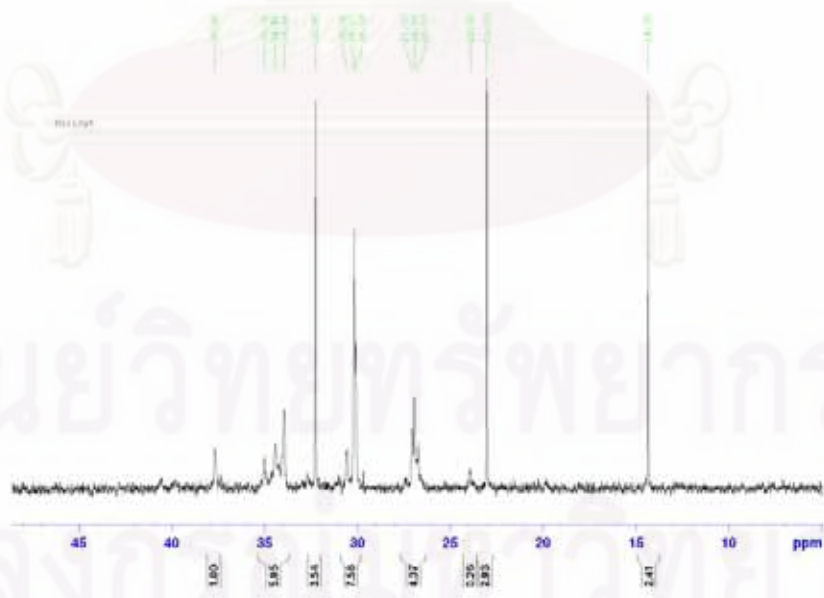


Figure C-4 ^{13}C NMR spectrum of ethylene/1-octene copolymer
(SiO_2 -5 μm by in situ impregnation)

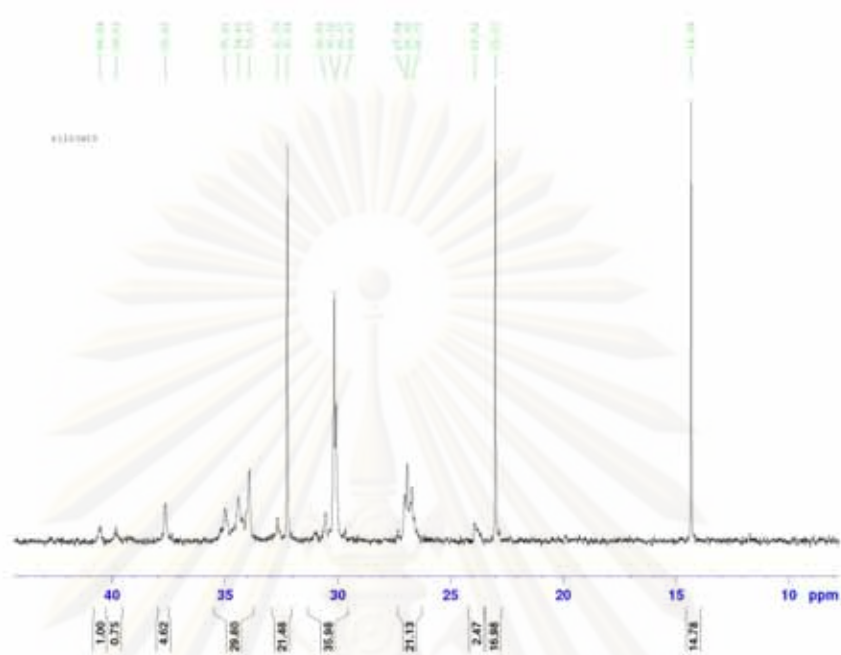


Figure C-5 ^{13}C NMR spectrum of ethylene/1-octene copolymer
(SiO_2 -10 μm by in situ impregnation)

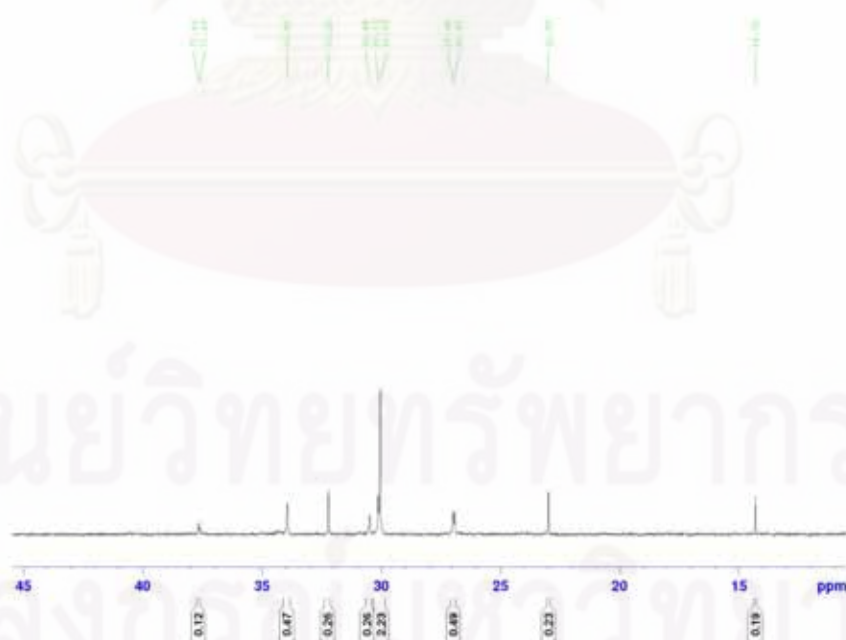


Figure C-6 ^{13}C NMR spectrum of ethylene/1-octene copolymer
(Homogenous by ex situ impregnation)

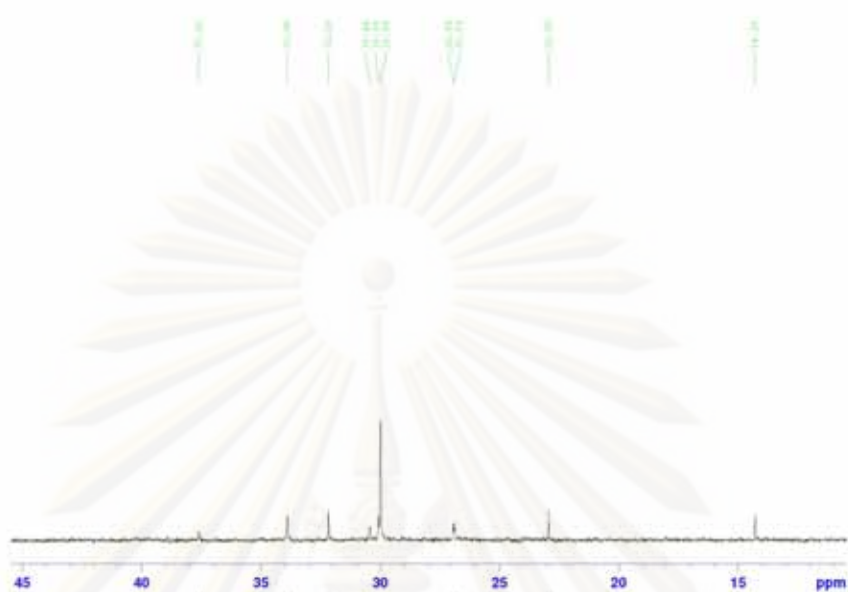


Figure C-7 ^{13}C NMR spectrum of ethylene/1-octene copolymer (SiO₂-0.56 μm by ex situ impregnation)

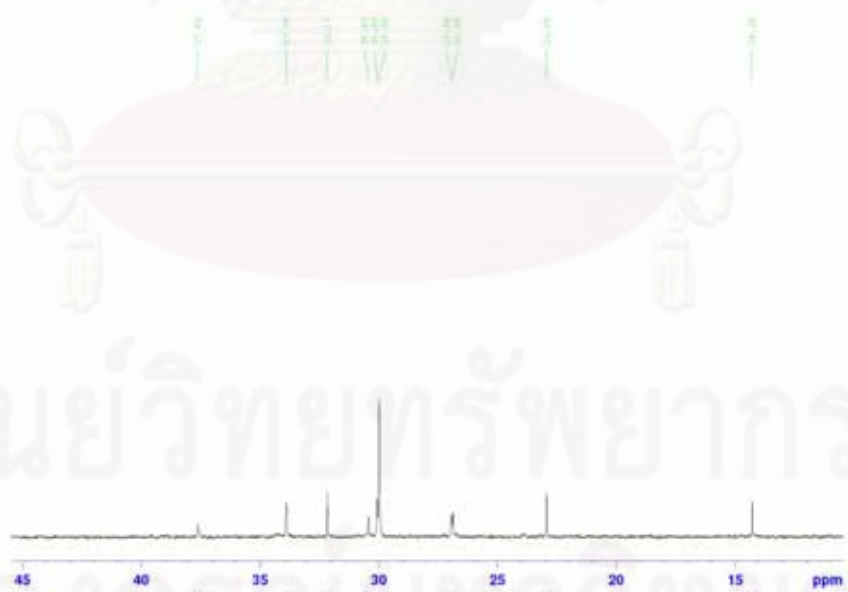


Figure C-8 ^{13}C NMR spectrum of ethylene/1-octene copolymer (SiO₂-3 μm by ex situ impregnation)

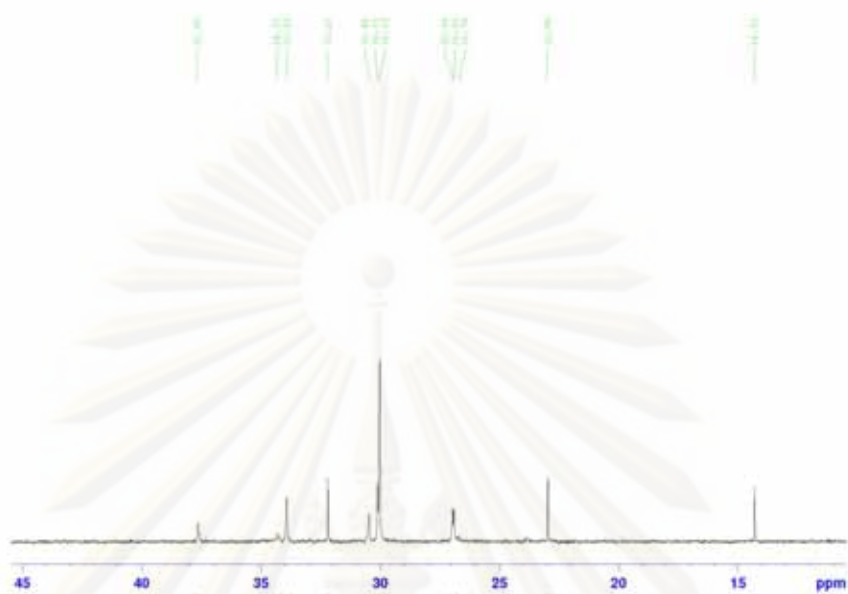


Figure C-9 ^{13}C NMR spectrum of ethylene/1-octene copolymer (SiO₂-5 μm by ex situ impregnation)

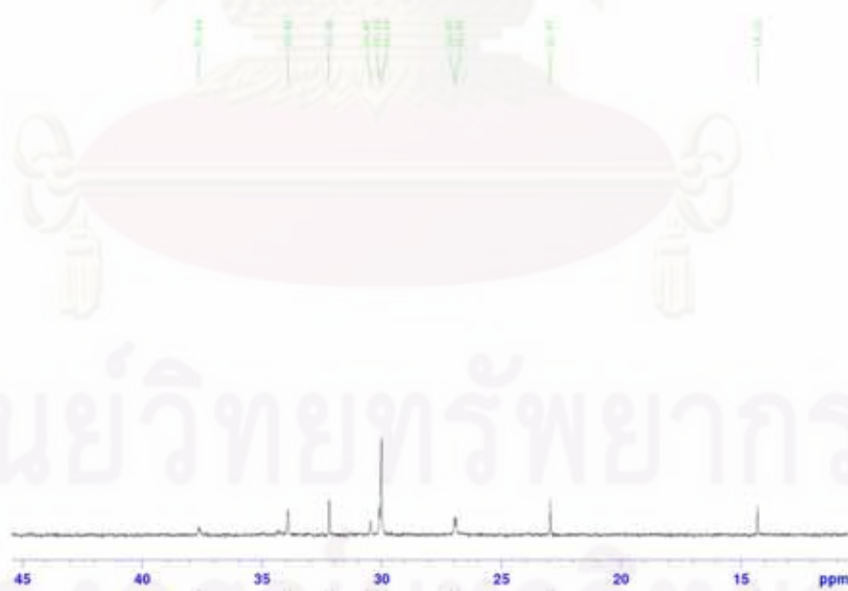
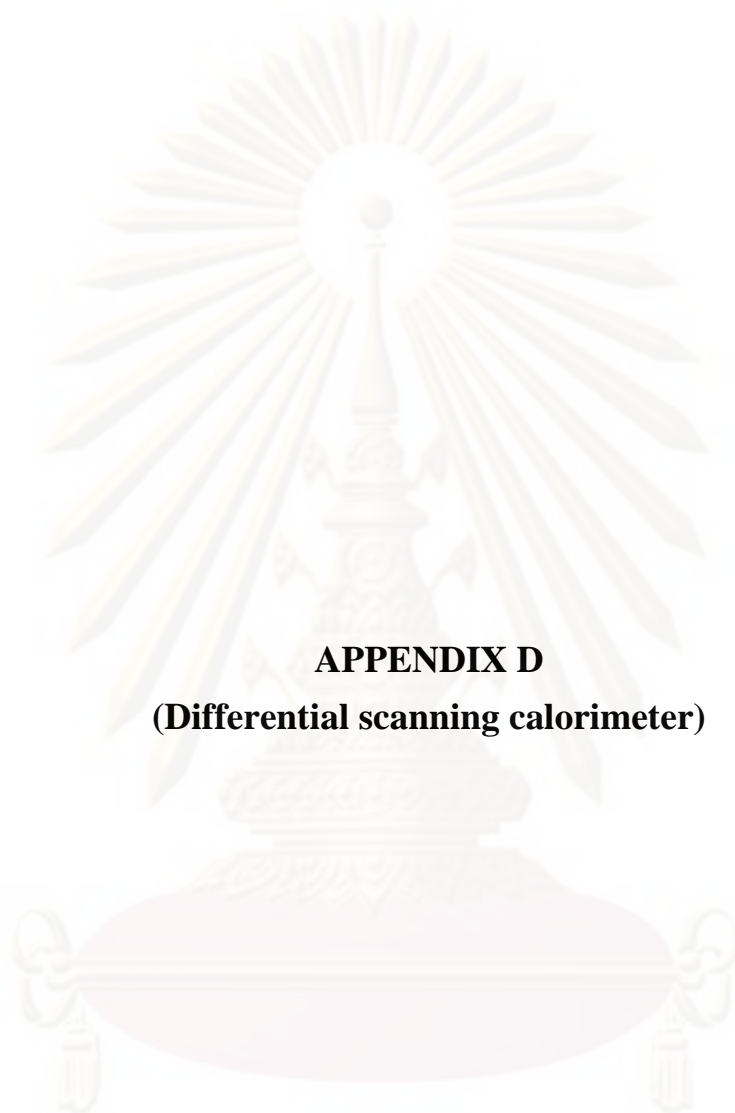


Figure C-10 ^{13}C NMR spectrum of ethylene/1-octene copolymer (SiO₂-10 μm by ex situ impregnation)



Figure C-11 ^{13}C NMR spectrum of polyethylene for all support types

ศูนย์วิทยทรัพยากร
จุฬาลงกรณ์มหาวิทยาลัย



APPENDIX D
(Differential scanning calorimeter)

ศูนย์วิจัยทรัพยากร
จุฬาลงกรณ์มหาวิทยาลัย

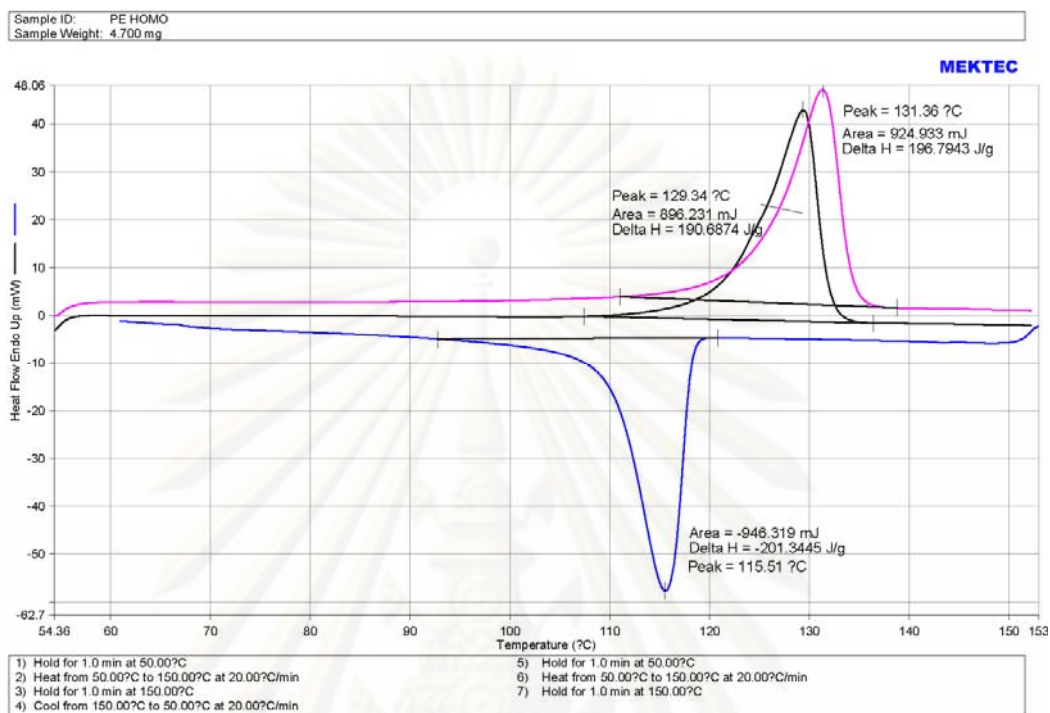


Figure D-1 DSC curve of polyethylene produce with homogenous

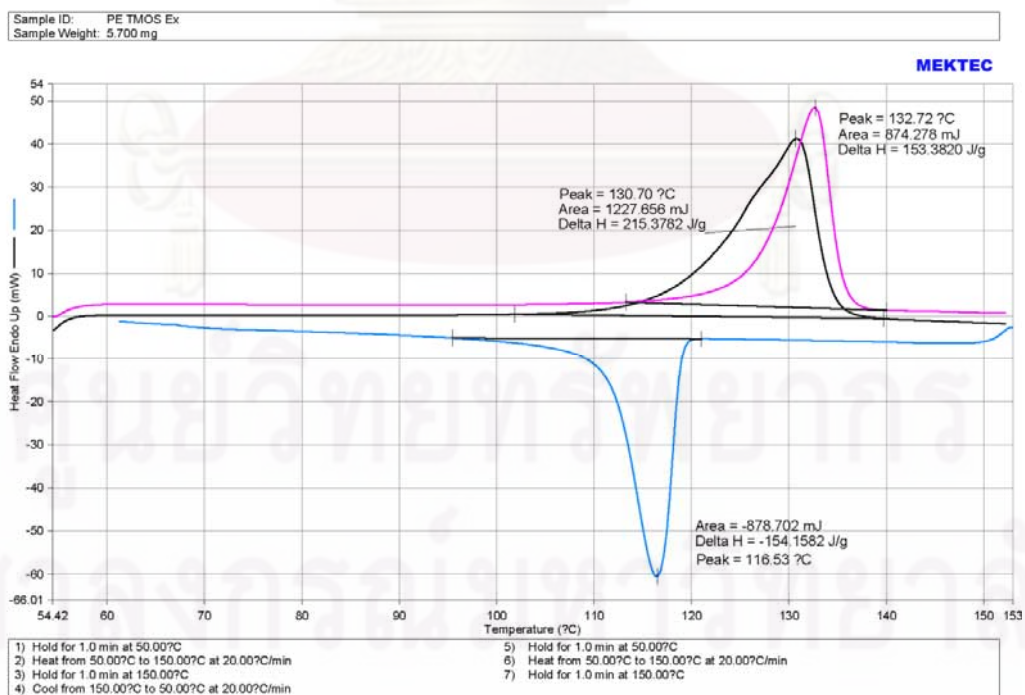


Figure D-2 DSC curve of polyethylene produce with SiO₂ (0.56 μm)

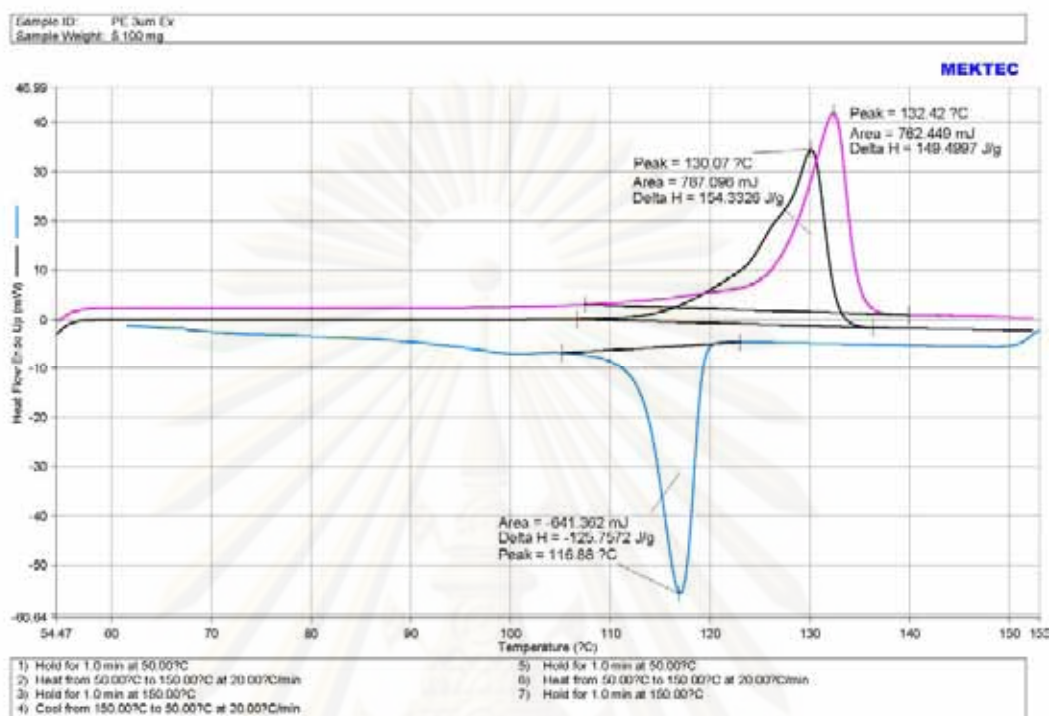


Figure D-3 DSC curve of polyethylene produce with SiO₂ (3 μm)

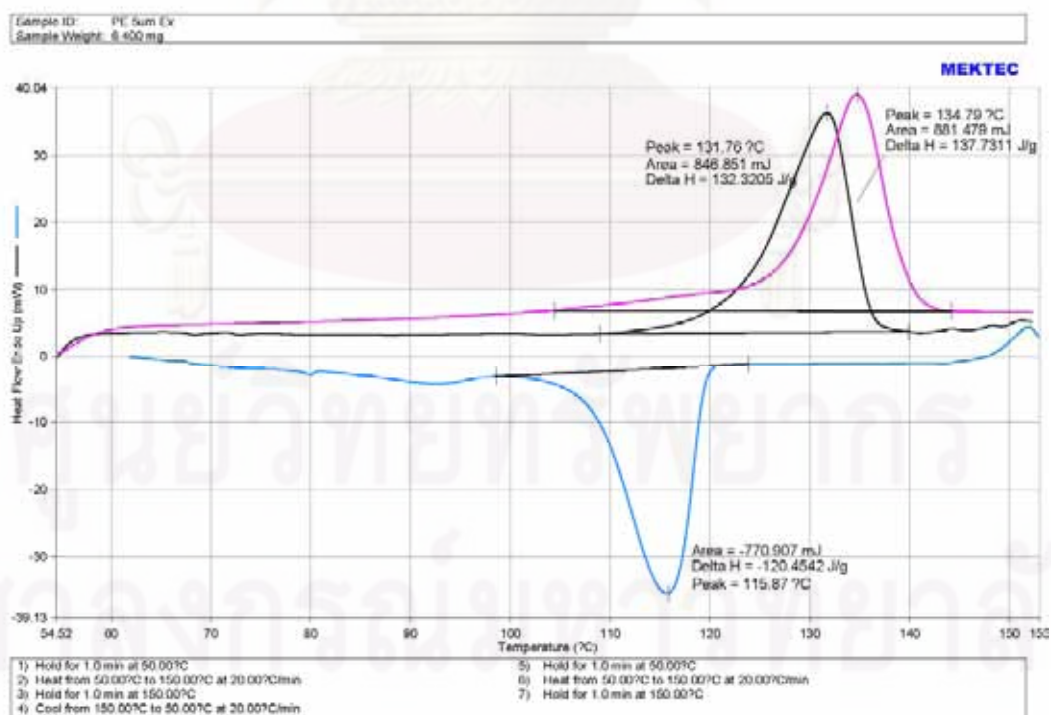


Figure D-4 DSC curve of polyethylene produce with SiO₂ (5 μm)

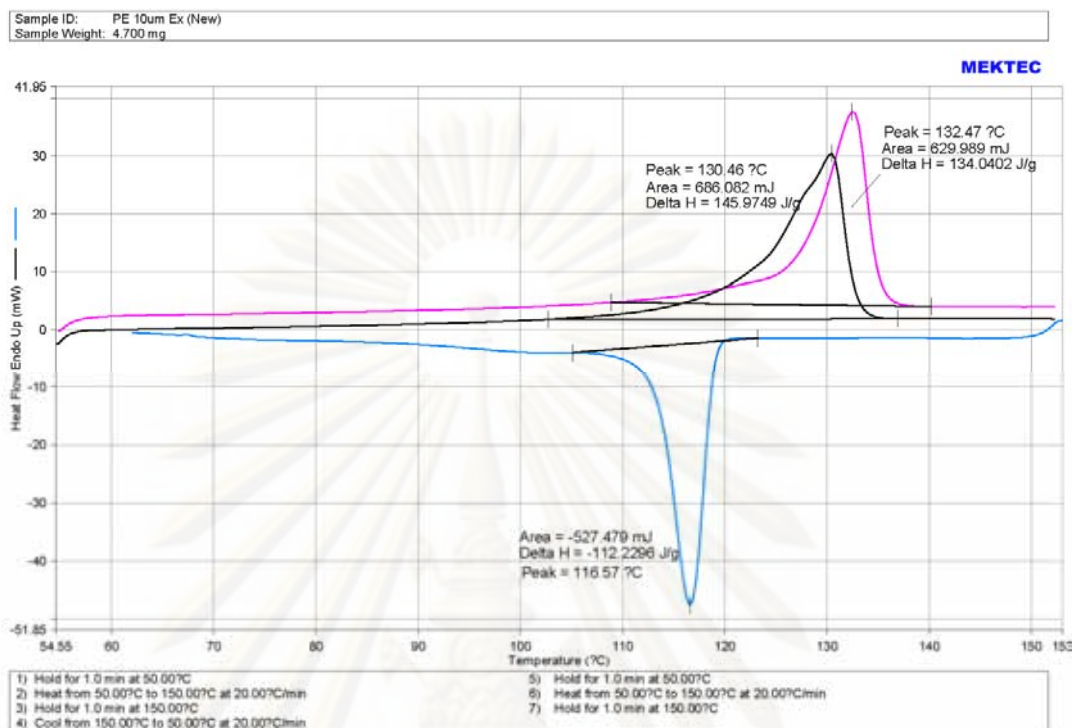


Figure D-5 DSC curve of polyethylene produce with SiO₂ (10 μm)

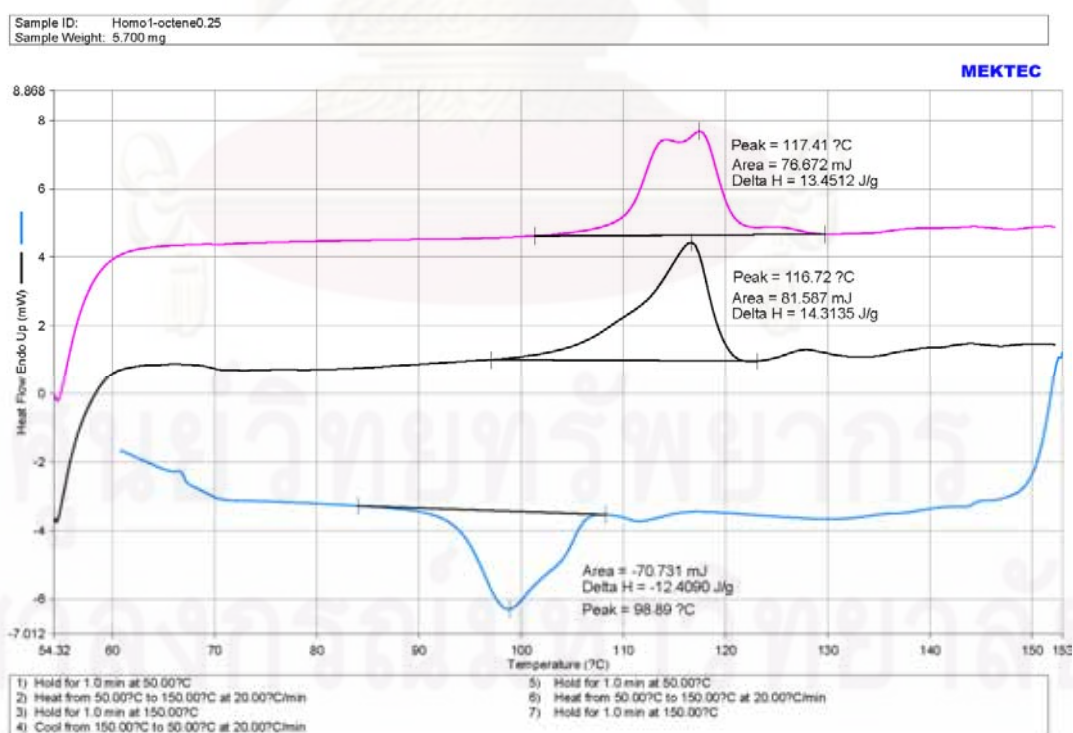


Figure D-6 DSC curve of ethylene/1-octene produce with homogenous

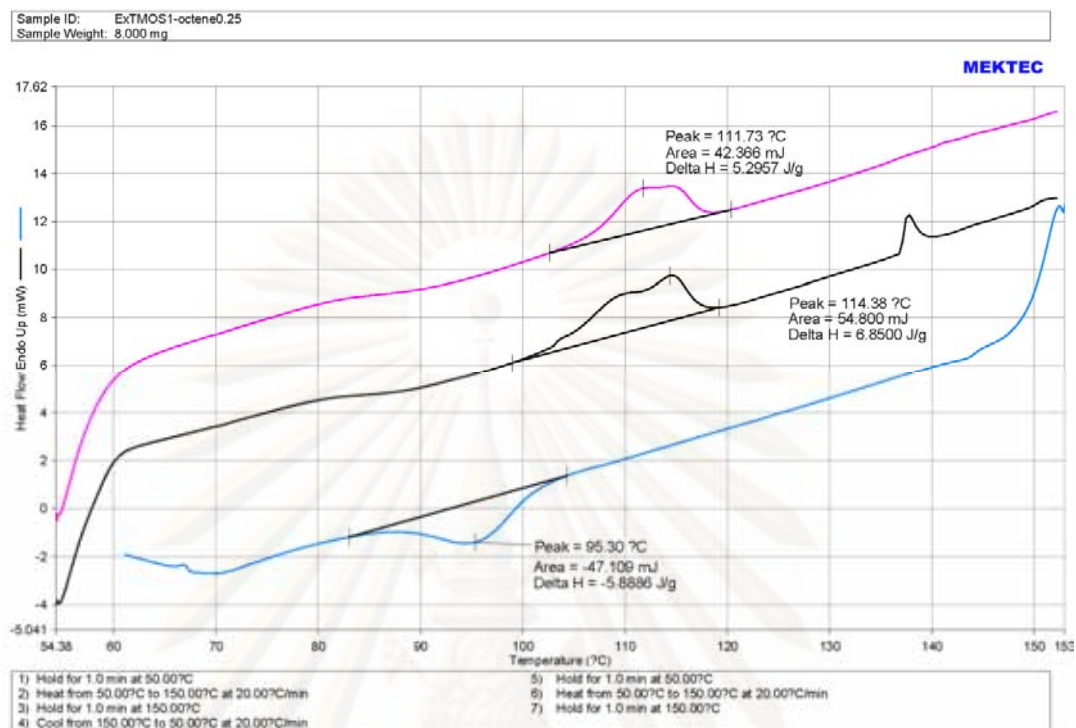


Figure D-7 DSC curve of ethylene/1-octene produce with SiO₂ (0.56 μm)

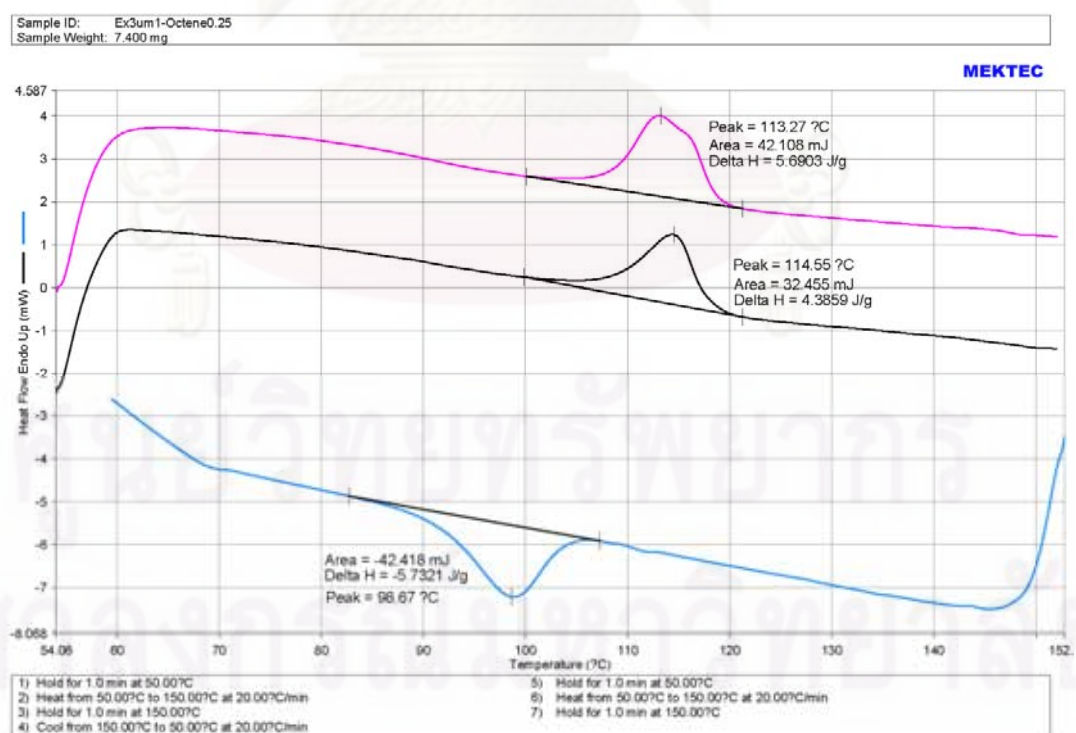


Figure D-8 DSC curve of ethylene/1-octene produce with SiO₂ (3 μm)

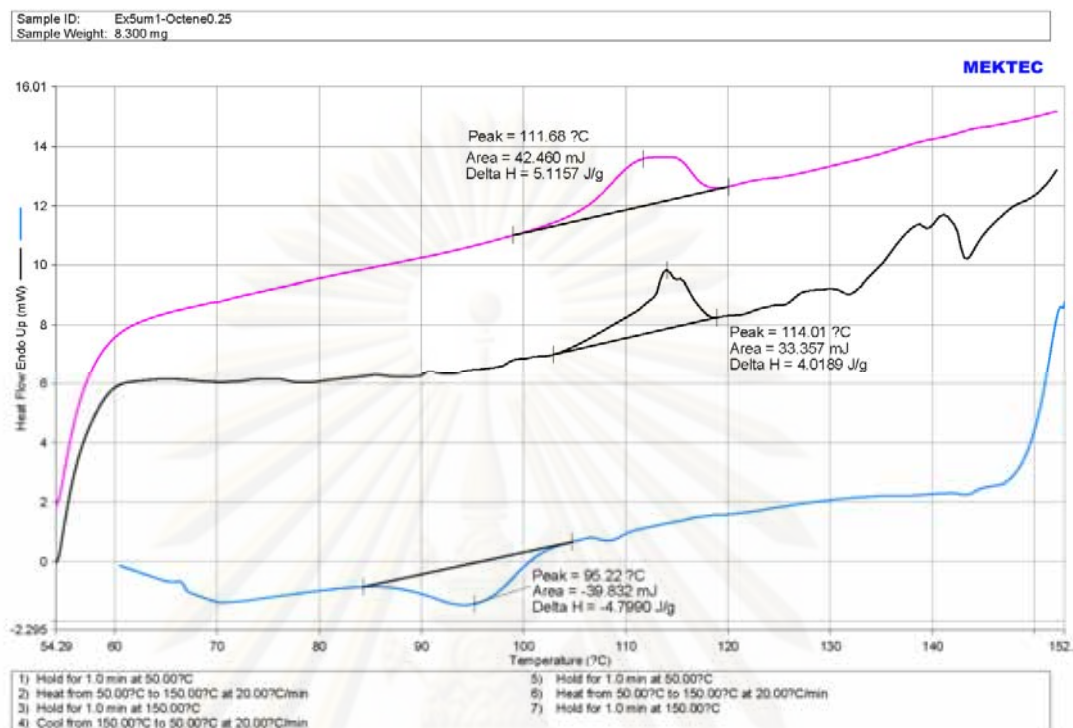


Figure D-9 DSC curve of ethylene/1-octene produce with SiO₂ (5 μm)

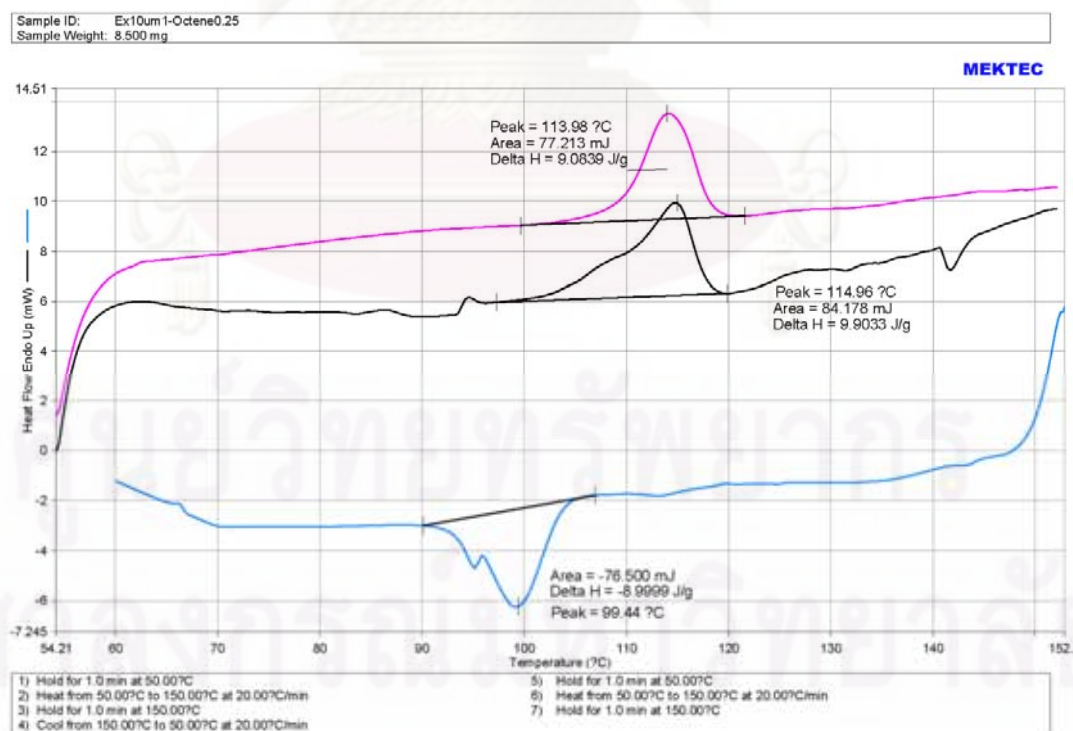
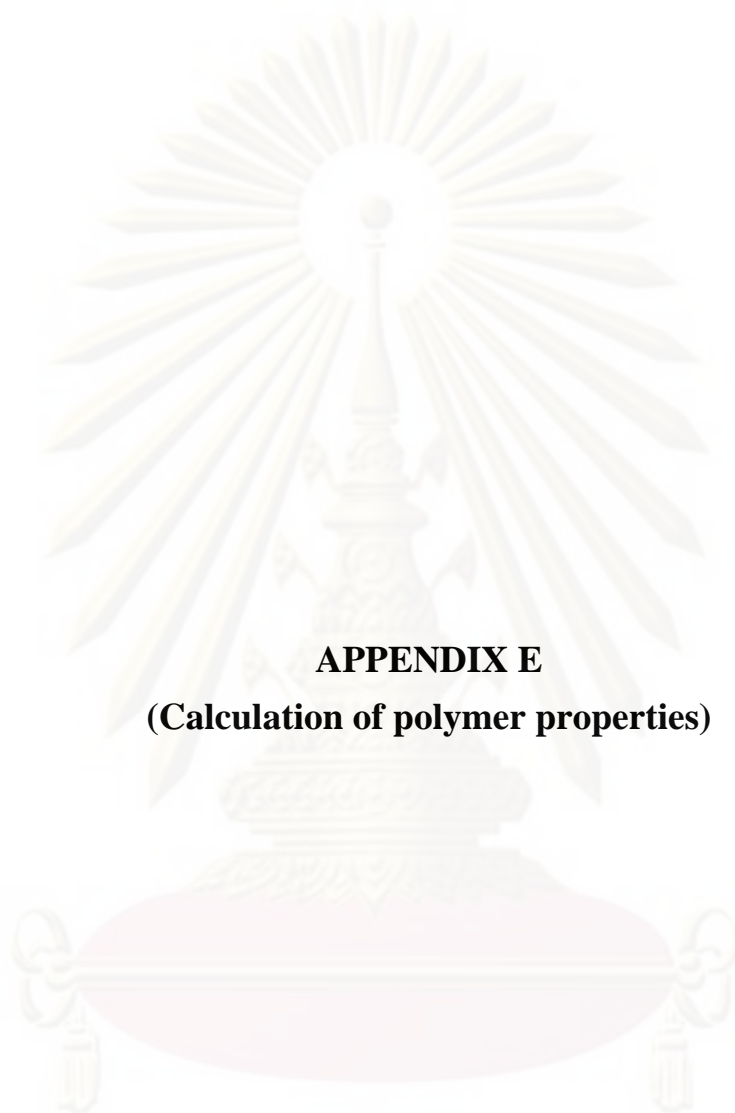


Figure D-10 DSC curve of ethylene/1-octene produce with SiO₂ (10 μm)



APPENDIX E
(Calculation of polymer properties)

ศูนย์วิจัยทรัพยากร
จุฬาลงกรณ์มหาวิทยาลัย

E-1 Calculation of polymer microstructure

Polymer microstructure and also triad distribution of monomer can be calculated according to the Prof. James C. Randall [Randall, 1989] in the list of reference. The detail of calculation for ethylene/ α -olefin copolymer was interpreted as follow.

1-Octene

The integral area of ^{13}C -NMR spectrum in the specify range are listed.

T_A	=	39.5 - 42	ppm
T_B	=	38.1	ppm
T_C	=	36.4	ppm
T_D	=	33 - 36	ppm
T_E	=	32.2	ppm
T_F	=	28.5 - 31	ppm
T_G	=	25.5 - 27.5	ppm
T_H	=	24 - 25	ppm
T_I	=	22 - 23	ppm
T_J	=	14 - 15	ppm

Triad distribution was calculated as the followed formula.

$k[\text{OOO}]$	=	$T_A - 0.5T_C$
$k[\text{EOO}]$	=	T_C
$k[\text{EOE}]$	=	T_B
$k[\text{EEE}]$	=	$0.5T_F - 0.25T_E - 0.25T_G$
$k[\text{OEO}]$	=	T_H
$k[\text{OEE}]$	=	$T_G - T_E$

Table E-1 Reactivity ratios of ethylene and 1-octene

Impregnation method	System	$r_E r_O$
In-situ	Homogeneous	0
	SiO ₂ 0.56μm	0
	SiO ₂ 3μm	0
	SiO ₂ 5μm	0
	SiO ₂ 10μm	1.01
Ex-situ	Homogeneous	0
	SiO ₂ 0.56μm	0
	SiO ₂ 3μm	0
	SiO ₂ 5μm	0
	SiO ₂ 10μm	0

All copolymer was calculated for the relative comonomer reactivity (r_E for ethylene and r_O for the 1-octene comonomer) and monomer insertion by using the general formula below.

$$r_E = 2[EE]/([EC]X) \qquad r_O = 2[CC]X/[EC]$$

where r_E = ethylene reactivity ratio

r_O = comonomer (1-octene) reactivity ratio

$[EE]$ = $[EEE] + 0.5[CEE]$

$[EO]$ = $[OEO] + 0.5[OEE] + [EOE] + 0.5[EOO]$

$[OO]$ = $[OOO] + 0.5[EOO]$

X = $[E]/[O]$ in the feed = concentration of ethylene (mol/L) / concentration of comonomer (mol/L) in the feed.

%E = $[EEE] + [EEO] + [OEO]$

%O = $[OOO] + [OOE] + [EOE]$

E.2 Calculation of crystallinity for ethylene/ α -olefin copolymer

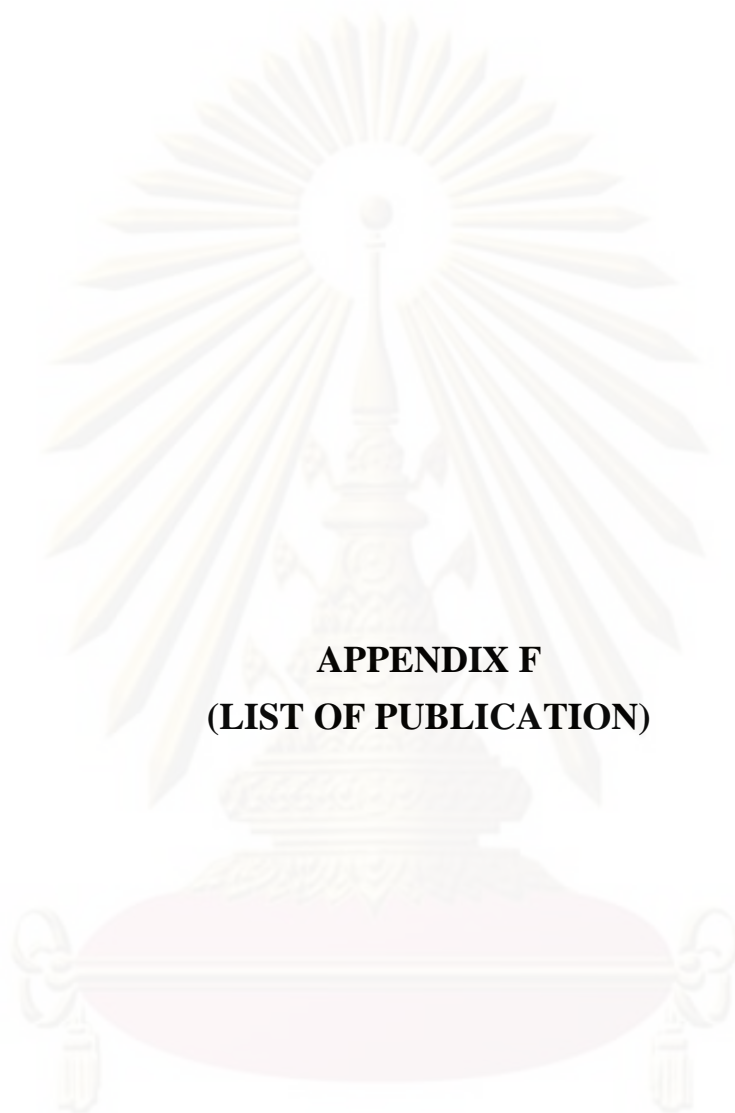
The crystallinities of copolymers were determined by differential scanning calorimeter. %crystallinity of copolymers is calculated from equation [Liu et al., 1997].

$$\chi(\%) = \frac{\Delta H_m}{\Delta H_{m_0}} \times 100$$

Where $\chi(\%)$ = %crystallinity

ΔH_m = the heat of fusion of sample (J/g)

ΔH_{m_0} = the heat of fusion of perfectly crystalline polyethylene
(286 J/g) [Galland et al., 1996]



APPENDIX F
(LIST OF PUBLICATION)

ศูนย์วิทยทรัพยากร
จุฬาลงกรณ์มหาวิทยาลัย

1. Rothakit, P. and Jongsomjit, B. “Effect of spherical silica-supported zirconocene/MAO catalyst on copolymerization of ethylene/1-octene” (The Proceeding of 19th Thailand Chemical Engineering and Applied Chemistry Conference, TIChe 2009, Kanchanaburi)



ศูนย์วิทยทรัพยากร
จุฬาลงกรณ์มหาวิทยาลัย

VITA

Miss Prae Rothakit was born on January 24, 1986 in Bangkok, Thailand. She graduated high school from Satreesamutprakarn School, Samutprakarn and received the Bachelor's Degree of Chemical Engineering from the Department of Chemical Engineering, Faculty of Engineering, Chulalongkorn University in April 2008. She continued her Master's Degree study at Chulalongkorn University in June, 2008.



ศูนย์วิทยทรัพยากร
จุฬาลงกรณ์มหาวิทยาลัย